

Downstream processing of fermented fine sieved fraction for biological nutrient removal

A comprehensive study on biodegradability
and biological nutrient removal performance
of fFSF, and a feasibility analysis of secondary
screening

by

Haozheng Lyu

to obtain the degree of Master of Science
at the Delft University of Technology,
to be defended publicly on Friday, 30 September at 15:00

Student number:	5210607
Project duration:	November 16, 2021 – September 30, 2022
Supervisors:	Prof. dr. ir. Merle de Kreuk TU Delft Dr. Magela Odriozola TU Delft Mathijs Oosterhuis Royal HaskoningDHV
Thesis committee:	Prof. dr. ir. Merle de Kreuk Sanitary engineering (Chair) Prof. dr. ir. Jules van Lier Sanitary engineering Dr. M. C. M. Bakker Resources & Recycling

Copyright © 2022 by Haozheng Lyu

An electronic version of this thesis is available at <http://repository.tudelft.nl/>.

Acknowledgement

Words cannot express my gratitude to my supervisors: Merle, Mathijs, and Magela, for their invaluable patience and feedback. I also could not have undertaken this journey without my defense committee, who generously provided many constructive suggestions. Additionally, this endeavor would not have been possible without the support from Royal HaskoningDHV and WWTP Aarle-Rixtel.

I am also grateful to my classmates, especially Sihan, for their kind help. Thanks should also go to Armand and other lab assistants from the Waterlab, who gave a lot of instructions on instrumental analysis.

Lastly, I would like to extend my sincere thanks to my parents. Their belief in me has kept my spirits and motivation high during my Master's study.

Abstract

Fine sieved fraction (FSF) is a solid waste generated from wastewater treatment plants (WWTPs). Cellulose fiber is the most important component of FSE, which can be fermented into volatile fatty acids (VFAs) and then be used as carbon sources in biological nutrient removal (BNR). This thesis measured and evaluated the aerobic & anaerobic biodegradability of solids in fermented FSF (fFSF) and the BNR performance of FSF-derived VFAs. In addition, this research tested the feasibility of using secondary sieving as a potential downstream processing technology. The products of secondary sieving (liquid: secondary filtrate, solid: secondary FSF) were compared with fFSF in terms of biodegradability and BNR performance. The aerobic biodegradability of raw FSF, fFSF and secondary filtrate were 52.3 ± 1.4 , 60.4 ± 4.7 and 72.1 ± 6.4 %, respectively. The anaerobic biodegradability of raw FSF, fFSF and secondary FSF are 56.8 ± 8.4 , 68.2 ± 6.4 , 51.5 ± 7.8 %, respectively. The results of biodegradability revealed that secondary sieving increased the proportion of readily biodegradable solids and reduced the overall organic load of activated sludge systems. The residual solids after secondary sieving could be converted into biogas or recovered as building materials. FSF-derived VFAs could substantially increase denitrification rates and phosphate release rates. fFSF and secondary filtrate could increase the denitrification rate by 40 - 50% and increase the phosphate release rate by around 200 % compared to blank. Theoretically, the effluent nitrogen load could be reduced by up to 53.7% if FSF-derived carbon sources are fully used for denitrification at WWTP Aarle-Rixtel. If used for phosphorus removal, the capacity provided by FSF-derived VFAs could nearly remove all phosphate from the effluent. To sum up, FSF-derived VFAs could effectively increase BNR rates and significantly reduce the effluent nitrogen and phosphorus load. The main advantages of FSF-derived VFAs over conventional carbon sources are sustainability and waste-reduction. Secondary sieving could reduce the solid load of activated sludge tank and achieve a combined recycling of VFAs and fibers, but the total COD available for BNR will be reduced as a compensation. The results in this thesis can facilitate the application of fFSF in WWTPs and the improvement of FSF-derived VFAs production.

Keywords: Batch activity test, biodegradability, biological nutrient removal, cellulose recycle, denitrification, downstream processing, enhanced biological phosphorus removal, fine sieved fraction, sieving.

Nomenclature

AMPTS	Automatic methane potential test system
AOB	Ammonia oxydizing bacteria
AST	Activated sludge tank
ATU	Allythiourea
BMP	Biomethane potential
BNR	Biological nutrient removal
BOD	Biochemical oxygen demand
C&F	Centrifugation & filtration
COD	Chemical oxygen demand
sCOD	Soluble chemical oxygen demand
tCOD	Total chemical oxygen demand
DN	Denitrification
DO	Dissolved oxygen
EBPR	Enhanced biological phosphorus removal
GC	Gas chromatography
GGA	Glucose-glutamic acid
FSF	Fine sieved fraction
fFSF	fermented fine sieved fraction
HRT	Hydraulic retention time
IC	Ion chromatography
MSM	Metrohm suppressor module
NOB	Nitrite oxidizing bacteria
OLR	Organic loading rate
PAO	Phosphate accumulating organism
PbSe	Polybutylene sebacate
PHA	Poly- β -hydroxyalkanoate
PHV	polyhydroxyvalerate
PR	Phosphate release
Poly-P	Polyphosphate
SS	Suspended solid
SB	Soluble substrate
XCB	Insoluble substrate
TN	Total nitrogen
TP	Total phosphorus
TS	Total solid
TSS	Total suspended solid
VFA	Volatile fatty acid
VS	Volatile solid
VSS	Volatile suspended solid
WWTP	Wastewater treatment plant

Contents

Acknowledgement	iii
Nomenclature	vii
1 Introduction	1
1.1 Background	1
1.2 Problem statement	2
1.3 Research questions	3
2 Literature review	5
2.1 Fine sieves for wastewater primary treatment	5
2.2 Characterization of fine sieved fraction	6
2.3 Biological nutrient removal	6
2.3.1 Biological nitrogen removal	6
2.3.2 Enhanced biological phosphorus removal	8
2.3.3 Carbon source for biological nutrient removal	8
2.4 Waste-derived VFAs for improving BNR performance	9
2.4.1 Factors influencing the fermentation of VFAs	9
2.4.2 Downstream processing of waste-derived VFAs	11
2.4.3 Performance of waste-derived VFAs in BNR	11
3 Methodology	13
3.1 Process flow diagram	13
3.1.1 Scenario 1	13
3.1.2 Scenario 2	14
3.2 Sample and inoculum collection	14
3.3 Morphology of samples	15
3.4 Physico-chemical analysis	15
3.4.1 Volatile fatty acids measurement with gas chromatography	16
3.4.2 Nitrate and Phosphate Measurement	17
3.5 Aerobic biodegradability test	17
3.5.1 Preparation of stock solutions	18
3.5.2 Execution of the BOD test	18
3.5.3 Data analysis and interpretation	19
3.6 Anaerobic biodegradability test	20
3.6.1 Pretreatment of anaerobic digestate inoculum	20
3.6.2 Execution of the BMP test	21
3.6.3 Data analysis and interpretation	22
3.7 Batch activity test	22
3.7.1 Denitrification batch activity test	23
3.7.2 Anaerobic EBPR batch activity test	25

4	Results	29
4.1	Sample characterization	29
4.1.1	Morphology	29
4.1.2	Sample composition	29
4.2	Aerobic biodegradability	32
4.3	Anaerobic biodegradability	34
4.4	Biological nutrient removal efficiency	36
4.4.1	Denitrification test	36
4.4.2	P-release test	37
4.4.3	Summary of batch activity test	39
4.5	Overall mass and COD balance	40
5	Discussion	43
5.1	Aerobic and anaerobic biodegradability analysis	43
5.1.1	Aerobic biodegradability	43
5.1.2	Anaerobic biodegradability	44
5.2	Biological nutrient removal performance	45
5.3	Comparison of FSF-derived VFAs with existing carbon source	47
5.4	Fiber reuse in construction sector	48
6	Conclusion	51
7	Recommendations	53
	Bibliography	55
A	Raw data	61
B	Solution preparation and program settings	73

1

Introduction

1.1. Background

Fine sieving is an emerging primary wastewater treatment technology and fine sieved fraction (FSF) is the solid waste from fine sieving. Fine sieving has been tested at many wastewater treatment plants (WWTPs) in the Nordic countries, and has been regarded as a substitution for primary clarification (Rusten and Ødegaard, 2006). Clarification can remove suspended solids (SS) at low cost, hence reducing the solid load of subsequent activated sludge system. However, clarifier cannot effectively remove cellulose, which originates from toilet paper and makes up 40% of the SS in municipal wastewater for many industrialized countries (Ruiken et al., 2010). Unremoved cellulose may not be completely degraded during the retention in aerobic tank, and thus increasing the cost of aeration and the volume of excess sludge (Ahmed et al., 2021). Compared to clarification, fine sieving has higher cellulose removal efficiency (Ruiken et al., 2013). FSF is mainly composed of cellulose derived from toilet paper, and FSF was found to have around 80% of cellulose and 90% of organic matters (on dry basis); while, the cellulose fraction and organic fraction of primary sludge are only approximately 35% and 80%, respectively (Ruiken et al., 2013). The Dutch government released the dutch roadmap report for WWTPs of 2030 and put energy & nutrient recovery at a high priority (Roeleveld et al., 2010). FSF has higher cellulose and organic content compared to primary sludge, which contributes to a higher recycling potential (Paulsrud et al., 2014). Consequently, appropriate FSF disposal and recycling could broaden the application of fine sieves in WWTPs.

Currently, incineration is the most common technology for organic waste disposal, including FSF. Incineration can recover the energy of the wastes and generate electricity; however, the efficiency of sludge incineration is low due to high water content (Sabbas et al., 2003). Ruiken et al. (2010) reported that the cost of sludge treatment accounts for more than half of the total wastewater treatment cost in The Netherlands. Moreover, incineration destroys the organic materials in the waste and releases the carbon as CO₂, which could limit the application of incineration in the foreseeable future (Kuo et al., 2011; Zhuang et al., 2020). As a result, finding efficient alternatives for FSF and sludge disposal could significantly decrease the cost of wastewater treatment and increase the sustainability of WWTPs.

Recycling of FSF can be achieved in different ways. Over the past decades, several utilization routes were proposed to valorize the FSF (Ghasimi, 2016; Kleerebezem et al., 2015). Previous studies indicate that the FSF can be digested under thermophilic or mesophilic conditions to produce biogas (Ghasimi et al., 2015). Recent research also revealed that the FSF can be converted into

volatile fatty acids (VFAs) by inhibiting the activity of methanogenesis during anaerobic fermentation process (Oosterhuis et al., 2019; Ros et al., 2020). This process is also referred to as acidogenic fermentation.

VFAs are short-chain fatty acids, which are mainly composed of C2-C6 compounds. VFAs are excellent carbon sources for microorganisms. Some studies showed that the waste-derived VFAs can be additional carbon sources to enhance the biological nutrient removal (BNR) processes of WWTPs, including denitrification and enhanced biological phosphorus removal (EBPR) (Elefsiniotis and Li, 2006; Lee et al., 2014). Recent research further optimized the yield of VFAs by studying the impacts of different operating parameters (Cadavid-Rodríguez and Horan, 2014; Fang et al., 2020; Ros et al., 2020), and the yield is about 264 g VFAs / kg dry-FSF (Cadavid-Rodríguez and Horan, 2014). Additionally, Liu et al. (2018) conducted an economic analysis for a full-scale waste-derived VFAs production plant, which uses sewage sludge as raw material. Their results indicate that the net profit of bio-based VFAs production is 2.5 times higher than bio-methanation.

In conclusion, considering FSF has higher organic contents than primary sludge, fermenting FSF and recycling the produced VFAs as additional carbon sources for biological nutrient removal in wastewater treatment might be possible and potentially profitable.

1.2. Problem statement

The above studies indicated that the application of FSF-derived VFAs as an additional carbon source for BNR might be feasible. WWTP Aarle-Rixtel built a pilot plant for the acidogenic fermentation of FSF. The pilot plant was operated until the end of 2021. A considerable conversion was achieved in this pilot plant. The concentration of VFAs in the product (fermented FSF) could reach 4g/L (approximately 6 g sCOD /L). The details of this pilot plant will be shown in section 3.2.

The fermented FSF (fFSF) produced at WWTP Aarle-Rixtel was regarded as an additional carbon source for activated sludge system and was planned to be used to enhance BNR in the future. However, the property of fFSF produced at WWTP Aarle-Rixtel has not been thoroughly studied yet. The extent of its contribution to BNR has also not been validated so far. Therefore, it is necessary to experimentally test the ability of fFSF to enhance BNR and to study the biodegradability to determine its effect on activated sludge system.

Furthermore, there are still some urgent issues for fFSF that need to be addressed. The produced VFAs in fFSF also contain other ions and cellulose fibers. Dosing the mixture as carbon source without downstream processing may cause the following problems.

1. fFSF contains nutrients and high organic content besides VFAs. The impurities in fFSF may increase the load of activated sludge tank (AST), posing a threat to effluent quality.
2. Only part of volatile solids can be converted to VFAs during the fermentation process (Ros et al., 2020), which means fFSF is still rich in cellulose. It is unknown whether the partly fermented cellulose could be completely biodegraded in activated sludge tank.
3. Residual cellulose fibers have poor settling performance, which may contribute to sludge bulking.

To overcome these obstacles, a proper downstream processing technology for fFSF is necessary. As waste-derived VFAs production is an emerging field, there is no universal downstream processing scheme to date. Previous research uses filtration to remove almost all remaining solids, and only

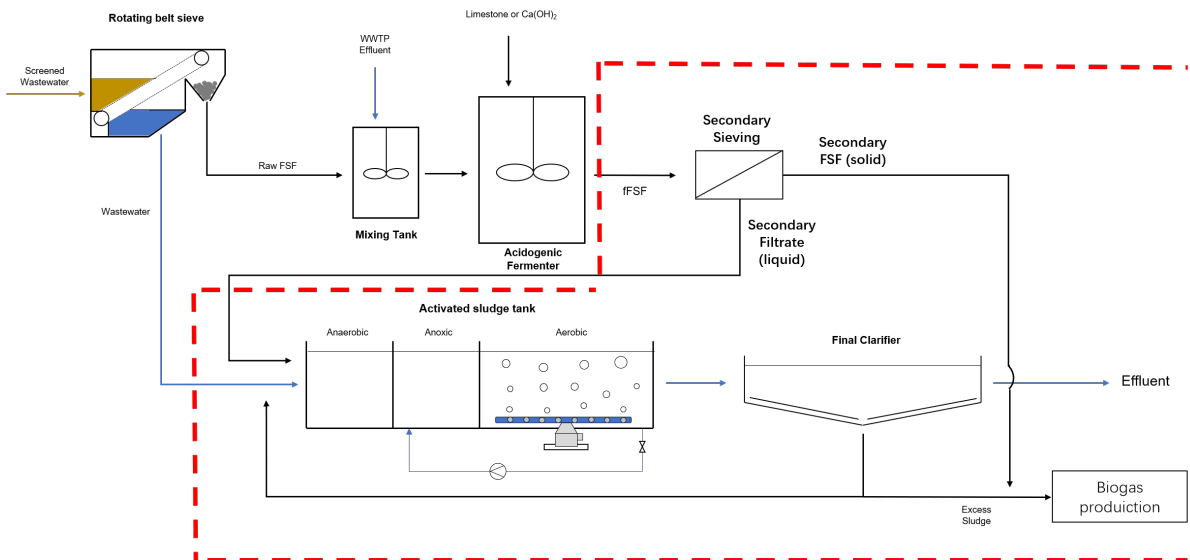


Figure 1.1: Process flow scheme of the FSF-derived VFAs fermentation and secondary sieving as downstream treatment. After bar screens, the wastewater influent could be treated by rotating belt sieve. The solid waste: Raw FSF is mixed with the effluent of this WWTP and fermented in a acidogenic fermenter. Limestone or $\text{Ca}(\text{OH})_2$ is used to maintain a slightly acidic conditions. The product of acidogenic fermenter is fFSF, which is then downstream processed by secondary sieving.

adds the liquid fraction into activated sludge tanks (Liu et al., 2018). In addition, membrane separation was used to concentrate VFAs if the fermentation liquid has low C:N or C:P ratios (Aktij et al., 2020). These technologies could alleviate the previously mentioned problems, but the operation cost also simultaneously increases. According to the observation of Oosterhuis et al. (2019), solid substrates can also be partly biodegraded in activated sludge system. It seems that removing large solid particles by sieving and retaining some small particles could increase the total available BOD for BNR. Simultaneously, the separated solids can be used for other applications such as biogas production. Therefore, using sieving as a downstream technology for fFSF might be able to both reduce operating costs and increase the total available BOD. Based on this assumption, the following flow diagram can be drawn. The focus of this thesis is the part enclosed by the red dashed line.

It is necessary here to clarify exactly the meaning of each terminology. "Raw FSF" and "FSF" referred to the organic solids from fine mesh sieving. The effluent of the fermentation tank is called "fFSF". Throughout this thesis, the "fine sieve" after the fermentation tank is referred to as "secondary sieving". The solids rejected are called "secondary FSF", and the liquid fraction is named "secondary filtrate". The term 'FSF-derived carbon sources' will be used to refer to both fFSF and secondary filtrate.

To bridge the knowledge gap between fFSF production and practical application, the main objective of this thesis is to evaluate the feasibility of using secondary sieving as a downstream treatment for fFSF and to investigate the biodegradability and BNR performance of fFSF and its downstream products.

1.3. Research questions

As stated in the problem statement, further downstream processing and research on its properties are required to apply fFSF in full-scale WWTPs. This thesis will focus on the following questions:

1. What are the solids content and VFAs composition of fFSF and downstream products of secondary sieving (secondary FSF & filtrate)?
2. What is the aerobic biodegradability of fFSF and secondary filtrate based on biochemical oxygen demand? How is the solids load of activated sludge tank affected by the use of FSF-derived VFAs?
3. What is the anaerobic biodegradability of fFSF and secondary FSF based on biomethane potential? Are there any material recovery routes for the cellulose fibers after acidogenic fermentation?
4. What are the effects of P release and denitrification from fFSF and secondary filtrate as additional carbon sources? What are the advantages and disadvantages compared to other conventional carbon sources?
5. By comparing the biodegradability and BNR performance of fFSF and secondary filtrate, what is potential of the proposed downstream processing scheme?

To answer these questions, several analyses were performed in this thesis. Solids content was determined by thermogravimetric analysis. VFAs composition was measured by gas chromatography (GC). Aerobic and anaerobic biodegradability are evaluated based on biochemical oxygen demand (BOD) and biomethane potential (BMP), respectively. The effects of P-release and denitrification were measured by batch activated sludge activity tests. The procedures to perform these measurements and experiments will be explicitly described in chapter 3. The answers to these questions could improve our understanding of FSF-derived carbon sources and provide data for future improvements in VFAs production and their application for BNR.

2

Literature review

In this chapter, background knowledge and previous studies related to this thesis are presented. Section 2.1 provides an introduction to the principle and technology used for fine sieving. Moreover, the pros and cons of fine sieving and other primary treatment technology are discussed in this section. Section 2.2 introduces some basic physiochemical properties and an overview of FSE. Section 2.3 gives a background of the basic principles of the biological nutrient removal process, including biological nitrogen removal and enhanced biological phosphorus removal (EBPR). This section also presents a summary of conventional carbon sources used in the BNR process. In the last section of this chapter, the studies on the production of VFAs from waste materials are reviewed. The factors affecting the waste-derived VFAs are also briefly discussed. In addition to waste-derived VFAs production, existing downstream treatment and BNR performance of waste-derived VFAs are presented at the end.

2.1. Fine sieves for wastewater primary treatment

Primary treatment is a physical process, which aims to remove a part of organic matter and suspended solids (SS) from wastewater. According to EUR-Lex (1991), primary treatment process should remove at least 20% of BOD₅ and 50% of SS from the influent. Sedimentation is the most common technology for primary treatment at moment. However, the BOD₅ and SS removal efficiency are usually unable to achieve the European standard at high overflow rates (Misund et al., 2004). The unsatisfied removal efficiency is usually caused by small particle size and morphology (Rusten and Ødegaard, 2006). To increase the settling performance, metal salts can be dosed to induce coagulation and precipitation. Although the removal rate can be increased by chemical dosage, the operating cost will inevitably increase as well. The Norwegian State Pollution Control Agency innovatively explored the possibilities of other technologies for primary wastewater treatment, and their results pointed out that fine mesh sieving could be a suitable and promising technology (Rusten and Ødegaard, 2006).

Fine sieving and primary sedimentation have their own advantages and disadvantages compared to each other. The pressure drop and energy loss of fine sieving are larger than that of traditional sedimentation tanks, but its retention time and required space are considerably smaller than that of sedimentation tanks. Based on a field study on WWTP Blaricum, the cost of primary treatment could be reduced by 40 % by sieving influent (Ruiken et al., 2013).

Until now, there are different types of fine mesh sieves equipment on the market. For example,

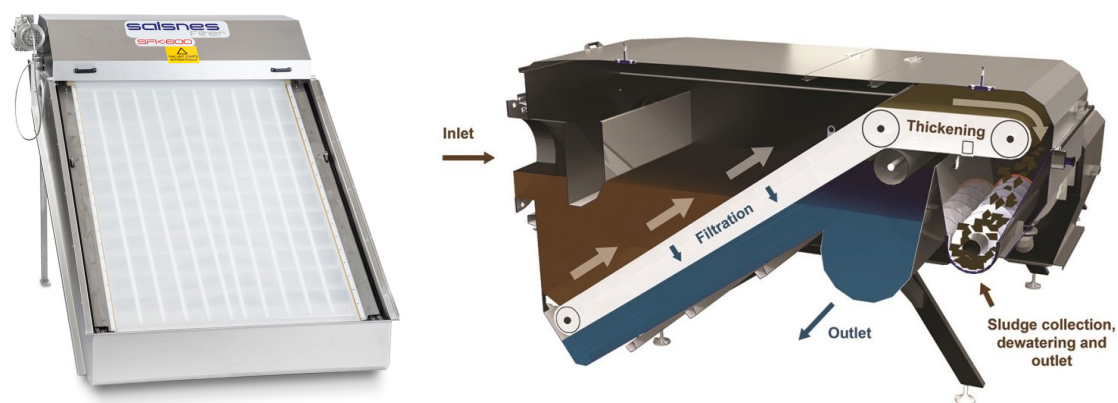


Figure 2.1: A rotating belt filter widely used in wastewater treatment. (Left) The appearance of a SFK-600 rotating belt filter. (Right) The section view of a SF-2000 rotating belt filter (reprinted from Salsnes (2022)).

stationary sieves, rotating belt sieves and rotating drum sieves. The SS removal efficiency of sieving is strongly related to mesh size and sieve rate (Rusten and Ødegaard, 2006). Rotating belt sieves with a fine mesh size $< 350 \mu\text{m}$ have been widely used in many countries. Fig 2.1 shows the principle of a rotating belt sieve (Salsnes, Norway). Once wastewater passes through the sieve, the solid waste will be blocked by the fine sieve. The sieve will rotate on the belt and transfer the solid waste to the other side. This device also has built-in solids thickening and dewatering units, which allows for continuous solids removal.

2.2. Characterization of fine sieved fraction

FSF is a solid organic waste similar to primary sludge, while the detailed compositions are different. As shown in Fig 2.2, raw FSF is brownish fiber aggregate. These fibers usually have a very high aspect ratio. The length may vary from $100 - 10000 \mu\text{m}$ and the width is usually around $10 - 50 \mu\text{m}$.

FSF is a highly heterogeneous material, therefore, it is difficult to accurately measure different characteristics. According to thermographic studies, 84 % of the organic mass (79 % of the overall mass) is made up of cellulose, and the percentage of inorganic fraction in FSF is 6% (Rusten and Ødegaard, 2006). The dry solids (DS) contents of FSF obtained from Norwegian WWTPs are ranging from 13.6 - 36.9 % (mean value = 27.3 %), and the total COD values are around $322 \text{ g O}_2/\text{L}$ (Paulsrud et al., 2014). One of the most prominent features of FSF compared to primary sludge is the high VS/TS ratio. According to Ghasimi et al. (2016), FSF can reach a VS/TS value higher than 90%; while the VS/TS value of primary sludge is only around 70 - 80 % (Odirile et al., 2021). Higher VS/TS ratio results in higher methane potential. Consequently, FSF is also very competitive for biogas production (Paulsrud et al., 2014).

2.3. Biological nutrient removal

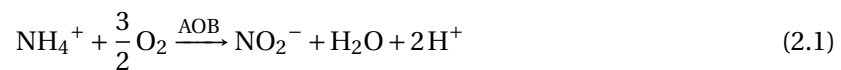
2.3.1. Biological nitrogen removal

Microorganisms can convert nitrate or nitrite into nitrogen via different biochemical reaction pathways. Biological nitrogen removal in AST is mainly contributed by heterotrophic microorganisms. Heterotrophic microorganisms are able to remove nitrogen via a consecutive process, which consists nitrification and denitrification. Nitrification is the biological oxidation of ammonia to nitrate. The nitrification process takes place in two steps under aerobic conditions, which are separately

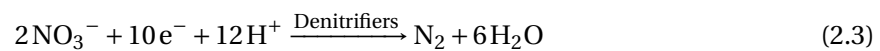


Figure 2.2: (Left) A picture of raw FSF (Ghasimi et al., 2016). (Right) Scanning electron microscopic picture of raw FSF from WWTP Blaricum (Ghasimi et al., 2015).

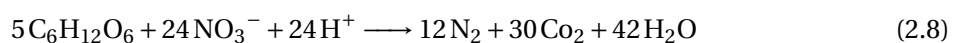
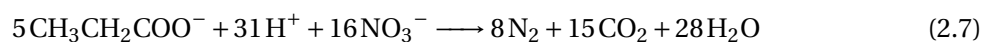
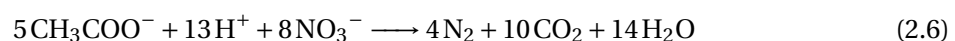
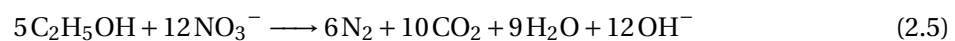
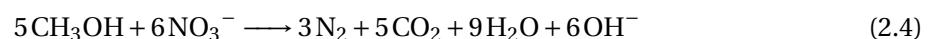
achieved by ammonia oxidizing bacteria (AOB) and nitrite oxidizing bacteria (NOB). The first step is the oxidation of ammonia to nitrite and the second step is the oxidation of nitrite to nitrate. The nitrification reactions are shown in Equation 2.1 and 2.2.



Contrary to nitrification, denitrification occurs in anoxic environments, where oxygen is limited. Once heterotrophic denitrifiers could not uptake enough oxygen from the environment, they will utilize external carbon source from wastewater as electron donor and nitrate as electron acceptor. Here, nitrate is converted to nitrogen gas. The general reaction is shown in Equation 2.3.



As shown in Equation 2.3, electron donors are required for denitrification process. Denitrifiers could utilize soluble carbon sources, for instance: alcohols, sugars and VFAs. The denitrification equation can be further written as following equations when different carbon sources are used (Elefsiniotis and Li, 2006; Pang and Wang, 2021).



Since the nitrogen in wastewater influent is mainly in the form of ammonia, nitrification is a prerequisite for denitrification. Therefore, Both nitrification and denitrification are indispensable for biological nitrogen removal.

2.3.2. Enhanced biological phosphorus removal

Phosphorus is an important component of all living organisms, and the organisms in activated sludge are no exception. For a conventional activated sludge system with only aerobic tank, the sludge can uptake and incorporate about 0.02 mg P / mg VSS, which leads to a net removal of about 15-25% of the influent P (Henze et al., 2008). Nevertheless, this removal percentage is far below the increasingly stringent effluent quality standard (EUR-Lex, 1991). To prevent the wastewater sector from discharging excessive phosphorus to nature, many phosphorus removal technologies have been proposed, such as enhanced biological phosphorus removal (EBPR).

EBPR refers to the biological uptake and removal of phosphorus that exceeds the amount removed by completely aerobic activated sludge systems. The EBPR system consists of an anaerobic tank followed by an anoxic tank and an aerobic tank. By applying this EBPR system, the amount of P incorporated into the sludge mass is increased from 0.02 mg $\text{PO}_4\text{-P}$ / mg VSS to roughly 0.06-0.15 mg $\text{PO}_4\text{-P}$ / mg VSS (Henze et al., 2008).

The higher phosphate removal of EBPR system is because of phosphate accumulating organisms (PAOs). PAOs are a group of heterotrophic bacteria that can effectively remove phosphorus by accumulating phosphate within their cells as polyphosphate (poly-P), which is not possible for ordinary heterotrophic bacteria in conventional activated sludge systems (Seviour et al., 2003). Figure 2.3 presents a simplified process flow scheme and biochemical model of EBPR process. After primary treatment, the wastewater will first pass through an anaerobic tank. Under anaerobic conditions, the PAOs can uptake carbon in wastewater (usually VFAs) and store the carbon within PAOs' cell in the form of poly- β -hydroxyalkanoates (PHAs). The energy and materials for forming PHAs originate from polyphosphate degradation, glycogen degradation, and orthophosphate release. Since OHOs cannot utilize the carbon source in wastewater without electron acceptors, the presence of the anaerobic tank gives PAOs higher selective advantages than OHOs. Under subsequent aerobic (and anoxic if denitrification is involved) conditions, the stored PHA is consumed to provide energy for phosphate uptake and poly-P synthesis. As a consequence of the growth of PAOs, more phosphorus is stored in the cells as poly-P and eventually removed from wastewater by sludge sedimentation (Henze et al., 2008).

2.3.3. Carbon source for biological nutrient removal

As illustrated in section 2.3.1 and 2.3.2, denitrifiers and PAOs are involved in heterotrophic organisms. Hence, the biological nutrient removal process and EBPR process both need carbon sources as electron donors. The carbon sources for biological nutrient removal can either naturally originate from wastewater itself or can be artificially dosed at WWTP. The former is also known as internal carbon sources and the later is referred to as external (or additional) carbon sources.

Internal carbon sources for the biological nitrogen removal and EBPR processes are typically derived from organics in domestic wastewater, for example, cellulose, proteins and lipids. During transport in the sewage system, these large organic molecules are partly degraded into soluble organic substances, which could be uptaken by microorganisms. However, some WWTPs have limited influent COD/N value (from 3:1 to 10:1), and the carbon sources in wastewater cannot satisfy the demand of biological nitrogen removal and EBPR process (Orhon et al., 1997; Phanwilai et al., 2020).

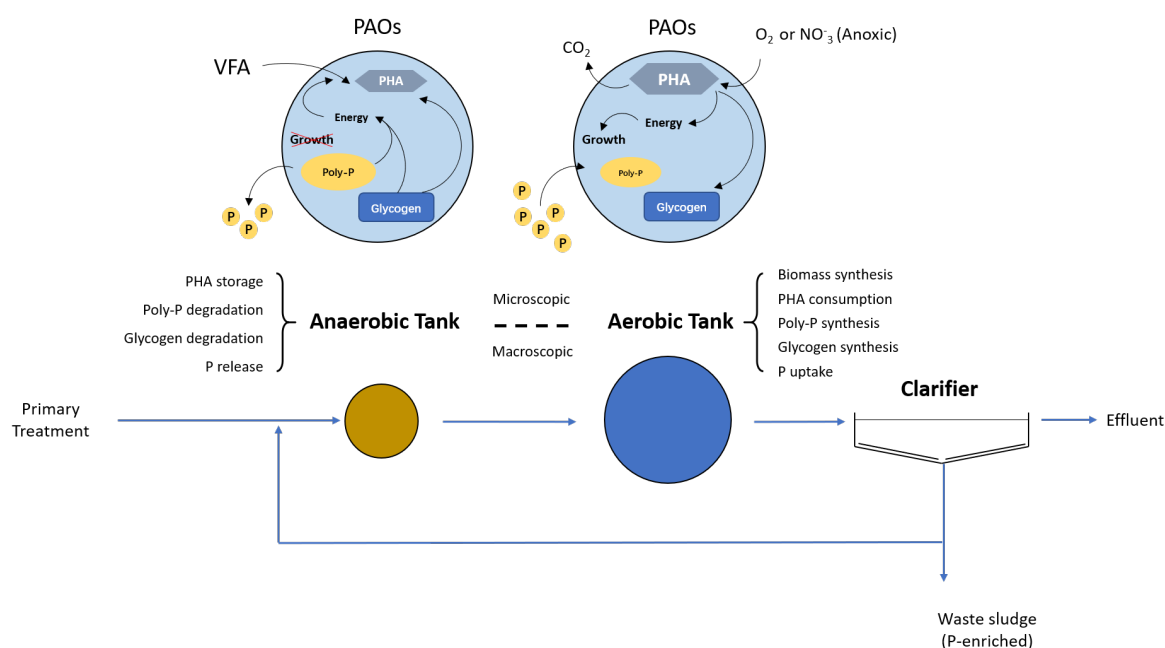


Figure 2.3: Process flow scheme and simplified biochemical model of EBPR process (adapted from Tchobanoglus et al. (2004) and Henze et al. (2008)).

To solve the problem of insufficient carbon sources, researchers proposed and validated that dosing additional carbon sources directly at anaerobic and anoxic stages can effectively improve the BNR performance (Isaacs and Henze, 1995; Isaacs et al., 1994). A large variety of external carbon sources could be dosed into anaerobic or anoxic tank to increase BNR performance (USEPA, 2013). Table 2.1 listed some carbon sources, including pure chemicals and commercial products. The most commonly used carbon sources on market are alcohols, VFAs and commercial mixed carbon sources.

Table 2.1: Possible carbon sources for improving BNR and respective properties(adapted from USEPA (2013)).

		Methanol	Ethanol	MicroC-g™	MicroC-glycerin™	56% Acetic Acid	30% sodium acetate
COD	mg/L	1,200,000	1,650,000	670,000	1,016,000	577,000	222,480
Bulk Density	kg/L	0.79	0.79	1.22	1.19	1.09	1.17
Yield	g COD/g COD	0.41	0.55	0.6	0.55	0.53	0.53
Total COD/N		4.82	6.36	6.45	6.36	6.09	6.09
Total dose	L C-source/ kg N removal	4.01	3.84	9.60	6.43	9.93	25.78

2.4. Waste-derived VFAs for improving BNR performance

2.4.1. Factors influencing the fermentation of VFAs

Most of VFAs are synthetically produced via carbonylation reaction in chemical plants (Cheung et al., 2000). Nevertheless, VFAs could also be fermented from waste materials, which is more sustainable than petrochemical production. To date, several studies have investigated how to ferment VFAs from organic waste and use these VFAs for BNR. Table 2.2 lists some waste-derived VFAs production technologies. As shown in this table, not only solid waste from the wastewater treatment process can be used for VFAs production, but also organic waste from the food industry can be used. The high raw materials availability allows waste-derived VFAs to be widely produced.

Notwithstanding the wide range of waste sources, the composition of each waste substantially varies from others, which results in different processing technologies and parameters. Many factors could affect the yield of the VFAs fermentation process, such as reactor configurations, temperature, pH, and organic loading rate (OLR). Although the sources of waste and processes are different, it is still possible to conclude some general trends from these studies. The remainder of this section will summarize the influences of operation conditions on the waste-derived VFAs fermentation process.

1. Reactor configurations

Due to the large amount of solids in the waste, the majority of VFAs production pilot plants are operated in batch or semi-continuous (regular addition of organic waste) mode. The fermentation can be carried out in batch reactors, sequential batch reactors, leach-bed reactors and so on. Due to the constraints of experiment design, the research on quantitatively comparing the pros and cons of different reactors and operation modes is still limited.

2. Temperature

In most of the processes, the fermentation temperature is controlled under mesophilic conditions. Zhang et al. (2009) also tried to ferment surplus activated sludge at thermophilic conditions and compared it with mesophilic conditions. Their results indicate that higher temperatures could slightly increase the optimal yield of VFAs; however, the increase in yield could not compensate for the cost of heat.

3. pH

pH also plays an important role during the fermentation process. Almost all studies controlled pH between 5.0 and 9.0. When pH is lower than 5.0, acidogenesis bacteria are inhibited, and alcohol is produced instead of VFAs; if pH is higher than 9.0, VFAs will be converted into corresponding salts and ammonia will be released during the fermentation process (Cadavid-Rodríguez and Horan, 2014). Researchers have reached a consensus on the approximate VFAs fermentation pH; however, a controversy has arisen on the specific optimal pH. According to Table 2.2, some studies revealed that the highest VFAs yields were achieved at pH 6.0, while others claimed that the highest yields were reached at weak alkaline environments (around pH 8.0 - 9.0). This contradiction might be due to the trade-off between hydrolysis and acidification steps. Ma et al. (2016) pointed out that higher pH is in favor of the hydrolysis process, while neutral and slightly acidic pH is appropriate for acidification process. Besides, the composition and degree of polymerization of organic wastes are different, hence, resulting in different optimal pH.

4. Organic loading rate

Similar to the impact of pH, OLR could also affect the waste-derived VFAs fermentation from two opposite perspectives. According to Jiang et al. (2013), the sCOD in the fermentation product increases as OLR increases, but the yield of VFAs decreased. Therefore if the main objective of the product is a higher sCOD, the OLR should be increased. While if waste reduction is a priority, the OLR should be reduced to achieve a higher conversion rate.

5. Hydraulic retention time

Generally, increasing HRT can effectively increase the contact time between microorganisms and substrates, and facilitate the production of VFAs (Bengtsson et al., 2008). However, this effect of HRT on VFAs production is not linear. For example, as the HRT increased from 4 to 12 hours, the production of VFA from dairy wastewater approximately doubled, while a further rise from 16 to 24 hours only slightly enhanced the VFA production (Fang and Yu, 2000).

In addition to VFAs yield, the above-mentioned factors could also influence the composition of VFAs. For example, Jiang et al. (2013) found that the percentage of acetic acid increased as OLR increased, while the propionic acid was predominant when OLR was low; Bengtsson et al. (2008) indicated that higher HRT could facilitate the production of propionic acid.

In conclusion, many factors could influence the production of VFAs, and the determination of an optimal set of parameters for a specific type of waste should be determined by experiment case by case. The process of FSF fermentation will be explained in section 3.2.

2.4.2. Downstream processing of waste-derived VFAs

The fermentation of VFAs from various wastes has been comparatively well understood. However, the applications of waste-derived VFAs and their respective downstream processing technologies have not been thoroughly studied. VFAs are versatile and can be used in many fields. To date, the waste-derived VFAs have been tested to produce polyhydroxyalkanoates (PHAs), bio-energy and used as carbon sources for BNR (Kleerebezem et al., 2015). Since this study focuses on the applications of BNR, the downstream processing described in this section is mainly for BNR.

Downstream processing could substantially increase the grade of VFAs. If solid wastes are used for VFAs production, the product of the acidogenic process is a mixture of VFAs, cellulose, biomass, nutrients, and other pollutants. Directly using this mixture might be detrimental to activated sludge tanks. For instance, the solid residuals in the product can significantly increase the OLR and solids load and may contribute to failures of the whole system (Palm, 1982). Therefore, the downstream processing primarily aims to separate solids residuals from produced VFAs.

Previously published studies on downstream processing are limited to lab-scale. As shown in Table 2.2, current downstream processing of waste-derived VFAs for BNR mainly includes membrane separation and centrifugation & filtration (C&F). Membrane technologies are scalable and can effectively concentrate the produced VFAs. However, the acidogenic fermentation product contains other organic solids like biomass, which can contribute to membrane fouling and other adverse effects (Le-Clech et al., 2006). As a consequence, membrane is difficult to use for continuous production and requires frequent cleaning. As for C&F technology, the energy consumption and cost make C&F available also only in lab-scale.

2.4.3. Performance of waste-derived VFAs in BNR

The research on applying waste-derived VFAs for BNR purpose are much less studied than the production of VFAs. Previous studies mostly dosed purified VFAs (solids reduced) in anaerobic and anoxic tanks. For instance, Li et al. (2016) fermented sludge liquor and removed the residual solids with C&F. They achieved 50% increase in denitrification compared to blank. Soares et al. (2010) fermented VFAs from brewery effluent and achieved a denitrification rate of 26.3 mg NO₃-N / (g VS · h). Furthermore, Soares et al. (2010) also apply the VFAs in EBPR culture and increased the P-release by 77.8% percent. Several research showed that applying waste-derived VFA produced better EBPR results than pure acetate, which is probably because of the synergistic effects of other organic compounds (Tong and Chen, 2007; Zheng et al., 2010).

Although the downstream processing is not fully established, it can be concluded from these results that the application of waste-derived VFAs for BNR purpose is promising.

Table 2.2: Various waste-derived VFAs production technologies and their application in BNR.

Waste Sources	Pretreatment	Anaerobic Fermentation		Product properties		Downstream processing		Application in Biological nutrient removal		Reference
Simulated food waste	N.A.	Batch fermentation reactor Temp = 35 °C HRT = 5 days pH = 6.0	Yield VFAs = 0.316 g VFAs / g VSfed sCOD = 39.46 g/L		Centrifugation & filtration	Nitrogen removal rate around 70% at C/N = 3.6	N.A.	Jiang et al. (2013) Zhang et al. (2016)		
Thickened surplus activated sludge	N.A.	N.A.	N.A.		Mechanical disintegration Integration time = 2-5 min Energy input = 2300 - 6200 KJ / Kg TS	Dis- 23.1 mg NO ₃ -N/(g VS * h)	44.4% increasing P-release compared to blank	Soares et al. (2010)		
Brewery effluent	N.A.	N.A.	Final sCOD = 680 mg/L		N.A.	26.3 mg NO ₃ -N/(g VS * h)	77.8% increasing P-release compared to blank	Soares et al. (2010)		
Surplus activated sludge	Settling	Batch fermentation reactor Temp = 35 °C HRT = 5 days pH = 9.0	VFAs Yield = 0.298 g VFA-COD / g VSS		N.A.	N.A.	N.A.	Zhang et al. (2009)		
Surplus activated sludge	Settling	Batch fermentation reactor Temp = 55 °C HRT = 9 days pH = 8.0	VFAs Yield = 0.368 g VFA-COD / g VSS		N.A.	N.A.	N.A.	Zhang et al. (2009)		
Municipal solid waste	N.A.	Plug flow reactor Temp = 37 °C HRT = 6 days	Final VFAs concentration = 23.1 g/L		N.A.	N.A.	N.A.	Sans et al. (1995)		
Primary Sludge	N.A.	Sequential batch reactor Temp = 30 °C	Unknown product properties due to simultaneous digestion & denitrification		N.A.	6.4 mg N / (g VSS * h)	N.A.	Cao et al. (2020)		
Sludge liquor	High-pressure homogenization	Sequential batch reactor Temp = 30 °C HRT = 3 days	1936.0 mg VFAs/L		Centrifugation & filtration	51% increasing denitrification compared to blank	N.A.	Li et al. (2016)		
Wastewater screenings (6 mm mesh size)	N.A.	Leach-bed reactor re-circulation ratio 8 BV/day pH = 6.0	264 g VFA / kg dry screenings Mostly Propionic acid.		N.A.	N.A.	N.A.	Cadavid-Rodriguez and Horan (2014)		
Organic municipal solid wastes	N.A.	Leach-bed reactor recirculation flow rate = 6.3 L/d Temp = 30 °C pH = 5.6	Acetate fraction increased from 24.7 % to 43.0%		Membrane contactor	N.A.	N.A.	Yesil et al. (2014)		
Fine sieved fraction	N.A.	Batch reactor Temp = 37 °C pH = 9	521 mg VFA-COD / g VSS 1% propionic acid of total VFAs		Centrifugation & filtration	N.A.	N.A.	Da Ros et al. (2020)		

3

Methodology

This chapter provides a detailed description of the methods used in this thesis. The general procedures of experiments and the parameters are listed in this Chapter. More specific experimental designs could be found in the Appendix.

Section 3.1 defines the framework of the research process, and section 3.2 describes the sources of the samples used in this study. The remaining section in this chapter corresponds to the research questions listed in Section 1.3, respectively. Section 3.3 and 3.4 focus on the first research question and characterize the morphology, solid contents and physiochemical properties of different samples. Section 3.5 mainly explained the method to measure BOD, which aims to evaluate the aerobic biodegradability. Section 3.6 is set for anaerobic biodegradability, which mainly presents the procedure and parameters of performing the biomethane potential test. Section 4.4 presents the method for measuring biological nutrient removal by using a batch reactor. The batch test is divided into two parts: nitrogen removal and phosphate release. The last question of this study is not related to a specific method, but will be a comprehensive evaluation of the results measured by the above methods.

3.1. Process flow diagram

Depending on different usages, there can be many possibilities for the downstream processing of fFSF. Each of these downstream processing technologies has unique pros and cons. However, this study mainly investigated the effect of secondary sieving as subsequent treatment. Their advantages and disadvantages will be covered in the subsequent Results and Discussion chapters. To test the effect of the secondary sieving, two process flow scenarios were proposed.

3.1.1. Scenario 1

In this thesis, the produced VFAs are designed to be used as additional carbon sources for BNR. Therefore, a very simple idea is to directly dose the fFSF into an activated sludge tank. As the fFSF is not treated before dosing into activated sludge tank, this scenario will be a reference to compare the impact of downstream processing. The process flow scheme is shown in Figure 3.1.

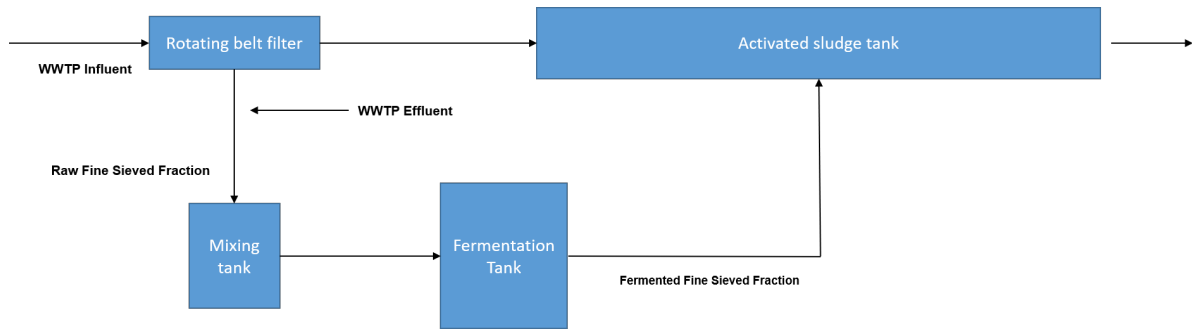


Figure 3.1: Process scheme of scenario 1: Reference scenario without downstream processing.

3.1.2. Scenario 2

In scenario 2, a secondary sieve is placed after the fermentation tank. The secondary filtrate is dosed into activated sludge tanks as a substitution for fFSF. The secondary FSF is fed into the anaerobic digester for further biogas production.

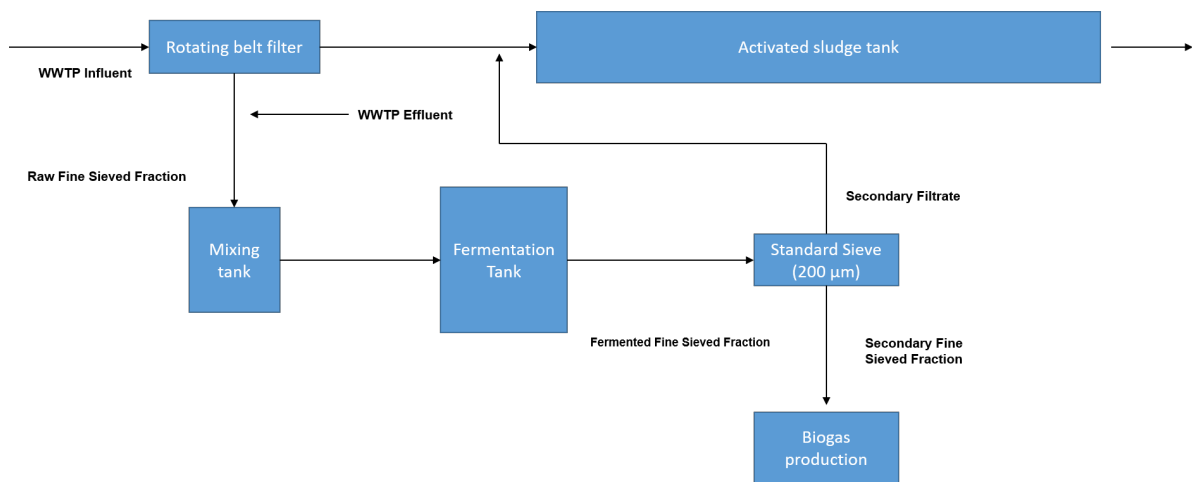


Figure 3.2: Process scheme of scenario 2: scenario with a secondary sieve as downstream processing technology.

3.2. Sample and inoculum collection

Two scenarios were proposed to utilize the produced fFSF. In order to assess the feasibility of secondary sieving, raw FSF, fFSF, secondary filtrate, and secondary FSF were comprehensively studied in this research.

The fFSF samples used in this research were collected from a FSF fermentation pilot plant at WWTP Aarle-Rixtel (Aarle-Rixtel, The Netherlands). The process flow diagram of this pilot plant is shown in Figure 3.3. The whole pilot process was operated semi-continuously. A 350 µm mesh size rotating belt filter (Salsnes Filter SA, Norway) is placed before the activated sludge tank to replace primary sedimentation tank. Dewatered raw FSF was manually added into a mixing tank. The effluent of WWTP Aarle-Rixtel was added into the mixing tank to dilute the raw FSF. The pH in the VFAs fermenter was controlled at 5.7 by adding CaCO_3 or Ca(OH)_2 . The hydraulic retention time (HRT) of the mixing tank and VFAs fermenters are 1 day and 2 days, respectively. The fermenter was operated under mesophilic conditions (around 27 °C). Unfortunately, the pilot fermenter at WWTP Aarle-Rixtel was shut down. Therefore, the FSF samples used in the study were collected in late

December 2021 and stored at $-18\text{ }^{\circ}\text{C}$ until the end of this study.

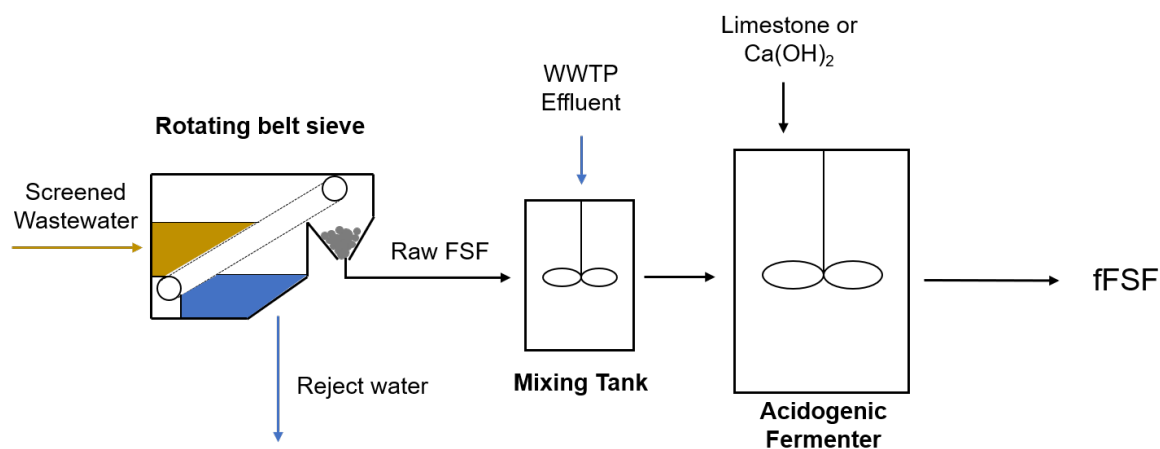


Figure 3.3: Process flow diagram of the FSF fermentation pilot plant at WWTP Aarle-Rixtel.

The raw FSF sample was collected at WWTP Beemster (Beemster, The Netherlands). In principle, raw FSF and fFSF should be sampled at the same WWTP; however, the rotating belt sieve at WWTP Aarle-Rixtel was under maintenance during this research. Therefore, WWTP Beemster, which has the same configuration as WWTP Aarle-Rixtel, was selected. The collected raw FSF samples were stored at $4\text{ }^{\circ}\text{C}$.

The secondary filtrate and secondary FSF were collected by filtering the fFSF through a $200\text{ }\mu\text{m}$ standard sieve. Secondary filtrate is the liquid fraction passing through the standard sieve, while secondary FSF is the solid remaining on the sieve. During the sieving process, the screen area was evenly used to prevent the interference of the filter cake.

In addition to the FSF-related samples, primary sludge, anaerobic digestate and activated sludge were also used in this thesis. They were taken from WWTP Harnaspolder, and stored at $4\text{ }^{\circ}\text{C}$.

3.3. Morphology of samples

Morphology was identified using a digital microscope VHX-5000 (Keyence, Belgium), which is equipped with a VH-Z20UR universal zoom lens and a VH-Z100UR universal zoom lens (Keyence, Belgium). By changing and zooming the lenses, this microscope can achieve a magnification from 20x to 1000x. fFSF and secondary filtrate were observed with this microscope. Prior to observation, samples were diluted 10 times for better visualization.

3.4. Physico-chemical analysis

In order to understand the properties of fFSF and its changes during downstream processing and applications, different physicochemical parameters were analyzed in this research. Table 3.1 briefly lists the parameters measured and equipment used in this research. The detailed procedures of anion and VFAs measurement will be explained in the remainder of this section.

Table 3.1: Summary of physico-chemical parameters and respective analyzing equipment

Parameter	Equipment
Total COD	HACH Lange LCK914 & DR 3900 (HACH, US)
Soluble COD	HACH Lange LCK914 & DR 3900 (HACH, US) & Chromafil®Xtra PES-45/25 0.45 µm (Macherey-Nagel, Germany)
Nitrate	HACH Lange LCK 340 & DR 3900 (HACH, US) & Chromafil®Xtra PES-45/25 0.45 µm (Macherey-Nagel, Germany) Ion chromatography (Metrohm, Switzerland)
Ortho-Phosphate	HACH Lange LCK348 & DR 3900 (HACH, US) & Chromafil®Xtra PES-45/25 0.45 µm (Macherey-Nagel, Germany) Ion chromatography (Metrohm, Switzerland)
Dissolved Oxygen	Multimeter Multi 3630 IDS (WTW, Germany) & FDO® Dissolved Oxygen Probe (Xylem, US)
pH	Multimeter Multi 9620 IDS (WTW, Germany) & pH probe SenTix®41 (WTW, Germany)
TS & VS	Thermogravimetric analysis
TSS & VSS	Glass Microfiber filters 0.7 µm (Whatman, Germany)
VFA	Gas Chromatography 7890A (Agilent Technologies, United States)

3.4.1. Volatile fatty acids measurement with gas chromatography

VFAs concentration was measured by gas chromatography (GC). GC 7890A with a 7693A auto-sampler (Agilent Technologies, United States) was used. The types of VFAs measured and their upper detection limits are shown in Table 3.2.

Table 3.2: Upper detection limits of VFAs using GC 7890A.

VFAs	Chemical formula	Upper limit (mg/L)	COD equivalent factor (mg COD / mg VFA)
Acetic acid	CH ₃ COOH	488.6	1.07
Propionic acid	CH ₃ CH ₂ COOH	621.7	1.51
Isobutyric acid	(CH ₃) ₂ CHCOOH	710.5	1.81
Butyric acid	CH ₃ (CH ₂) ₂ COOH	710.5	1.81
Isovaleric acid	(CH ₃) ₂ CHCH ₂ COOH	843.2	2.04
Valeric acid	CH ₃ (CH ₂) ₃ COOH	843.2	2.04
Isocaproic acid	(CH ₃) ₂ CH(CH ₂) ₂ COOH	932.1	2.21
Caproic acid	CH ₃ (CH ₂) ₄ COOH	932.1	2.21

A series of pre-treatments are required before injecting samples into the GC system. Sludge and FSF samples were centrifuged at 10,000g for 5 to 10 minutes. The supernatant after centrifuge was filtered with a 0.25 µm syringe filter. High concentration samples are then diluted with 320 mg/L pentanol. In addition, 6.67 µL of formic acid was added per mL of diluted sample. After these pre-treatment processes, VFAs concentration was measured automatically following the program. The program settings and parameters of gas chromatography are shown in Table B.1.

3.4.2. Nitrate and Phosphate Measurement

After adding a carbon source, the changes in nitrate and phosphate concentrations in wastewater can indicate the activity of denitrification and P-release processes. In this study, nitrate and phosphate concentrations were measured by both HACH test kits and ion chromatography (IC). HACH kits were mainly used to quickly determine the initial concentration for biological nutrient removal tests. The procedure of using these HACH kits was based on the official guideline (Hach, 2019, 2020). IC was used to test samples collected during the batch activity tests. Metrohm 919 auto-sampler combined 818 anion IC system was used in this study. A standard anion column Supp-5-150/4.0 was installed in this IC system. The eluent for this system is 3.2 mM Na₂CO₃ and 1 mM NaHCO₃, which run at 0.7 mL/min. Background signal is chemically and physically suppressed by Metrohm Suppressor Module (MSM) and CO₂ stripper. The MSM should be regenerated by a 150 mM H₃PO₄ solution, and rinsed with ultrapure water.

3.5. Aerobic biodegradability test

Aerobic biodegradability has been widely used to quantify the extent of biodegradation of a substance under aerobic conditions. Measuring the biological oxygen demand (BOD), and carbon dioxide consumption are typical methods for determining aerobic biodegradability (García-Depraect et al., 2022).

This thesis used BOD to represent aerobic biodegradability. This section will mainly describe the required materials and the procedure of the BOD test. The preparation of solutions and experiment procedures are adapted from APHA standard 5210B and is specifically designed for the BOD measurement with OxiTop® OC110 & C/B (WTW, Germany) (Baird et al., 2017).

OxiTop® is a BOD measuring device based on the respirometric method, which can measure the pressure change in a closed vessel (WTW, 2021). The oxygen in the vessel is consumed because of aerobic respiration and the generated carbon dioxide is absorbed by sodium hydroxide, causing a negative pressure. The BOD value can be then calculated from the pressure difference as follows (WTW, 2021):

$$BOD = \frac{M(O_2)}{R \cdot T_m} \cdot \left(\frac{V_{tot} - V_I}{V_I} + \frac{T_m}{T_0} \right) \cdot \Delta p(O_2) \quad (3.1)$$

Where:

$M(O_2)$	Molecular weight of oxygen (32000 mg/mol);
R	Gas constant (83.144 L*hPa/(mol*K));
T_0	Temperature (273.15 K);
T_m	Measuring temperature (293.15 K for BOD Test);
V_{tot}	Bottle volume (mL);
V_I	Sample volume (mL);
α	Bunsen absorption coefficient (0.03103);
$\Delta p(O_2)$	Difference of the partial oxygen pressure (hPa).



Figure 3.4: Oxitop® system for BOD measurement. Aerobic biodegradation was taken place in 250 mL Duran® bottles. These bottles were connected to Oxitop® pressure measuring heads and covered with aluminium foil to prevent the growth of algae.

3.5.1. Preparation of stock solutions

Phosphate buffer solution, magnesium sulfate solution, calcium chloride solution and ferric chloride solution should be added to the dilution water to ensure nutrients are sufficient for the growth of microorganisms. HCl and NaOH solutions were used to adjust the pH of the sample. Additionally, nitrification inhibitor solution was added to the sample to prevent the oxidation of ammonium. Control and quality check of the BOD test was performed by measuring the BOD of a standard GGA solution. The chemicals and concentrations of stock solutions are shown in Table B.2.

3.5.2. Execution of the BOD test

Five groups of BOD tests were simultaneously performed in this study. The components of each group are listed as follows:

- Blank: inoculum + medium
- Control 1: glucose-glutamic acid (GGA) solution + inoculum + medium
- Sample 1: Raw FSF + inoculum + medium

- Sample 2: fFSF + inoculum + medium
- Sample 3: Secondary filtrate + inoculum + medium

Three types of sample: Raw FSF, fFSF and secondary filtrate were tested. The blank group was set to remove the influence of seed suspension. The standard group was set to check the quality of the BOD test.

Table B.3 shows the settings of OxiTop® Controller OC110 and how each experimental group was prepared. The prepared solution were mixed and transferred to Duran® bottles. The transferred volume for each bottle is equal to the Fill. Vol. shown in Table B.3. The dissolved oxygen (DO) concentration and pH value of the mixture were checked before the test. The pH value was maintained to around 6.6 - 7.2 with acid solution or alkali solution, and the DO concentration was higher than 7.5 mg/L to maintain sufficient initial available oxygen (Baird et al., 2017).

After all experimental group solutions were transferred to Duran® bottles, 4 sodium hydroxide pellets were placed in each rubber sleeve. Rubber sleeves, OxiTop® measuring heads were then connected to the Duran® bottles. The BOD test was started with OxiTop® Controller OC110 by respectively inputting the setting parameters mentioned in Table B.3. Finally, the Duran® bottles were placed in an Innova 43 incubator shaker (Eppendorf, Germany) at 20 °C, 130 rpm.

3.5.3. Data analysis and interpretation

BOD value usually increases with time and eventually converge to an equilibrium value. The BOD value at time t could be modeled by applying first-order kinetics (Weijers, 2000).

$$BOD_t = BOD_u \cdot (1 - e^{-kt}) \quad (3.2)$$

where:

- BOD_t BOD at time t (mg/L);
- BOD_u Ultimate BOD (mg/L);
- k First-order reaction rate constant (1/d).

The aerobic biodegradability was calculated as follows:

$$D_{\text{aerobic,tot}} = \frac{BOD_{\text{tot}}}{tCOD_{\text{tot}}} \cdot 100\% \quad (3.3)$$

The aerobic biodegradability calculated here is total aerobic biodegradability, which considered the contribution of both VS and VFAs. Generally, VFAs concentration is neglectable in conventional sludge samples, and the total aerobic biodegradability could effectively reflect the degradation of solids. However, this equation could not accurately represent the biodegradability of samples with high VFAs concentration. The difference in VFAs concentrations between raw FSF and fFSF is significant. Hence, using total aerobic biodegradability may overestimate the biodegradability of fFSF. Therefore, the influence of VFAs should be subtracted from the total, and use the biodegradability of VS only to get a comparable result. In order to measure the aerobic biodegradability of VS for a given sample, it is necessary to exclude the BOD and tCOD of VS. To simplify this correction, it is assumed that the BOD of FSF samples only consisted of VS and VFAs. Therefore, the total BOD and total tCOD can be expressed as Equation 3.4 and 3.5.

$$BOD_{\text{tot}} = BOD_{\text{VS}} + BOD_{\text{VFAs}} \quad (3.4)$$

$$tCOD_{\text{tot}} = tCOD_{\text{VS}} + tCOD_{\text{VFAs}} \quad (3.5)$$

The BOD of VS could be further calculated by the following equation. The unit of BOD is changed to per gram of VS here, because it is hard to measure the volume of solid samples.

$$BOD_{\text{VS}} \left[\frac{\text{g O}_2}{\text{g VS}} \right] = \frac{BOD_{\text{tot}} \left[\frac{\text{g O}_2}{\text{L}} \right] - BOD_{\text{VFAs}} \left[\frac{\text{g O}_2}{\text{L}} \right]}{VS \left[\frac{\text{g VS}}{\text{L}} \right]} \quad (3.6)$$

The BOD and tCOD of VFAs were assumed the same and were calculated based on the VFAs concentrations c_i and respective COD equivalent factors α_i .

$$tCOD_{\text{VFAs}} = BOD_{\text{VFAs}} = \sum_{i=\text{CH}_3\text{COOH}}^{\text{C}_5\text{H}_{11}\text{COOH}} C_i \cdot \alpha_i \quad (3.7)$$

Based on equation 3.4 - 3.6, we can calculate the aerobic biodegradability for VS using the following equation.

$$D_{\text{aerobic,VS}} = \frac{BOD_{\text{VS}}}{tCOD_{\text{VS}}} \cdot 100\% \quad (3.8)$$

3.6. Anaerobic biodegradability test

Anaerobic digestion has been widely used in municipal waste sludge treatment to produce biogas. Anaerobic biodegradability reflects the ability of a substance to produce methane under anaerobic conditions (García-Depraect et al., 2022). Biomethane potential (BMP) is a significant indicator for anaerobic biodegradability of organic solids, which is expressed in N-mL CH₄ / g VS (Angelidaki et al., 2009).

The BMP test was conducted for raw FSE, fFSF and secondary FSE. Additionally, primary sludge and cellulose were also tested for comparison. This experiment was carried out using an analytical device designed for online BMP measurements at laboratory scale. The device: AMPTS II is shown in Figure 3.5. Bioprocess Control (2016) and Guo (2016) have published several experiment manuals and experiment parameters. The BMP test of this study is mainly based on these manuals.

3.6.1. Pretreatment of anaerobic digestate inoculum

As the samples were frozen for a longer period, additional anaerobic inoculum should be added. Prior to the BMP test, several pretreatments should be done on the inoculum. First, the anaerobic digestate was sieved with a 710 μm standard sieve to remove non-biomass particles. After sieving, the anaerobic digestate was incubated at 35 °C under anaerobic conditions for 5 days. This process could remove the initial substrate and methane from the anaerobic digestate, and prevent temperature disturbance during the subsequent inoculation process.



Figure 3.5: A picture of Automatic methane potential test system II (AMPTS II) (Bioprocess Control, Sweden) used in this experiment. The setup is divided into three parts. The bottom part is a sample incubation unit, which consists of a water bath and Duran® bottle reactors. The reactors were sealed with AMPTS mixers. The middle part is a CO₂ absorption unit, which is filled with 3 mol/L NaOH. The top part is a flow cell array & DAQ unit, which is connected to a PC for data collection.

3.6.2. Execution of the BMP test

The BMP test was performed in triplicate. The anaerobic digestion was taken place in 500 mL Duran® bottles. Six groups and 18 bottles were used in this test. The components of each group are listed as follows:

- Blank: inoculum + medium
- Control 1: Cellulose + inoculum + medium
- Control 2: Primary sludge+ inoculum + medium
- Sample 1: Raw FSF + inoculum + medium
- Sample 2: fFSF + inoculum + medium
- Sample 3: Secondary FSF + inoculum + medium

To begin the measurement, standard solutions should be prepared. Phosphate buffer was added to maintain the pH of the media. Macro-nutrients and micro-nutrients solution were added to prevent nutrient deficiency. The preparation and dosage of these standard solutions can be found in Table B.5.

Generally, the sample volume and sludge volume were determined by volatile solids concentration and were calculated based on Equation 3.9 and 3.10.

$$\frac{V_{\text{sub}} \cdot VS_{\text{sub}}}{V_{\text{sludge}} \cdot VS_{\text{sludge}}} = 0.5 \quad (3.9)$$

$$V_{\text{sub}} + V_{\text{sludge}} + V_{\text{nutrients}} + V_{\text{buffer}} = 0.4L \quad (3.10)$$

After adding the calculated amount of inoculum and substrate, the nutrients solutions, and phosphate buffer solutions were added. The total volume in each bottle was kept at 0.4 L. Initial pH values were measured and adjusted to 7.0 with NaOH or HCl solution. The Duran® bottles were sealed with rubber lids and AMPTS stirrers. All bottles were flushed with nitrogen to achieve anaerobic conditions. The detailed parameters of BMP test are shown in Table B.4.

Finally, all Duran® bottles were placed in a 35 °C water bath to maintain mesophilic environments. Tygon® tubing was used to connect all units to avoid methane diffusion.

3.6.3. Data analysis and interpretation

Anaerobic biodegradability was calculated based on the measured BMP and tCOD of substrates. The calculation is highly similar to aerobic biodegradability. The same assumptions were made in the BMP measurements as for the BOD test. The BMP directly measured from the BMP test is defined as total BMP here, which includes both VS and VFAs.

$$BMP_{VS} = BMP_{\text{tot}} - BMP_{\text{VFAs}} \quad (3.11)$$

The BMP contributed by VFAs were calculated from VFAs concentrations C_i and COD equivalent factors α_i .

$$BMP_{\text{VFAs}} = \sum_{i=\text{CH}_3\text{COOH}}^{\text{C}_5\text{H}_7\text{COOH}} (C_i \cdot \alpha_i) \cdot 350 \frac{\text{mL CH}_4}{\text{g COD}} \cdot V_{\text{sample}} \quad (3.12)$$

The anaerobic biodegradability, which is based on VS, can be hence calculated as follows:

$$D_{\text{anaerobic,VS}} = \frac{BMP_{VS}}{350} \cdot \frac{VS}{tCOD_{VS}} \cdot 100\% \quad (3.13)$$

3.7. Batch activity test

Batch activity tests can measure the performance of biological nutrient removal. In this study, denitrification batch activity test and anaerobic EBPR batch activity test were performed. Raw FSF, fFSF and Secondary filtrate were tested for both batch activity tests. Figure 3.6 shows the experiment

setup of these two batch activity tests. The remainder of this section will explain the procedures for these two activity tests in detail.



Figure 3.6: The experiment set up for batch activity test. The tests were performed in duplicate. Each Duran® bottle was equipped with a gas inlet, gas outlet, sampling port and electrode probe port (for pH and DO measurement).

3.7.1. Denitrification batch activity test

Denitrification tests are designed to evaluate the anoxic biomass growth yield and the maximal denitrification rate of a sludge sample fed with a specific substrate. Based on different purposes, two types of denitrification test are usually conducted. The first test (DEN.CHE.1) uses a known easily biodegradable carbon source to determine the denitrification rate and anoxic growth yield, while the second (DEN.CHE.2) uses real wastewater or mixed sample to mainly evaluate the denitrification capacity of this mixed sample (van Loosdrecht et al., 2016). The aim of this study is to determine the denitrification capacity of ffSF, which contains both easily biodegradable carbon sources and hardly biodegradable carbon sources. Therefore, the second method (DEN.CHE.2) was chosen.

The procedure of this test is briefly shown in Figure 3.7 (van Loosdrecht et al., 2016). The pH was controlled between 6.6 - 7.2, and the temperature was controlled at 20 °C. The activated sludge concentration used in this test was 3 - 4 g VSS / L. To prevent nutrient deficiency, micro-nutrient and macro-nutrient solutions were also added. The concentrations of all substrates were fixed at 50 mg VS / L. The details of solution preparation and dosage can be found in Appendix B. Each batch test lasted for 4 hours after the addition of the substrate and nitrate. Samples were taken at 0, 5, 10, 15, 20, 30, 45, 60, 90, 120, 150, 180, 210, 240 minute (14 times in total). The samples were then stored in a 4 °C fridge for subsequent IC and GC measurements.

Due to the different experiment times for different substrates, weather, operating conditions of WWTP and other factors may have impact on the activated sludge. Therefore, acetate was used as a

standard control to normalize the differences in activated sludge.

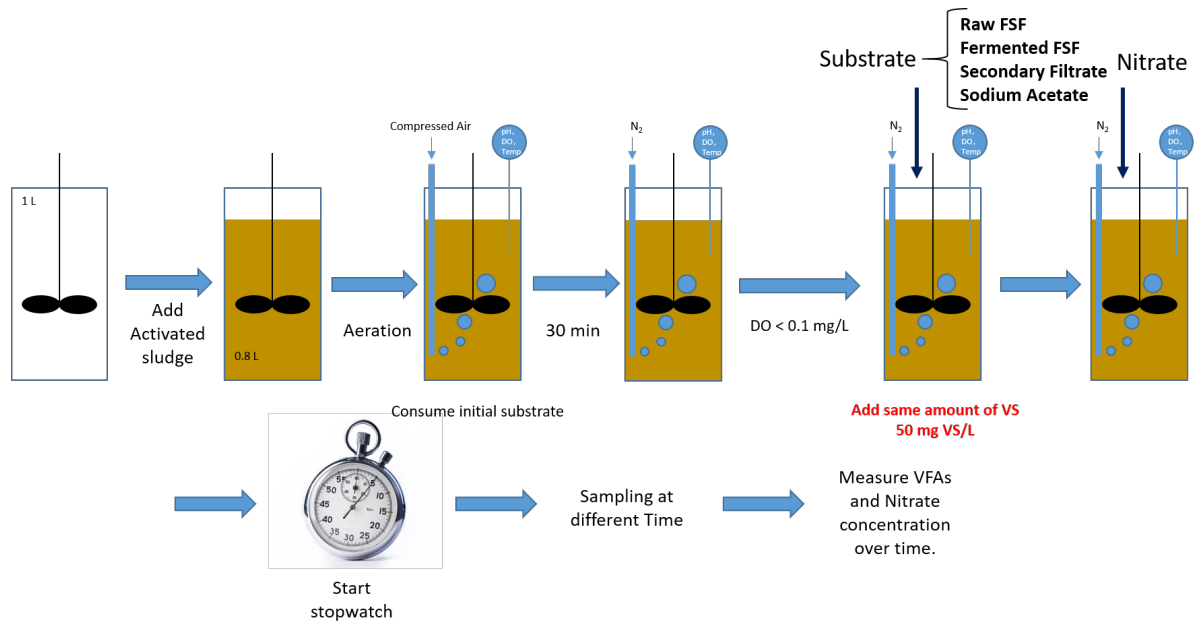


Figure 3.7: A scheme of denitrification batch activity test. The denitrification process was taken place in a 1L bottle. 0.8 L of activated sludge was added and aerated for at least 30 min to remove all initial substrates. After 30 min, the bottle was purged with nitrogen gas until the end of the test. When the DO was less than 0.1 mg/L, the substrate, standard nitrate solution and nutrient solutions were added. T0 is the moment when nitrate is added.

Figure 3.8 shows a typical result of this denitrification test. Different denitrification rates can be observed from this figure. The whole denitrification process can be divided into three phases. The soluble substrates SB are consumed at the beginning, resulting in the highest denitrification rate. Once all soluble substrates are consumed, the hydrolyzed insoluble organic solids XCB are the only available carbon sources, causing a slow denitrification phase. If both soluble and biodegradable solid substrates are completely consumed, endogenous denitrification will start.

The results of denitrification test are usually interpreted by denitrification rate r_{DN} (in $\frac{\text{mg N}}{\text{L} \cdot \text{min}}$), specific denitrification rate q_{DN} (in $\frac{\text{mg N}}{\text{g VSS} \cdot \text{min}}$) and denitrification potential DP (in $\frac{\text{mg N}}{\text{L sample}}$).

$$q_{DN,SB} = \frac{r_{DN,SB} - r_{DN,endo}}{X_{VSS}} \quad (3.14)$$

$$q_{DN,XCB} = \frac{r_{DN,XCB} - r_{DN,endo}}{X_{VSS}} \quad (3.15)$$

$$q_{DN,endo} = \frac{r_{DN,endo}}{X_{VSS}} \quad (3.16)$$

The denitrification potential can be computed as follows:

$$DP_{SB} = \frac{\Delta S_{NO_3/SB,eq} \cdot V_{tot}}{V_{sample}} \quad (3.17)$$

$$DP_{XCB} = \frac{\Delta S_{NO_3/XCB,eq} \cdot V_{tot}}{V_{sample}} \quad (3.18)$$

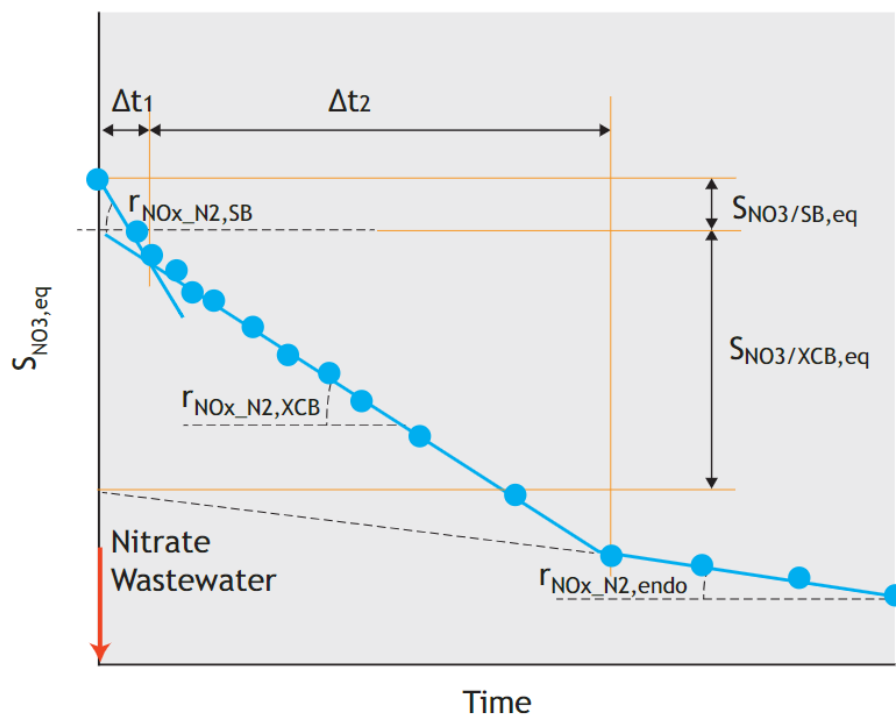


Figure 3.8: Typical nitrate concentration profiles of denitrification test. The red arrow shows the addition of standard nitrate solution and tested substrate. This figure is reprinted from van Loosdrecht et al. (2016).

3.7.2. Anaerobic EBPR batch activity test

The key microorganism in EBPR cultures is PAOs. As mentioned in section 2.3.2, they are able to survive in aerobic, anoxic and anaerobic conditions. Because this study focuses on the effect of waste-derived VFAs on biological nutrient removal, anaerobic conditions were hence selected for this batch test. As PAOs can uptake carbon sources and release phosphate under anaerobic conditions, this test is also referred to as the phosphate (P) release test.

Similar to denitrification tests, the P-release test can also be divided into different methods depending on the experiment settings. The procedure of this study was based on Method EBPR.ANA.2, which is mainly interested in P-release to carbon consumed ratio (van Loosdrecht et al., 2016). In this method, a defined concentration of substrate was added and completely consumed. Figure 3.9 shows the working flow scheme of this test. The pH and temperature were controlled between 6.6 - 7.2 and 20 °C. The P-release test requires a higher restriction on DO concentration than the denitrification test. Anaerobic conditions should be maintained throughout the experiment. Besides nutrient solution, allylthiourea was added before aeration to avoid the formation of nitrate. The food to biomass ratio was controlled at 0.05 g VS / g VSS for all substrates. If the phosphate concentration in the activated sludge was constant, the substrate could be dosed. The duration and sampling time of the P-release experiment was also consistent with that of the denitrification test. To eliminate the impact of different activated sludge, acetate was used as a standard control.

The process of phosphorus release can also be divided into soluble (SB), insoluble substrate (XCB), and endogenous phase. The results of P-release test could be processed in a similar way as the denitrification test.

Specific P-release rate q_{PR} (in $\frac{mgP}{L\ Sample}$) can be calculated as follows:

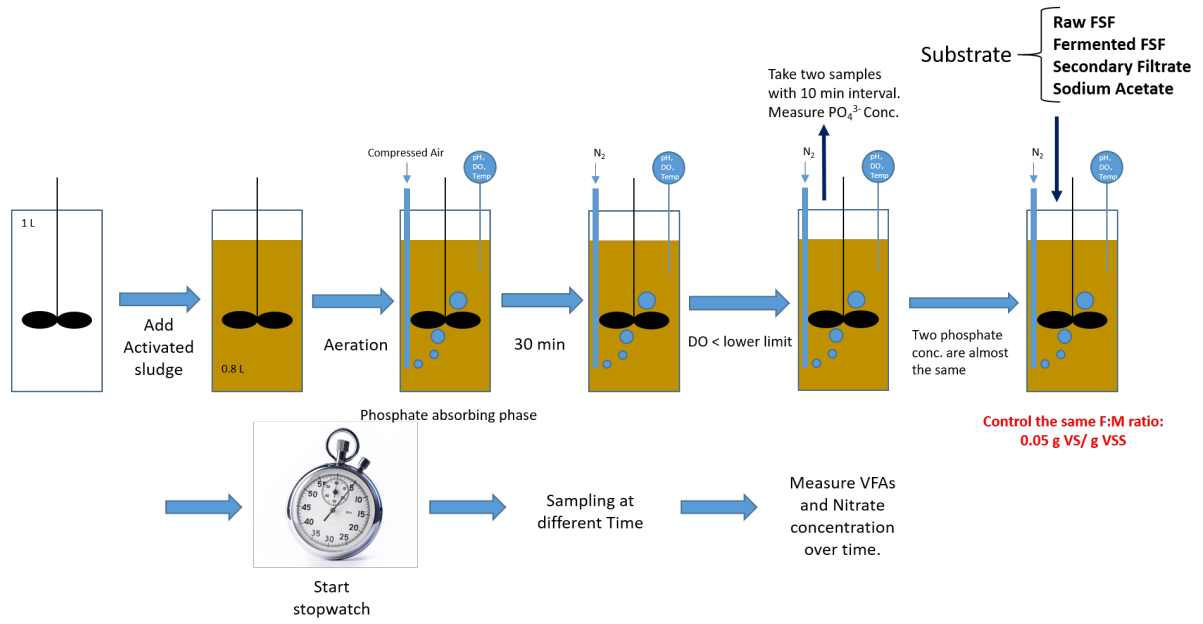


Figure 3.9: A scheme of P-release test based on EBPR.ANA.2. The set up was the same as the denitrification test.

$$q_{PR,SB} = \frac{r_{PR,SB} - r_{PR,endo}}{X_{VSS}} \quad (3.19)$$

$$q_{PR,XCB} = \frac{r_{PR,XCB} - r_{PR,endo}}{X_{VSS}} \quad (3.20)$$

$$q_{PR,endo} = \frac{r_{PR,endo}}{X_{VSS}} \quad (3.21)$$

The P-release potential PRP (in $\frac{mgP}{gVSS \cdot min}$) can be computed as follows:

$$PRP_{SB} = \frac{\Delta S_{PO4/SB,eq} \cdot V_{tot}}{V_{sample}} \quad (3.22)$$

$$PRP_{XCB} = \frac{\Delta S_{PO4/XCB,eq} \cdot V_{tot}}{V_{sample}} \quad (3.23)$$

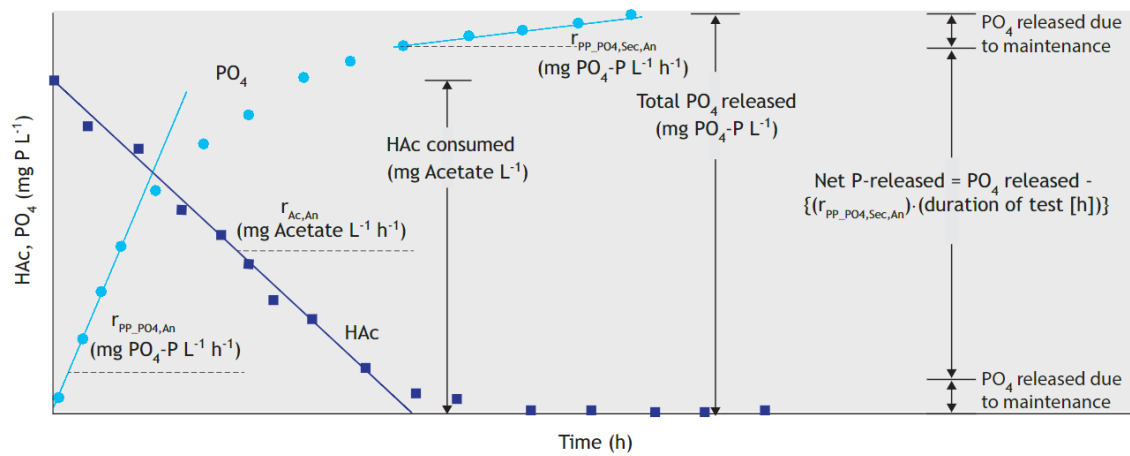


Figure 3.10: Typical phosphate and VFAs concentrations profile of p-release test. This figure is reprinted from van Loosdrecht et al. (2016).

4

Results

4.1. Sample characterization

4.1.1. Morphology

Figure 4.1 shows some microscopic structures of diluted fFSF and diluted secondary filtrate. The most common solid component of the fFSF is fiber. Nevertheless, as can be seen from Fig 4.1a and Fig 4.1b, there are many impurities in the fFSF sample, such as plant cells, sludge flocs and bacteria. The fibers usually exist in the sample as aggregates with each other or impurities.

The morphology of fibers in fFSF and raw FSF are slightly different. As shown in Fig 4.1e and Fig 4.1d, the length of the fiber is usually shorter than 1000 μm and the width is around 15 μm , which is shorter and thinner than the raw fibers shown in Fig 2.2 (Ghasimi et al., 2015). The decrease in fiber length and width indicates that the fermentation process could convert cellulose into soluble organic compounds.

Secondary sieving (mesh size = 200 μm) present a good solids removal efficiency in this study. Fig 4.1f is a digital microscopic picture of secondary filtrate. It can be seen from this graph that most of the aggregates and fibers were removed by the secondary sieving.

4.1.2. Sample composition

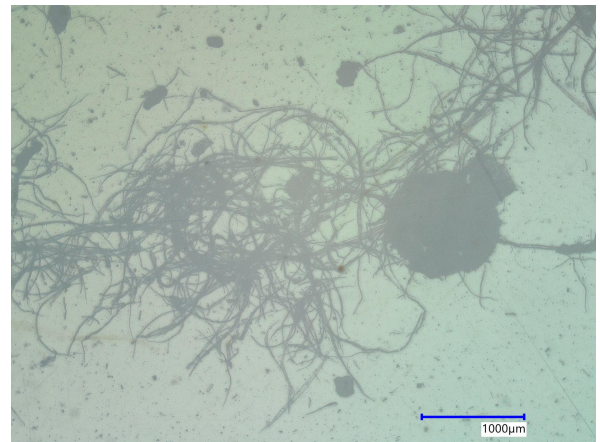
The composition of raw FSE, fFSE, secondary filtrate and secondary FSF were analyzed by thermogravimetric analysis and GC. The results are shown in Figure 4.2 and Table 4.1. The term "residual" refers to the ash remaining on aluminum tray after 550 $^{\circ}\text{C}$ combustion. The main component of the residuals might be inorganic salts.

As can be seen from the graph, the mass fraction of water in all four samples exceed 90%. Secondary filtrate has the highest water content among these samples, and secondary FSF has the lowest water content. Due to the relatively low water content, both raw FSF and secondary FSF are in solid form. Although they behave like solid more than liquid, there is a still certain amount of water entrapped in the fiber aggregates. On the other hand, fFSF and secondary filtrate are basically liquid, in which FSF fibers and impurities are heterogeneously dispersed.

Secondary sieving was effective to remove organic solids and increase the percentage of VFAs. It is apparent from Fig 4.2 (right) and Table 4.2 that secondary filtrate has the lowest volatile solids



(a) fibers, sludge flocs and plant cells found in the fFSF sample.



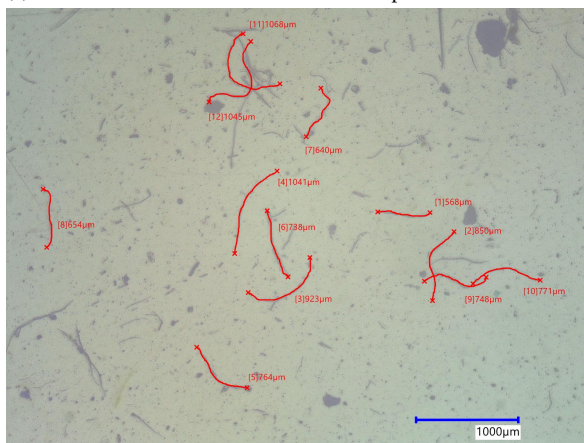
(b) A fiber aggregate found in the fFSF sample.



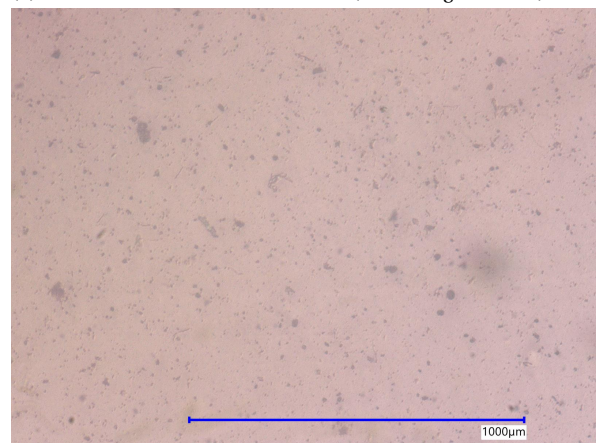
(c) Some intact fibers found in the fFSF sample.



(d) A measurement of fFSF fiber width (1000x magnification).



(e) A measurement of fFSF fiber length.



(f) Small sludge flocs found in secondary filtrate.

Figure 4.1: Digital microscopic pictures of fFSF and secondary filtrate under different magnifications.

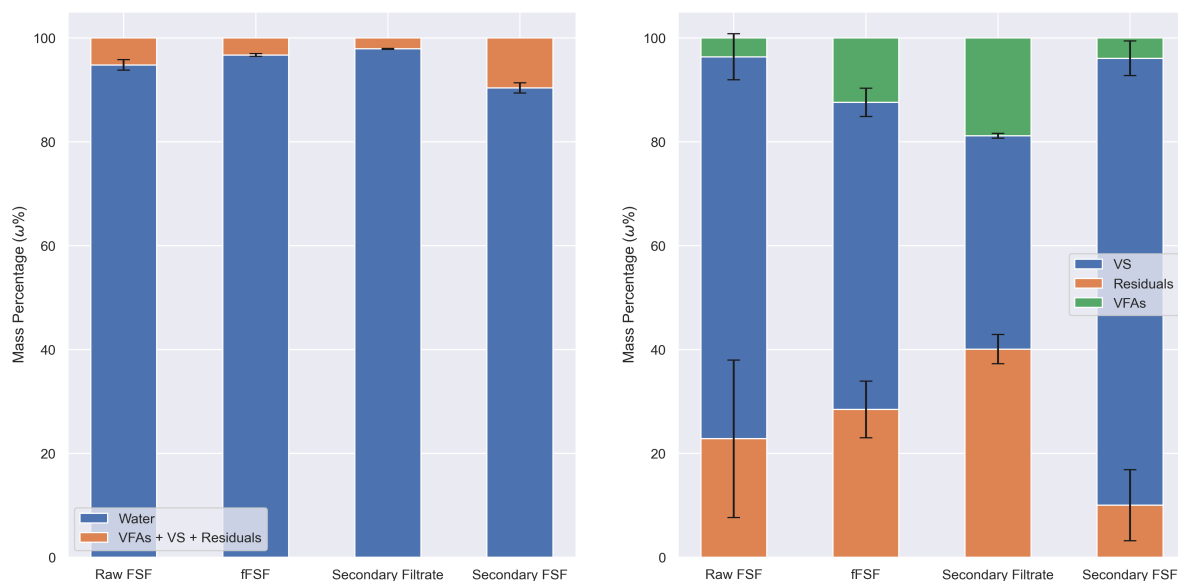


Figure 4.2: (Left) Water content of different samples . (right) VS, VFAs and residuals content on dry basis. The values are in mass fraction.

concentration. Additionally, the data shown in Figure 4.2 is in mass fraction. As a result, it does not mean that the secondary filtrate has the highest residuals concentration. The standard deviation of raw FSF is much higher than others. The inaccuracy is mainly due to the highly heterogeneous structure of raw FSF.

Table 4.1: VS, ash, VFAs and water content of the samples.

	Volatile Solids %	Ash %	VFAs %	Water %
Raw FSF	3.83 ± 0.23	1.19 ± 0.79	0.19 ± 0.00	94.79
fFSF	1.95 ± 0.09	0.94 ± 0.18	0.41 ± 0.01	96.70
Secondary Filtrate	0.87 ± 0.01	0.85 ± 0.06	0.40 ± 0.00	97.88
Secondary FSF	8.30 ± 0.32	0.97 ± 0.66	0.38 ± 0.01	90.35
Primary Sludge	4.80 ± 0.12	1.30 ± 0.25	0.36 ± 0.01	93.54

The proportion of VFAs is relatively small, but it is still much higher than conventional organic wastes. The GC results showed that these samples had a large variety of VFAs. As shown in Figure 4.3, acetic acid and propionic acid are predominant VFA species in all samples. The percentage of these two acids exceeds 90 % in all four types of samples. Acetic acid has a comparatively higher share in raw FSF, while this percentage is decreased from 45% to 15% in fFSF, secondary filtrate and secondary FSF. The percentage of acetic acid in raw FSF is replaced by newly generated acids during the fermentation process. According to Table 4.2, the VFAs concentration was increased from 215.90 mg/L to 4129.90 mg/L after the fermentation. All VFAs concentrations in fFSF were substantially increased compared to raw FSF, and the highest increase was observed in propionic acid. Some macro-molecules were also fermented and decomposed into C5 and C6 fatty acids. By comparing the VFAs concentration in fFSF, secondary filtrate and secondary FSF, it can be concluded that the secondary sieving has little influence on VFAs distribution and concentration. The percentages of different VFAs in these three samples were almost the same.

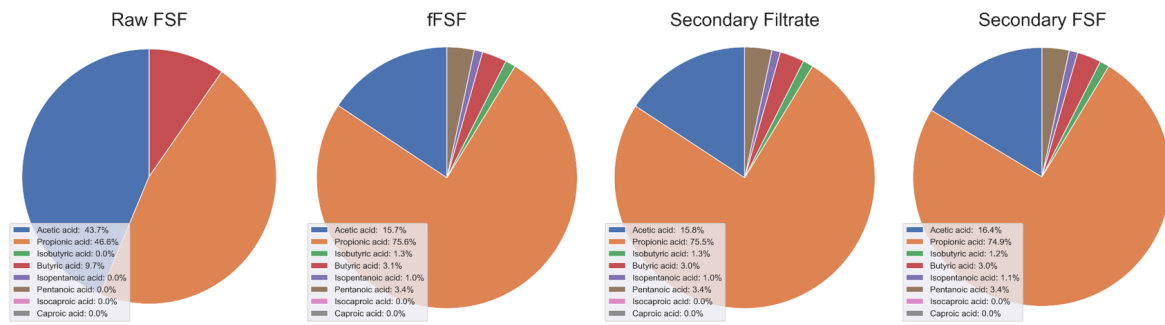


Figure 4.3: The percentage of different VFAs in raw FSF, fFSF, secondary filtrate and secondary FSF.

Table 4.2: VFAs compositions. N.A.: Not applicable; N.D.: Not detected.

Sample	Sample mass Conc. g sample / L	Acetic acid mg/L	Propionic acid mg/L	I-C4 mg/L	Butyric Acid mg/L	I-C5 mg/L	Valeric acid mg/L	I-C6 mg/L	Caproic acid mg/L	Total VFAs Conc. mg/L	VFAs content g VFAs /g sample
Raw FSF	114.52	94.4 ± 1.4	100.7 ± 2.4	N.D.	20.9 ± 0.1	N.D.	N.D.	N.D.	N.D.	215.9 ± 3.9	0.0019
fFSF	N.A.	647.7 ± 2.0	3121.1 ± 31.3	52.4 ± 2.9	126.2 ± 1.4	43.1 ± 0.3	139.5 ± 1.0	N.D.	N.D.	4129.9 ± 38.1	0.0040
Secondary Filtrate	N.A.	633.2 ± 2.5	3032.8 ± 22.7	51.2 ± 2.9	121.6 ± 0.6	42.1 ± 0.8	135.4 ± 0.5	N.D.	N.D.	4016.3 ± 28.8	0.0040
Secondary FSF	97.71	61.0 ± 1.5	278.9 ± 3.4	4.5 ± 0.1	11.2 ± 0.2	4.0 ± 0.2	12.7 ± 0.2	N.D.	N.D.	374.6 ± 8.9	0.0038
Primary Sludge	109.61	150.2 ± 1.4	83.2 ± 0.6	15.4 ± 0.1	76.0 ± 1.0	31.5 ± 0.3	34.5 ± 0.2	7.1 ± 0.1	3.3 ± 0.1	398.8 ± 4.7	0.0036

Table 4.3 provides the equivalent COD values for different types of VFAs. These values were calculated based on the VFAs concentration shown in Table 4.2 and COD equivalent factors presented in Table 3.2. The COD data will be used for subsequent aerobic and anaerobic biodegradability calculations.

Table 4.3: VFAs-contributed COD values of different samples.

	Acetic acid mg O ₂ /L	Propionic acid mg O ₂ /L	I-C4 mg O ₂ /L	Butyric Acid mg O ₂ /L	I-C5 mg O ₂ /L	Valeric acid mg O ₂ /L	I-C6 mg O ₂ /L	Caproic acid mg O ₂ /L	Total VFAs COD mg O ₂ /L	Total VFAs COD mg O ₂ / g sample
Raw FSF	101.0 ± 1.5	152.0 ± 3.6	N.D.	37.8 ± 0.2	N.D.	N.D.	N.D.	N.D.	290.8 ± 5.3	2.5 ± 0.1
fFSF	693.0 ± 2.1	4712.9 ± 47.3	94.9 ± 5.3	228.4 ± 2.5	87.8 ± 0.6	80.5 ± 2.0	N.D.	N.D.	5897.5 ± 59.8	5.9 ± 0.1
Secondary Filtrate	677.5 ± 2.6	4579.6 ± 34.3	92.6 ± 5.2	220.1 ± 1.1	85.8 ± 1.6	276.3 ± 1.1	N.D.	N.D.	5931.9 ± 45.9	5.9 ± 0.1
Secondary FSF	65.2 ± 1.6	421.1 ± 5.1	8.1 ± 0.2	20.2 ± 0.3	8.1 ± 0.3	25.8 ± 0.4	N.D.	N.D.	548.5 ± 8.0	5.6 ± 0.1
Primary Sludge	160.7 ± 1.5	125.6 ± 0.9	27.9 ± 0.2	137.5 ± 1.7	64.3 ± 0.5	70.3 ± 0.3	15.7 ± 0.2	7.3 ± 0.2	609.3 ± 5.4	5.6 ± 0.1

4.2. Aerobic biodegradability

The BOD results of samples are shown in Figure 4.4. As can be seen, raw FSF (green dots) has the highest ultimate BOD among the samples. This phenomenon is because the raw FSF has higher VS content. During the fermentation process, part of the substrate is consumed by the microorganisms, and also some COD is converted into gas. As a result, the initial tCOD of raw FSF is higher than fFSF. Similarly, as a considerable portion of VS was removed by secondary screening, the total BOD and tCOD of fFSF were also higher than secondary filtrate.

The trends of BOD above are generally in agreement with the first-order reaction kinetic equation proposed by Weijers (2000). However, the previous figure is not convenient for comparison as the initial concentration of the three samples are different. To compare the BOD and aerobic biodegradability, the values should be normalized to the same VS concentration. Figure 4.5 shows the average BOD value after normalization and first-order kinetic functions.

Surprisingly, the order of BOD shown in Figure 4.5 is the reverse regarding to the data in Figure 4.4. According to the fitted BOD curves, the normalized ultimate BOD of secondary filtrate is higher than fFSF, and fFSF is higher than raw FSF. The detailed results are summarized in Table 4.4.

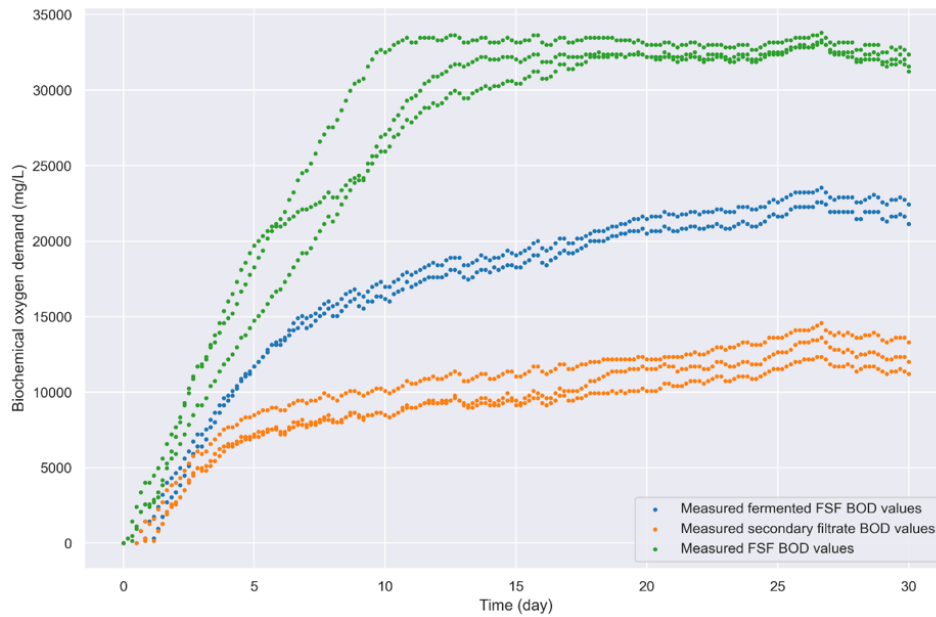


Figure 4.4: Measured BOD values of raw FSF, fFSF and secondary filtrate without correction and normalization. The unit of BOD is $\text{mg O}_2/\text{L}$. The measurement was performed in triplicate. One of the fFSF bottle was clogged during the test, and hence, there is only two sets of data.

Table 4.4: BOD test results and first-order kinetics parameters. The BOD, tCOD and Ultimate aerobic biodegradability are total values, which include both VS and VFAs.

Sample	$\text{BOD}_{\text{ult,tot}}$ $\text{mg O}_2/\text{g VS}$	k $1/\text{d}$	tCOD_{tot} $\text{mg O}_2/\text{L}$	VS g/L	tCOD_{tot} $\text{mg O}_2/\text{g VS}$	$\text{D}_{\text{aerobic,tot}}$ %
Raw FSF	888 ± 10	0.160 ± 0.007	62560 ± 1379	38.18 ± 2.25	1639 ± 104	54.18 ± 3.49
Fermented FSF	1160 ± 12	0.136 ± 0.004	33500 ± 2245	19.46 ± 0.90	1721 ± 140	67.40 ± 5.53
Secondary Filtrate	1418 ± 25	0.154 ± 0.010	14600 ± 638	8.59 ± 0.09	1700 ± 76	83.41 ± 4.01

The results in Table 4.4 suggest that secondary filtrate has the highest aerobic biodegradability. However, these results are still not accurate enough. As discussed in section 3.5.3, VS concentration measured by thermogravimetric analysis does not include VFAs. Consequently, the normalized BOD and aerobic biodegradability of samples with high VFAs concentration are overestimated. One possible solution to this problem is to subtract the BOD of VFAs from the total BOD. Since the kinetics of the VFAs biodegradation under aerobic conditions are unknown, the correction is only applicable for ultimate BOD values. The final BOD result and aerobic biodegradability are shown in Table 4.5. The final BOD results show that 60.4 % of the COD from VS is aerobically biodegradable for fFSF, which is higher than that of raw FSF. The proportion of VFAs-contributed COD in raw FSF is small, while the proportion of COD in VS is significant. As to the secondary filtrate, 72.1% of the COD from VS is aerobically biodegradable, which is the highest value among all samples.

In summary, these results indicate that both acidogenic fermentation and secondary sieving could increase the aerobic biodegradability of waste solids and alleviate the burden of activated sludge systems. Using secondary filtrate as an additional carbon source for the activated sludge system can reduce nearly 50% of the hardly-biodegradable fraction compared to fFSF.

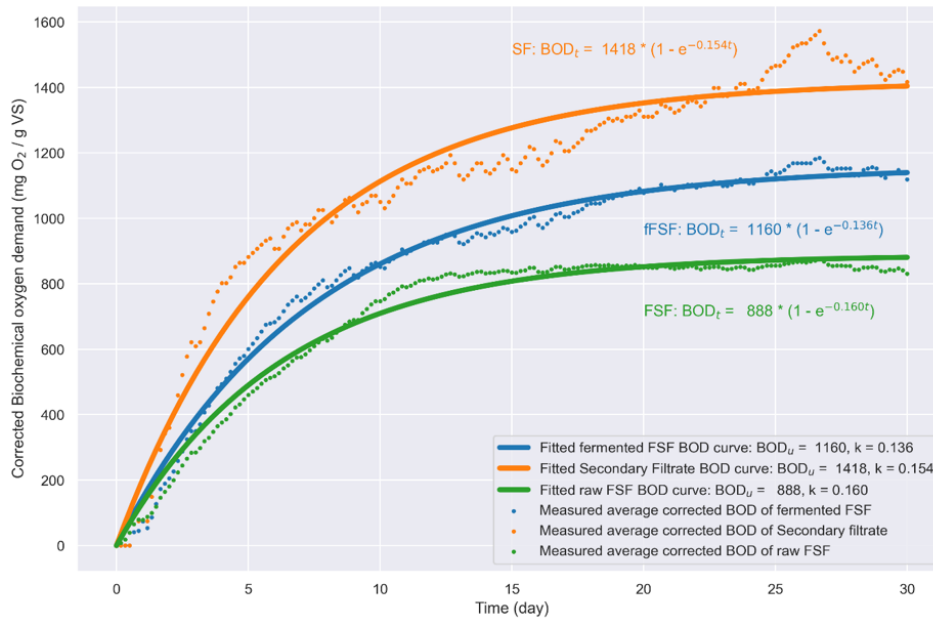


Figure 4.5: Measured average BOD values after normalization. The unit of BOD is $\text{mg O}_2 / \text{g VS}$. The dots are average values after normalization, the curves are modeled BOD according to first-order kinetics (equation 3.2). The fluctuation at the end might be due to changes in ambient temperature.

Table 4.5: Corrected BOD and aerobic biodegradability results.

	$\text{BOD}_{\text{ult,VS}}$	tCOD_{VS}	$\text{D}_{\text{aerobic,VS}}$
	$\text{mg O}_2 / \text{g VS}$	$\text{mg O}_2 / \text{g VS}$	%
Raw FSF	822 ± 11	1572 ± 38	52.3 ± 1.4
fFSF	857 ± 15	1418 ± 108	60.4 ± 4.7
Secondary Filtrate	727 ± 30	1009 ± 80	72.1 ± 6.4

4.3. Anaerobic biodegradability

Evaluation of anaerobic biodegradability of samples is based on the results of the BMP test. The raw BMP results measured by AMPTS II are shown in Figure 4.6. As can be seen, the BMP of raw FSF, secondary FSF, primary sludge and cellulose are between 300 - 400 $\text{N-mL CH}_4 / \text{g VS}$. The BMP of cellulose is $328.53 \pm 6.84 \text{ CH}_4 / \text{g VS}$, which is in the range of standard value 315 - 439 $\text{N-mL CH}_4 / \text{g VS}$. These results are also in accord with existing research, which showed similar patterns and values (Guo et al., 2020).

What stands out in this figure is the special pattern of fFSF. The equilibrium biomethane production of fFSF is much higher than others, exceeding the normal range of 300 - 400 $\text{N-mL CH}_4 / \text{g VS}$. This unexpected value could be explained by higher VFAs concentration. As shown in Table B.4, the VS content of different bottles are the same, while fFSF group contains 5 - 8 times higher VFAs concentration. Hence, for fFSF, the total organic matter in the BMP measuring bottles were more than other samples. As a result, the BMP contributed by VS also needs to exclude the effect of VFAs.

Additionally, a large change in slope can be seen from the curve of fFSF. Initially, the biomethane production rate of fFSF is similar to other samples, while the slope suddenly decreases on day 3 and

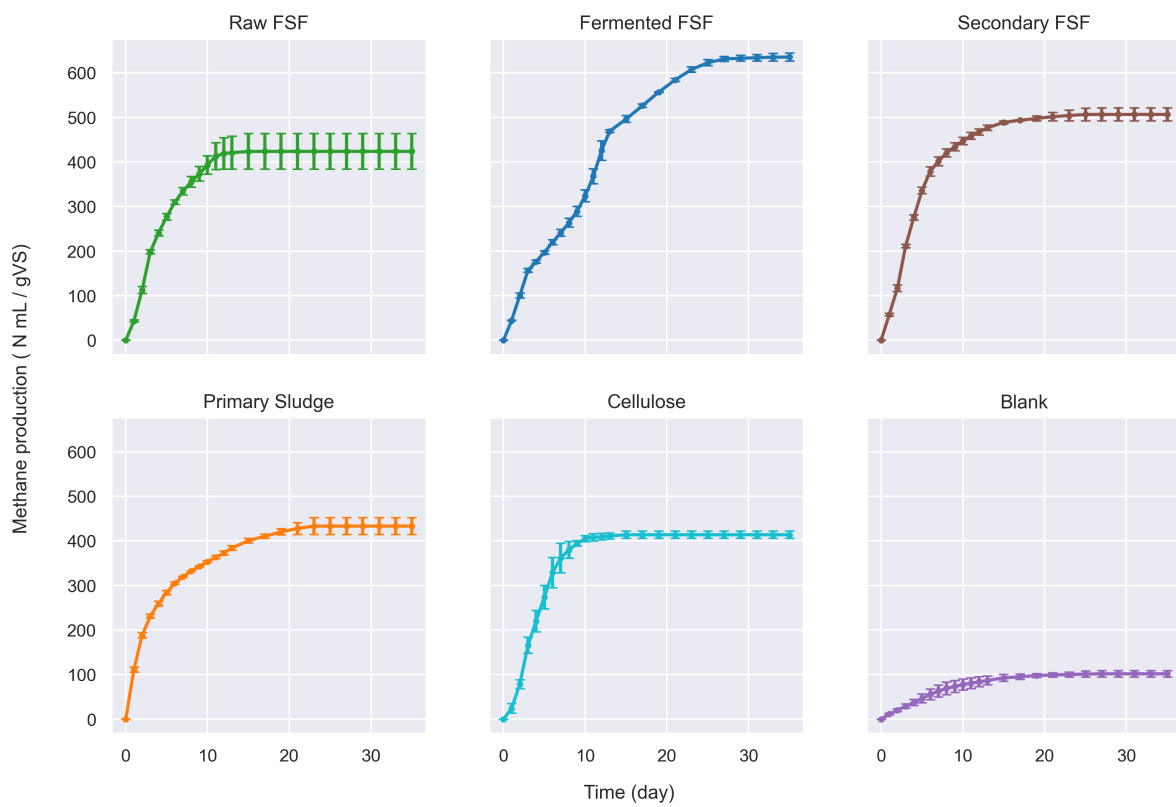


Figure 4.6: Cumulative biomethane potential of different samples. The experiment was performed in triplicate. The BMP values of tested samples have been calibrated to standard temperature and pressure. Blank value is not removed in this figure.

gradually increases until day 12. In the later phase, the trend of fFSF BMP curve is very similar to other substrates; however, a longer time is required to achieve equilibrium.

If we now turn to anaerobic biodegradability, as mentioned in Equation 3.13, it should be corrected to VS basis. Considering that the kinetics of VFAs degradation were not measured in this thesis, the VFAs corrections for anaerobic biodegradabilities were only performed for the equilibrium values. Table 4.6 presents the BMP on the basis of total substrates, VFAs and VS. As can be seen, after subtracting the contribution of VFAs, the BMP of fFSF decreases from 529 to 352 N-mL CH₄ / g VS, which is more reasonable. Based on the corrected BMP value (BMP_{VS}), the calculated anaerobic biodegradability of fFSF is 68.23 %. The anaerobic biodegradability of raw FSF and secondary FSF are 56.8 % and 51.5%, respectively.

In summary, fFSF has the highest anaerobic biodegradability on VS basis. The difference in the anaerobic biodegradability of raw FSF and secondary FSF is small. Since the samples are highly viscous and heterogeneous solid-liquid mixtures, the relative error is comparatively higher than liquid substrates. Considering the error, the anaerobic biodegradability of raw FSF and secondary FSF are similar, which indicates the anaerobic biodegradability of cellulose fibers before and after the acidogenic fermentation process are almost the same. While the anaerobic biodegradability of cellulose fibers are substantially increased from 55 % to around 70% if the fibers are co-digested with VFAs (analogous to the case of fFSF). Therefore, VFAs might play an important role in improving the anaerobic biodegradability of cellulose. Simultaneously, it is probably that the existence of VFAs could inhibit the rate of the methanogenesis process, causing a sharp decrease in biogas production rate during the BMP test. A limitation of the anaerobic results is that the fFSF sample and raw FSF are from different WWTPs, and were stored at different temperature conditions. Therefore, the measured values might slightly deviate from the true values.

Table 4.6: Anaerobic biodegradability, total COD and BMP of different substrates.

Sample	BMP _{tot}	BMP _{VFAs}	tCOD _{VS}	BMP _{VS}	D _{anaerobic,VS}
	N-mL CH ₄ / g VS	N-mL CH ₄ / g VS	mg O ₂ / g VS	N-mL CH ₄ / g VS	%
Raw FSF	323.3 ± 38.2	7.7 ± 0.2	1628 ± 147	315.3 ± 38.2	56.8 ± 8.4
Fermented FSF	529.2 ± 11.1	176.3 ± 1.8	1477 ± 128	352.7 ± 12.8	68.2 ± 6.4
Secondary FSF	402.1 ± 13.6	11.5 ± 0.1	2166 ± 322	390.5 ± 14.1	51.5 ± 7.8

4.4. Biological nutrient removal efficiency

To demonstrate that FSF-derived VFAs are actually able to improve the performance of BNR and to evaluate the effect of secondary sieving on fFSF, the denitrification test and P-release test were conducted in this research. This section will present the outcome of these two tests.

4.4.1. Denitrification test

The results of denitrification test are shown in figures 4.7a (raw FSF), Fig 4.7b (fFSF) and Fig 4.7c (secondary filtrate). Generally, the NO₃ – N concentration decreases over time, while the slope is not constant. Two decreasing stages were discovered for fFSF and secondary filtrate, but only one stage was found for raw FSF. As can be seen, the slope of the first stage is steeper than the second stage. It can be noticed that the intersection of these two stages is approximately occurs at the same moment when the VFAs are completely consumed. Therefore, it can be roughly inferred that the

first faster stage is the SB stage, at which VFAs are the main substrates. Based on this assumption, we can use the linear regression method to fit these two stages. The green and red lines are fitted $\text{NO}_3\text{-N}$ concentrations. As VFAs were not detected for the test of raw FSF, therefore there is only a green line in Fig 4.7a. Additionally, as mentioned in section 3.7.1, sodium acetate was used to eliminate the impact of different sludge on the BNR process. The stars in these figures represent the result of acetate standard, and the dots are the results for real samples. The fitted rate parameters are summarized in Table 4.7.

Table 4.7: Denitrification rates and specific denitrification rates based on the denitrification test results. The denitrification rates have been normalized with the mean blank denitrification rate measured in the standard group. The unprocessed rates can be found in the previous denitrification curves.

	r_1 mg N/(L · min)	r_2 mg N/(L · min)	r_{Ac} mg N/(L · min)	r_{blank} mg N/(L · min)	$q_{DN,SB}$ mg N/(g VSS · min)	$q_{DN,endo}$ mg N/(g VSS · min)
Raw FSF	-0.065	-	-0.134	-0.078	-	-0.020
fFSF	-0.169	-0.052	-0.177	-0.075	-0.035	-0.016
Secondary filtrate	-0.144	-0.063	-0.218	-0.058	-0.025	-0.019

In addition to kinetics, denitrification potential was used to elaborate the efficiency of FSF-based carbon sources. The results are compiled in Table 4.8.

Table 4.8: Denitrification potential of soluble substrates (VFAs) in FSF-based carbon sources.

	$\Delta S_{\text{NO}_3,SB}$ mg $\text{NO}_3\text{-N}$ /L	V_{tot} L	V_{sample} L	DP_{SB} g $\text{NO}_3\text{-N}$ /L sample	DP_{SB} g $\text{NO}_3\text{-N}$ /g VS
Raw FSF	0	0.808	0.0021	0	0
fFSF	1.795	0.808	0.0038	0.382	0.034
Secondary filtrate	2.960	0.813	0.0074	0.325	0.059

4.4.2. P-release test

The results of P-release test were plotted in the same way as the denitrification test. Two P-release stages with different slopes were discovered, and the P-release rates were fitted with the linear model. The P-release curve can be found in Figure 4.7d, Figure 4.7e and Figure 4.7f.

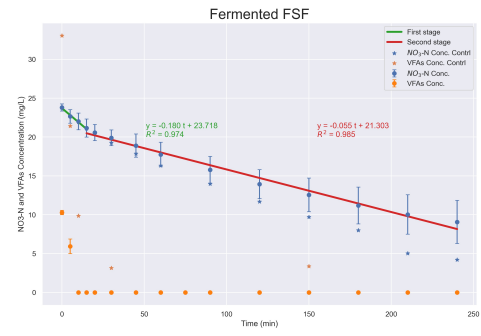
Similarly, P-release rates, specific P-release rates and P-release potential were calculated and listed in Table 4.9 and Table 4.10, respectively. The results of P-release rates and specific P-release rates will be discussed together with denitrification parts in section 4.4.3.

Table 4.9: P-release rates and specific denitrification rates based on the P-release test results. The P-release rates have been normalized with the mean blank P-release rate measured in the standard group. The unprocessed rates can be found in the previous P-release curves.

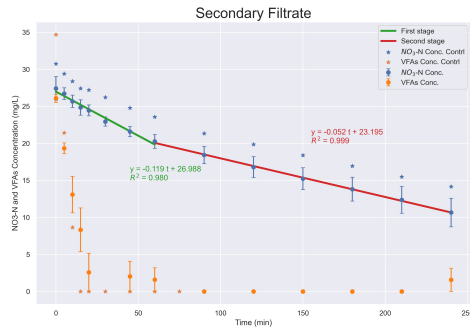
	r_1 mg P/(L · min)	r_2 mg P/(L · min)	r_{Ac} mg P/(L · min)	r_{blank} mg P/(L · min)	$q_{PR,SB}$ mg P/(g VSS · min)	$q_{PR,endo}$ mg P/(g VSS · min)
Raw FSF	0.130	-	0.913	0.067	-	0.039
fFSF	0.321	0.081	0.793	0.063	0.073	0.025
Secondary filtrate	0.300	0.050	1.016	0.061	0.076	0.015



(a) Denitrification curve for raw FSE.



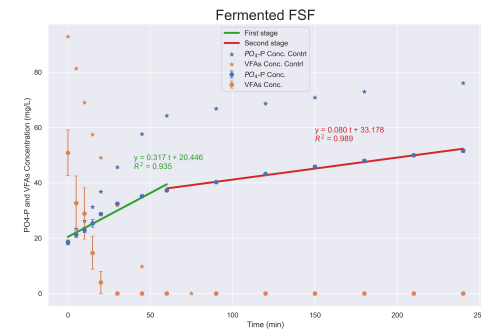
(b) Denitrification curve for fFSF.



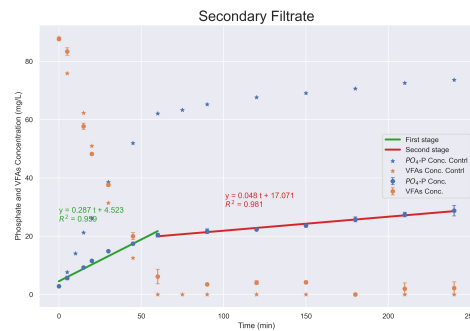
(c) Denitrification curve for secondary filtrate.



(d) P-release curve for raw FSE.



(e) P-release curve for fFSF.



(f) P-release curve for secondary filtrate.

Figure 4.7: Denitrification curves and P-release curves of raw FSE, fFSF and secondary filtrate.

Table 4.10: P-release potential of soluble substrates (VFAs) in FSF-based carbon sources.

	$\Delta S_{PO_4,SB}$	V_{tot}	V_{sample}	PRP_{SB}	PRP_{SB}
	mg PO_4-P/L	L	L	g PO_4-P/L sample	g PO_4-P/g VS
Raw FSF	0	0.811	0.0058	0	0
fFSF	13.978	0.815	0.0094	1.212	0.108
Secondary filtrate	17.546	0.825	0.0192	0.754	0.137

4.4.3. Summary of batch activity test

This section summarizes the results of the two activity tests and provides a comprehensive comparison of the performance of the different samples from perspectives of kinetic and BNR efficiency.

From the view of kinetics, the first stage rates ($r_{DN,1}$ and $r_{PR,1}$) are significantly higher than the second stage rates ($r_{DN,2}$ and $r_{PR,2}$), except for raw FSF, which only has one stage. This correlation is also confirmed in specific rates ($q_{SB} > q_{endo}$).

Interestingly, the measured curves are different from the standard curves shown in section 3.7.1 and 3.7.2. Only two stages were discovered rather than three stages. Based on the curves only, it seems that the solid substrates (fibers) do not play any role during the denitrification tests and the P-release test. Nevertheless, if $q_{PR,endo}$ is considered, the specific endo P-release rate of raw FSF is greater than fFSF and secondary filtrate, which indicates that solid substrates increase the so-called specific "endo" P-release rates in the case of raw FSF. If the specific endo P-release rates of the blank group (r_{blank}) are further compared with the specific endo P-release rates of raw FSF, it can be found that the latter is much faster. If compared to fFSF, the difference still exists but less significant. Based on this observation, a more likely explanation is that the degradation rate of fibers during the experiments was slow. Hence it is difficult to separate the XCB stage from endogenous stage within 4 hours. But XCB do provide extra COD for EBPR process. If now turning to the denitrification test, the $q_{DN,endo}$ for three samples are very similar. which means the impact of solid substrates on endogenous denitrification rate is less significant than P-release process. The reason for the difference between denitrification and P-release has not been investigated.

So far this section has presented a brief summary of kinetics parameters. The remainder of this section will discuss the efficiency of different samples mainly based on denitrification and P-release potentials. The DN and PRP are given in two different forms. g nutrient / L sample or g nutrient / g VS. Using per liter sample basis is more convenient for real case operation, while using per gram VS basis is easier to be compared with different carbon sources.

According to Table 4.8, per liter of fFSF could remove 0.382 g NO_3-N , while secondary filtrate could only remove 0.325 g NO_3-N . If converting into per g VS basis, the removal efficiency of secondary filtrate is approximately 40 % higher than fFSF. A similar phenomenon is also shown in P-release test. On a per liter sample basis, dosing a liter of fFSF could release 1.212g of PO_4-P , which is approximately 40% higher than secondary filtrate. However, on a per gram VS basis, secondary filtrate showed 20% higher P release performance.

Briefly speaking, fFSF and secondary filtrate showed promising BNR results compared to raw FSF. They did work as additional carbon sources for activated sludge systems. fFSF and secondary filtrate have different pros and cons. Improving BNR with fFSF leads to higher total nutrient removal, but lower efficiency per gram of VS, which may increase the organic solids burden of the

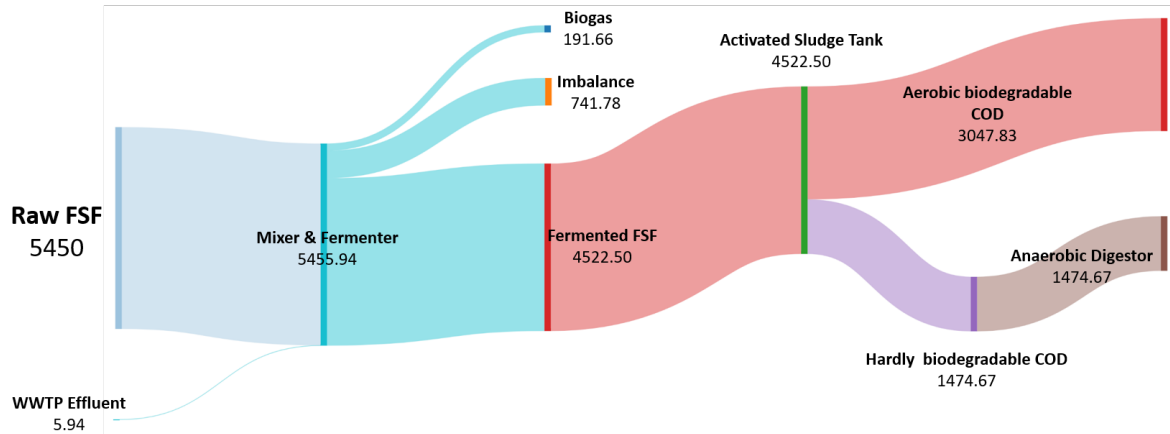
activated sludge system. The use of secondary filtrate could alleviate the problem of organic solid burden on AST, but will lose a certain amount of nutrient removal potential as compensation. Besides, fFSF contributes to higher P-release rates, which may be due to higher organic solids concentration.

4.5. Overall mass and COD balance

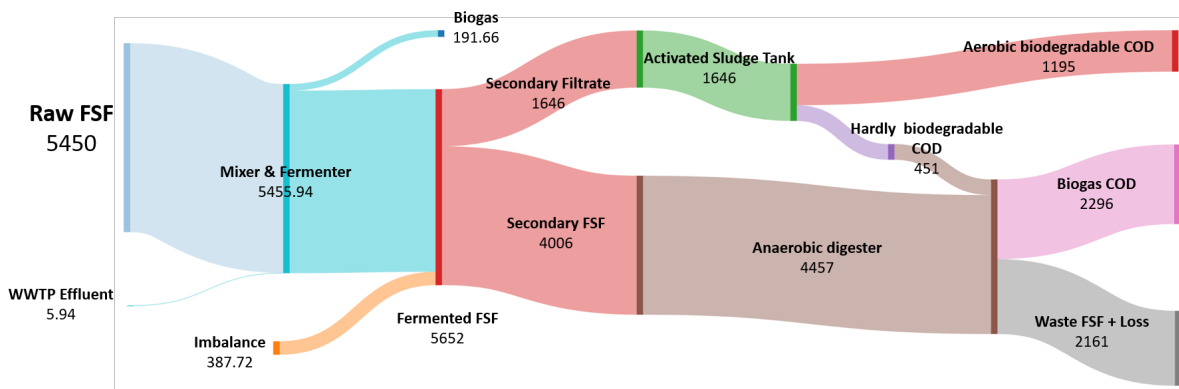
Two different scenarios were proposed in section 3.1. This section will show the differences between these two scenarios mainly based on COD balance. To present an overview of the flux of fFSF and subsequent COD flows, this section will combine the properties of different samples and the results of aerobic & anaerobic biodegradability.

Figure 4.8 shows three COD load flow diagrams. Figure 4.8a is a flow diagram of the reference process. The fFSF produced from raw FSF is used directly in AST without any downstream treatments. This process would result in an additional COD load of 4522.50 kg per day to the activated sludge tank. About 3000 kg of this increasing COD is aerobically biodegradable. The remaining part will enter the anaerobic treatment process along with waste sludge to produce biogas. Adding fFSF could at least release 163.62 kg $\text{PO}_4 - \text{P}/\text{day}$ or remove 51.57 kg $\text{NO}_3 - \text{N}/\text{day}$.

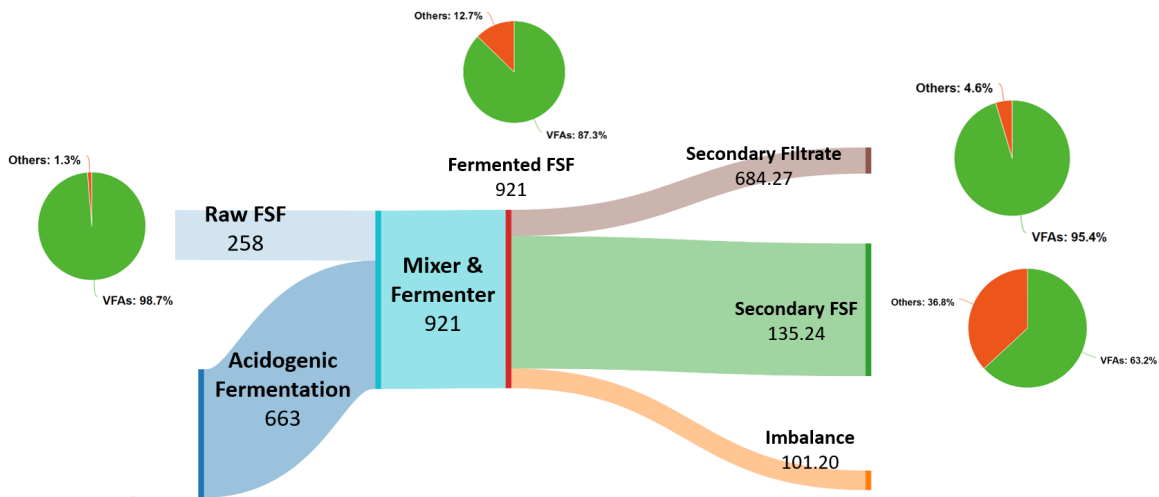
If using the second scenario instead, the COD entering activated sludge is 1646 kg/day, which will lead to at least a release of 85.01 kg $\text{PO}_4 - \text{P}/\text{day}$ or removal of 36.64 $\text{NO}_3 - \text{N}/\text{day}$. Since no obvious XCB stage was observed in the BNR curves, these data were calculated only based on soluble substrates.



(a) Total COD balance of Scenario 1.



(b) Total COD balance of Scenario 2.



(c) Soluble COD balance of Scenario 2. The pie charts represent the proportion of VFAs in sCOD.

Figure 4.8: COD balance of different scenarios. The unit of the data is kg COD /day. The fFSF and raw FSF used in this thesis were collected from two different wastewater treatment plants, which may cause imbalance of COD values. Additionally, the solid contents of these samples are higher than conventional wastewater, and hence the the accuracy of COD measurement might be limited and contribute to imbalance.

5

Discussion

5.1. Aerobic and anaerobic biodegradability analysis

5.1.1. Aerobic biodegradability

As discussed in section 4.2, the results of the BOD test indicate that acidogenic fermentation and secondary sieving could increase the aerobic biodegradability of cellulose fibers.

Compared to raw FSF, the improved aerobic biodegradability of fFSF might be benefit from higher sCOD. As can be seen in Figure 4.8, the concentration and the percentage of sCOD increase after the fermentation tank. The increasing fraction of sCOD other than VFAs might be due to soluble carbohydrate and protein hydrolyzed under acidic environment. After acidogenic fermentation, the pH of raw FSF dropped to 5 - 6. The principle of this phenomenon is analog to acid pretreatment. This also accords with other observations on waste activated sludge samples, which showed a 20 % increase in soluble carbohydrate and protein concentrations after 1 day of HCl treatment at pH 5 compared to uncontrolled pH (Devlin et al., 2011). Nonetheless, these data must be interpreted with caution because the fFSF sample has been stored for months before the experiment. Despite being stored at - 17 °C and exposed to low pH and temperature in long term may cause the measured sample to differ from the original fFSF.

Concerning the impacts of secondary sieving, a possible reason for the higher aerobic biodegradability of secondary filtrate might be the removal of large particles. This might be explained from two perspectives. For one thing, after the secondary sieving, the reduction of tCOD is greater than the decrease of BOD. Most of the soluble substrates of fFSF retain in the secondary filtrate, while the large solid organics are removed. For another, smaller solid organic particles may also be better aerobically biodegradable. Although particle size does not affect the chemical composition of substrates and the amount of substance, there appears to be a threshold at which particle size could significantly affect biodegradability. Polybutylene sebacate (PbSe) is a biodegradable polymer, which is widely used in the production of bioplastics. Chinaglia et al. (2018) conducted a soil biodegradability test on PbSe and found that the aerobic biodegradability showed a significant decrease at a specific surface area of 33 cm²/g, while there was no significant effect in the range of 89 - 825 cm²/g (see Figure 5.1 for details). Modelli et al. (1999) and César et al. (2009) also reported the similar phenomenon on polyhydroxybutyrate, polycaprolactone and starch. However, the experimental conditions of the soil biodegradability test and BOD test are considerably different. To date, there is limited research in aqueous medium. Therefore, further research is required to verify whether it is

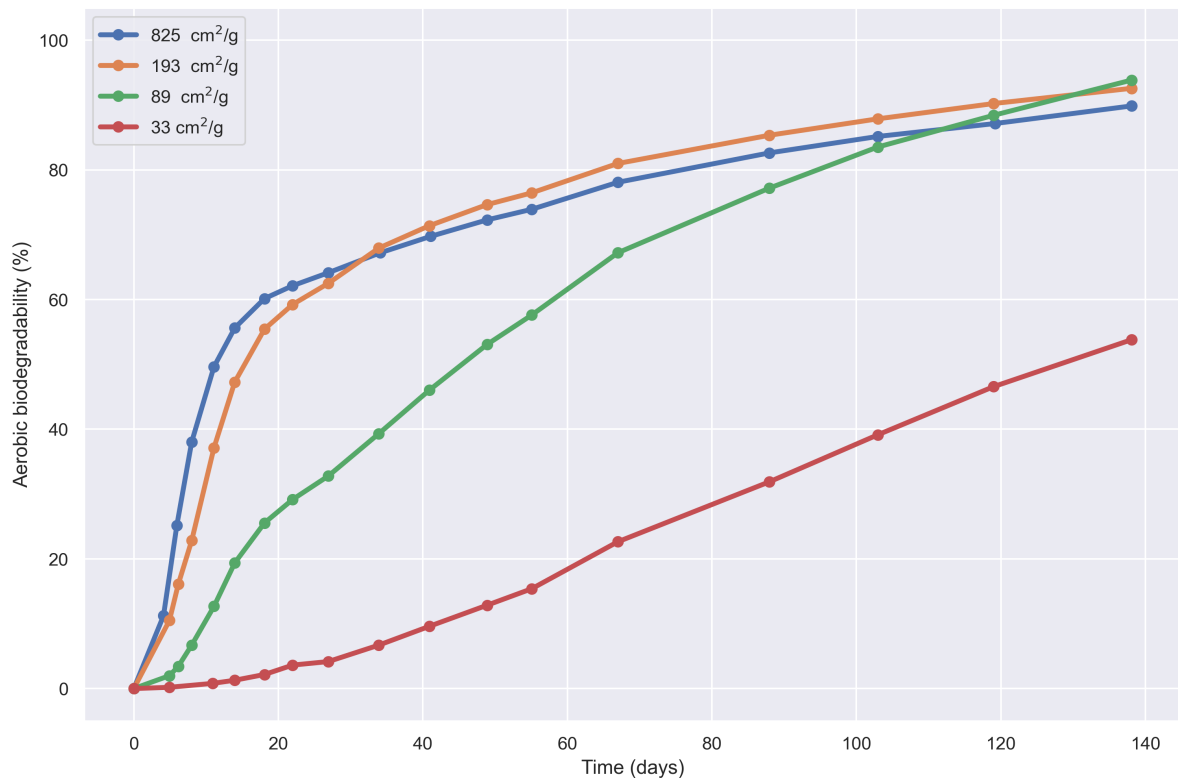


Figure 5.1: Aerobic biodegradability curves of PBSe (1 gram) with different specific surface area (adapted from Chinaglia et al. (2018)). The experiment was performed in duplicate.

applicable to fFSF (cellulose fibers) and the BOD test.

5.1.2. Anaerobic biodegradability

In this study, fFSF was found to have higher anaerobic biodegradability than raw FSF and secondary FSE, while the anaerobic biodegradability of raw FSF and secondary FSF are nearly the same. This could also be explained by the acidogenic fermentation as mentioned in 5.1.1. VFAs in fFSF contribute to a much higher total anaerobic biodegradability than other samples. Hydrolyze carbohydrate and protein is remained in fFSF, resulting in a slightly higher anaerobic biodegradability on VS basis.

In addition to different anaerobic biodegradability, surprisingly, the biomethane production rate of fFSF was found substantially different from others. Biomethane production seems to be limited by some factors from day 4 to day 12. Since there is no corresponding experiment to carefully investigate what happened for fFSF during the BMP test, we can only make some assumptions based on existing literature to explain this phenomenon. According to Romsaiyud et al. (2009), for batch anaerobic reactors, VFAs concentration and pH could have different effects on different phases of anaerobic digestion process. If VFAs concentration is ≥ 2 g/L, the cellulose hydrolysis process could be inhibited; If the VFAs concentration increases above 4 g/L, it could lead to the inhibition of subsequent acidogenesis process (Siegert and Banks, 2005). The concentration of VFAs in fFSF samples is 4 g/L, and the initial VFAs concentration in BMP measuring bottle is around 1.6 g/L. Therefore, VFAs concentration is likely to accumulate above 4 g/L and decrease the biomethane production rate. In addition to VFAs concentration, pH value could also decrease biomethane production rate by suppressing cellulase synthesis (Romsaiyud et al., 2009). The rate of cellulase production could

decrease by more than 80% if the pH decreases from 7 to 5. However, the pH value was not monitored during the BMP test, and hence solid evidences to this assumption are currently not available.

In general, based on previous studies, we could infer that the decreasing pH and the accumulation of VFAs concentration during the BMP test may be responsible for the inhibition shown in Figure 4.6. To validate this explanation, VFAs concentration and pH in BMP measuring bottles need to be sampled and measured periodically during the BMP test.

5.2. Biological nutrient removal performance

According to the results of batch activity test, it can be confirmed that fFSF and secondary filtrate could both improve the BNR performance. The denitrification rates were increased by 40 - 50% compared to blank, and the P-release rate is around 3 times higher than blank group. Previous studies have found similar increases in denitrification rates (Li et al., 2016); while the rates found in this thesis are 10 times lower than liquid substrates (Soares et al., 2010).

Applying FSF-derived carbon sources could effectively decrease the effluent TN and TP concentrations. Table 5.1 presents the water quality and load of WWTP Aarle-Rixtel. External carbon sources are not added in this WWTP. If FSF-derived carbon sources are used at WWTP Aarle-Rixtel, the effluent TN and TP concentrations could be further decreased. Figure 5.2 shows the effluent nitrogen load and phosphorus load if FSF-derived carbon sources are used for nitrogen removal or EBPR. Based on experimentally measured denitrification potential, by adding fFSF, the effluent TN load could be reduced by 53.7%. Secondary filtrate could achieve 17.9 % of TN reduction. Accurately calculating the effect of additional carbon sources to EBPR is difficult. The P-release to P-uptake ratio for PAOs could fluctuates between 1.10 and 1.45 (Ge et al., 2013). Here, the mean value 1.275 is chosen for estimation, which means that PAOs could uptake 1.275 g of $\text{PO}_4\text{-P}$ at the subsequent aerobic stage if 1 g of $\text{PO}_4\text{-P}$ is released at anaerobic stage. As shown in figure 5.2, theoretically, secondary filtrate could nearly remove all phosphorus from the effluent. fFSF could even provide more phosphorus removal capacity than requirement. However, due to limitations of mass transfer, PAOs cannot uptake all phosphorus from the effluent, hence it is impossible to decrease the phosphorus concentration to zero.

Table 5.1: Influent and effluent quality of WWTP Aarle-Rixtel.

	Flow	COD	BOD ₅	TN	TP	BOD ₅	TN	TP
	m ³ /d	mg/L	mg/L	mg N/L	mg P/L	kg/d	kg N/d	kg P/d
Influent	69552	625	241	46.1	7.22	16762	3206	502
Effluent	69474	40.4	3.72	5.31	0.62	258	369	43

To better evaluate the performance, the results were compared with the results of pure chemicals. Figure 5.3 shows the DP and PRP of FSF-derived carbon sources compared to acetate. The results are presented as the ratio of FSF-derived carbon sources to acetate. As can be seen, the performance of FSF-derived carbon sources is not as efficient as pure substances; however this phenomenon should be interpreted with cautious. Due to the limitation of sampling, the experimental removal might be smaller than the actual removal, and the optimal amount of carbon sources required is usually higher than that from theoretically calculated value. Furthermore, it is also found that fFSF has higher DN and PRP efficiencies compared to the secondary filtrate, which is probably contributed by slowly biodegradable organic compounds. This finding was also reported by Drewnowski and Makinia (2014).

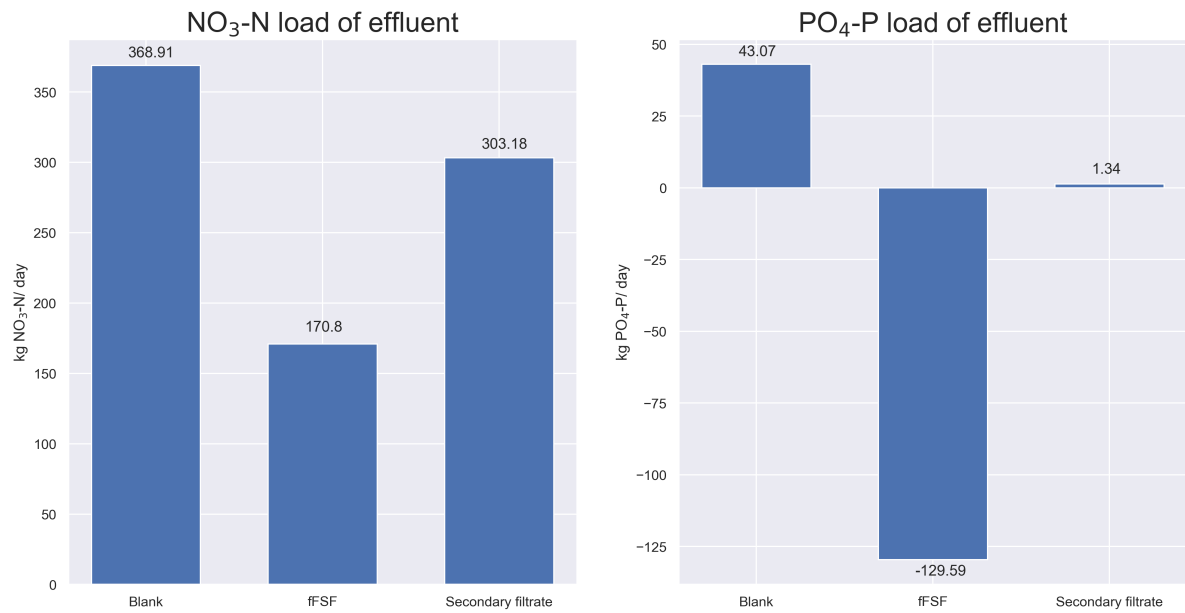


Figure 5.2: Effluent nutrients load under different carbon source conditions. (Left) Nitrogen, (right) Phosphorus. Blank indicates no additional carbon source. Negative value means the provided COD exceeds total requirement.

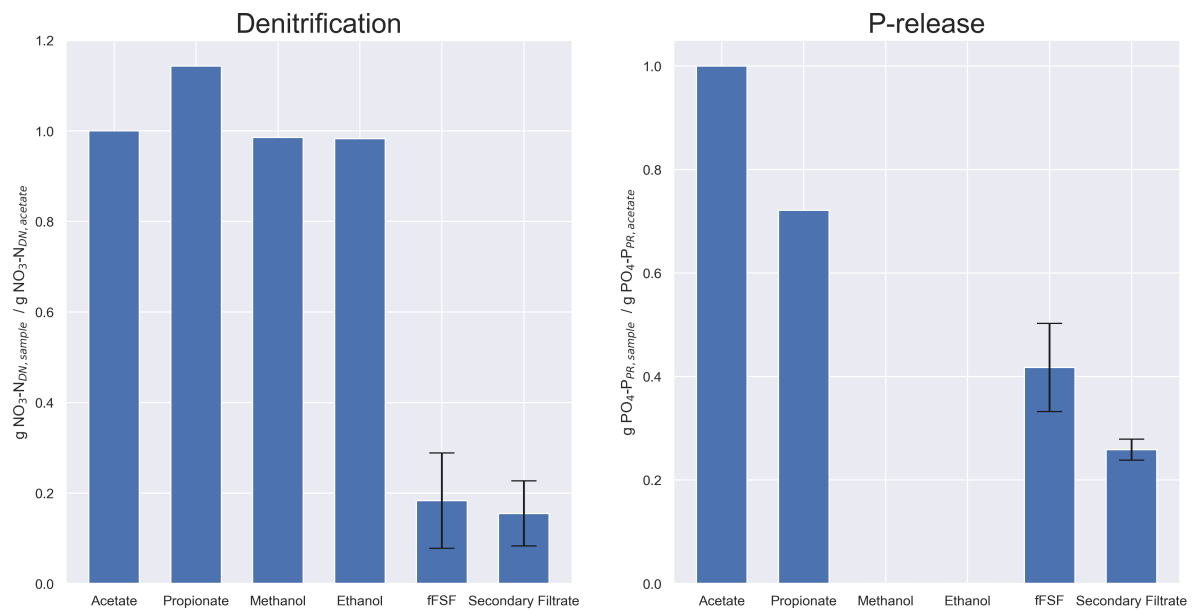


Figure 5.3: Denitrification and P-release performance of FSF-derived carbon sources and pure acetate. The denitrification performance of acetate, propionate, methanol and ethanol are stoichiometrically calculated based on equation 2.4-2.7. The P-release performance are experimentally determined with pure PAOs culture (Oehmen et al., 2005; Smolders et al., 1994). Methanol and ethanol are not suitable carbon sources for P-release in short-term tests, therefore the data is missing in this figure (Puig et al., 2008).

5.3. Comparison of FSF-derived VFAs with existing carbon source

The main objective of the project is to apply FSF-derived VFAs in BNR. Section 5.2 confirmed that FSF-derived carbon source could increase both denitrification and P-release rate. Nevertheless, it is necessary to compare FSF-derived VFAs with existing carbon sources from the view of application and operation. Table 5.2 presents an evaluation of different carbon sources for biological nutrient removal purpose. To better investigate the future possibilities of using FSF-derived carbon sources in WWTP, fFSF and secondary filtrate were incorporated in the following table.

Table 5.2: Evaluation of different external carbon sources for biological nutrient removal (adapted from USEPA (2013)). The number indicates ranking of each attribute, where 1: poor, 2: fair, 3: good, 4: very good. The ratings are qualitatively given. There are no strict criteria to classify the various ratings.

Attributes	Alcohols		Acetate		Carbohydrates		Commercial Products	Waste-derived Carbon sources	
	Methanol	Ethanol	Acetic acid	Sodium acetate	Corn Syrup	Sucrose solution	MicroC-glycerin	Fermented FSF	Secondary Filtrate
Safety & Flammability	1	1	2	4	4	4	4	4	4
Shelf life	4	4	3	3	2	2	3	1	1
Price Volatility	1	1	2	2	2	2	2	4	4
BNR performance	2	4	4	4	3	3	4	3	3
Viscosity & Handling	4	4	4	3	2	2	4	1	3
Freezing Point	4	4	4	1	2	2	4	1	1
Product Stability	4	4	4	4	2	1	4	1	2
Supply Availability	4	4	4	4	3	3	3	1	1
Quality Control	4	4	4	4	4	3	4	1	1
Cost	4	3	1	1	1	2	3	3	3
Technical data availability	4	4	4	4	2	2	3	1	1
Sustainability	1	1	1	1	2	2	2	4	4

From the table, it could be concluded that FSF-derived carbon sources have many advantages compared to conventional carbon sources. As discussed in section 4.4, the BNR performance of the fFSF and secondary filtrate is significant compared to blank, but slightly inferior to pure acetate. Furthermore, Waste-derived carbon sources have significant advantages over synthetic alcohols, acetates, carbohydrates and commercial carbon sources in terms of safety, cost, price volatility, and sustainability. fFSF and secondary filtrate have high water content and hence are inflammable. Some researchers argue that VFAs are volatile and may cause unpleasant odors, but the concentration is very low. It is significant to note that fFSF and secondary filtrate may contain pathogenic bacteria or release H_2S , which could lead to health problems (Phenova, 2017). Therefore, ventilation and prevention of skin contact should be taken care of when using this material. Since the raw materials for the VFAs fermentation originate from the waste of WWTP, the price is very stable and not subjective to commodities. Also because part of the waste is converted into valuable material, which reduces the demand for incineration, fFSF and secondary filtrate are more environmental-friendly and sustainable than conventional carbon sources.

On the other hand, the drawbacks of applying FSF-derived carbon sources are also prominent. Due to high water content, the freezing point of these two substances is around $0\text{ }^{\circ}\text{C}$. Using and storing these FSF-derived carbon sources in cold areas require heating installations or insulation. Not only the threat of freezing, fFSF and secondary filtrate will also deteriorate under mesophilic temperature. Since these materials are mixtures of bacteria and VFAs, the bacteria may completely consume the soluble substrates if they are stored for a long period. Hence, the shelf life and product stability of FSF-derived carbon sources are not competitive. Furthermore, transferring and operating these materials are extremely difficult. Based on these disadvantages, if FSF-derived carbon

sources are going to be applied in large-scale WWTP, a better approach is to use them as soon as possible and avoid long term storage. However, this also raises the level of quality control and increases the difficulty of process control, requiring more rapid responses to changing parameters.

In summary, the BNR performance and advantages of FSF-derived carbon sources show that they are capable to substitute conventional carbon sources, like methanol, and increase the denitrification & P-release rates. Their shortcomings in terms of storage, transportation, and operation limit the large-scale application of fFSF and secondary filtrate. Further treatment of fFSF and secondary filtrate might compensate some of the shortcomings, but the additional costs should be carefully considered.

5.4. Fiber reuse in construction sector

The results of the anaerobic biodegradability test proved that separating cellulose fibers from fFSF by using secondary sieving and using those fibers for biomethane production is feasible. However, in terms of waste management, energy recovery is less favorable than material recovery. Recycled cellulose fibers from other industries like waste paper pulp have been used in construction sector to produce cellulose fiber-reinforced materials (Andrés et al., 2015). In order to further utilize the waste cellulose fibers, recycling fibers from FSF as building materials might be a possible option.

The mechanical properties of cellulose are competitive compared to conventional building materials such as steel and glass fibers, which is one of the main reasons why it can be used for building materials. Linear unbranched cellulose (β -1,4-linked d-glucose polysaccharide) has Young's modulus of 138 GPa (Chen et al., 2004). Although the Young's modulus of cellulose fiber is smaller than steel (Steel: 190 - 215 GPa), the lower density of cellulose gives it a higher specific stiffness and specific tensile strength than many metals (Huber et al., 2012).

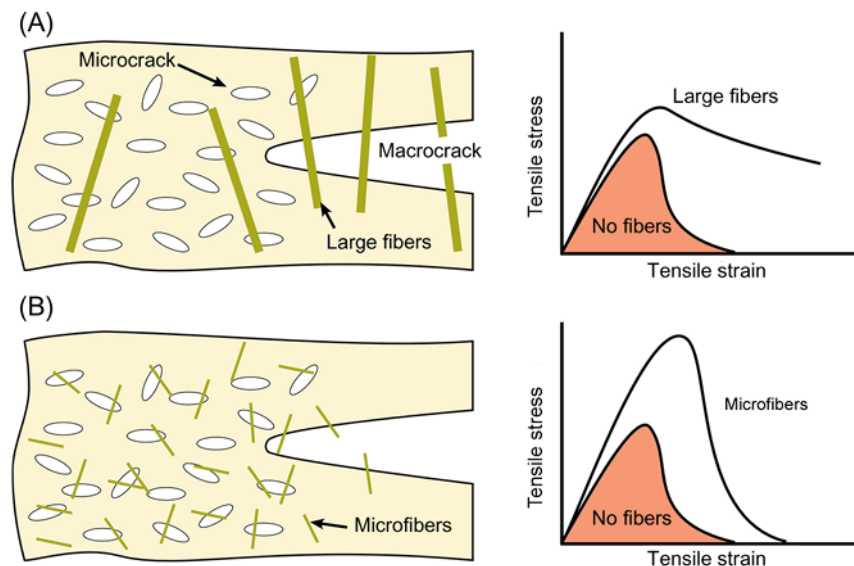


Figure 5.4: Schematic and mechanism of fiber-reinforced materials based on different fiber length. (A) Large fibers and (B) microfibers (Reprinted from Fu et al. (2017)).

Figure 5.4 illustrates the mechanisms of how cellulose fibers increase the strength of mortar. The fibers have high aspect ratios, so that they could attach and connect the air cavities in mortar formed during mixing. As mentioned before, cellulose fibers have high specific Young's modulus

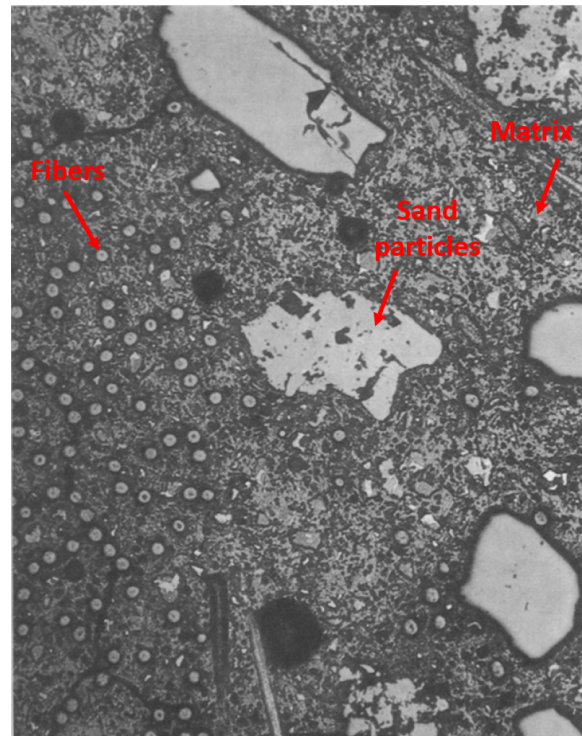


Figure 5.5: Cross-section microscopic picture of a cellulose-reinforced mortar (100x magnification). This picture is adapted from Betterman et al. (1995).

and specific tensile strength. Hence the fibers can increase the strength of mortar and prevent small cracks inside materials. Mortars with large fibers are usually more ductile than conventional mortars. On the other hand, mortars with small microfibers could fill more air cavities and could withstand higher tensile stress. Figure 5.5 presents a microscopic structure of a fiber-reinforced mortar. The volume fraction of cellulose fibers is 4%. The average length of fiber is 7 mm. As shown in the figure, the fibers are distributed in the mortar in various orientations, creating a matrix of fibers and other components.

Palmieri et al. (2019) recycled cellulose fibers from wastewater and mixed them with mortar at different mixing ratios. Their results indicate that with increasing fiber volume fraction, the density and compressive strength of the mortar seems to decrease. While the flexural strength increased from 0.5 MPa to 1.05 Mpa (0 - 20 vol%). Furthermore, they also found that mortar with recycled fibers from WWTPs has higher water vapor permeability and moisture buffering capacity, which can improve people's health and living comfort.

6

Conclusion

The majority of this study is based on the results of the pilot fermentation plant at WWTP Aarle-Rixtel. Starting from the fFSF produced by this pilot plant, this study made an exploration on the downstream processing by applying secondary sieving after the fermentation tank, and investigated the biodegradability and BNR performance of various FSF-derived VFAs. At the end of this thesis, the research questions are separately answered.

1. What are the solids content and VFAs composition of fFSF and downstream products of secondary sieving (secondary FSF & filtrate)?

Based on the result of thermogravimetric analysis, more than 90% of raw FSE, fFSE, secondary filtrate and secondary FSF were water. VS content was significantly decreased by applying secondary sieving. Through GC measurements, this study has shown that fFSF and secondary filtrate contains way more VFAs than raw FSE. The VFAs concentration of fFSF and secondary filtrate are 4129.90 ± 38.06 and 4016.31 ± 28.77 mg/L, respectively. Propionic acid and acetic acid are the two most abundant VFAs in fFSF, secondary filtrate. The VFAs concentration of secondary FSF is only 374.55 ± 8.87 mg/L, but the composition is similar to fFSF and secondary filtrate.

2. What is the aerobic biodegradability of fFSF and secondary filtrate based on biochemical oxygen demand? How is the solids load of activated sludge tank affected by the use of FSF-derived VFAs?

Both fFSF and secondary filtrate are better biodegraded than raw FSF under aerobic conditions. $60.4 \pm 4.7\%$ of fFSF and $72.1 \pm 6.4\%$ of secondary filtrate are aerobically biodegradable on VS basis. The use of fFSF and secondary filtrate could both increase the organic load of activated sludge tank, while using secondary filtrate could reduce 70% of hardly biodegradable COD than fFSF.

3. What is the anaerobic biodegradability of fFSF and secondary FSF based on biomethane potential? Are there any material recovery routes for the cellulose fibers after acidogenic fermentation?

According to the BMP test, both fFSF and secondary FSF are promising for biogas production. The BMP of fFSF and secondary FSF are 352.7 ± 12.8 and 390.5 ± 14.1 N-mL CH₄ / g VS, respectively. The anaerobic biodegradability of fFSF and secondary FSF is 68.2 ± 6.4 and 51.5

± 7.8 %, respectively. Inhibition was found during the fermentation of fFSF. The reason may be due to the accumulation of VFAs. In addition to biogas production, the cellulose fiber in fFSF and secondary FSF can also be recycled as a building material. The microfibers could effectively increase the maximum tensile stress of mortar.

4. What are the effects of P release and denitrification from fFSF and secondary filtrate as additional carbon sources? What are the advantages and disadvantages compared to other conventional carbon sources?

fFSF and secondary filtrate can significantly enhance biological nutrient removal compared to blank. Denitrification rate was increased by 40 - 50 % compared to blank. The P-release rate after adding FSF-derived carbon sources was almost 3 times higher than blank. Based on theoretical calculations, the effluent nitrogen load could be reduced by 53.7% with fFSF and 17.9% with secondary filtrate. The COD provided by FSF-derived carbon sources could completely satisfy the phosphorus removal requirements of WWTP Aarle-rixtel.

Particulate COD (XCB) could be partly biodegraded and contribute to the BNR process. However, the solids could also pose a higher organic burden on activated sludge tank. Using secondary filtrate could alleviate the problem of organic burden, but will lose a certain amount of nutrient removal capacity. Interestingly, FSF-derived carbon sources could enhance P-release to a greater extent than denitrification. Moreover, the DP and PRP of FSF-derived VFAs were found inferior to pure VFAs. The causes of these phenomena are not well understood yet.

In general, FSF-derived VFAs showed a promising BNR performance, and higher sustainability, which make them a competitive substitution compared to conventional carbon source. However, its complex composition causes some obstacles in terms of storage and operation.

5. By comparing the biodegradability and BNR performance of fFSF and secondary filtrate, what is potential of the proposed downstream processing scheme?

As a solid-liquid separation unit, secondary sieving could separate part of the solids from the fFSF and achieve separate recycling of fibers and VFAs. By separating the fibers, secondary sieving could reduce 70% of hardly biodegradable COD, which will enter activated sludge tank with FSF-derived VFAs. Furthermore, the application of secondary sieving could broaden the usage of fFSF. fFSF will not be limited to BNR purpose only. Biogas production and fibers recovery could also be achieved.

7

Recommendations

This thesis has some limitations. Due to the shut down of the pilot plant at WWTP Aarle-Rixtel, the fFSF sample used in this study has been stored for months. Furthermore, the effects of freezing on the samples have also not been evaluated in this thesis. Hence, the properties may not be identical to the fresh sample. Furthermore, this research only tested the biodegradability and BNR performance of the samples in batch tests. The degradation and recirculation of VS after entering aeration tank were not considered in this study. For instance, although particulate COD could enhance BNR, remaining solids entering the aeration tank will inevitably increase the energy consumption of aeration. Therefore, the results could not perfectly represent the actual conditions that occur in continuous WWTPs. The impacts of FSF-derived carbon sources and the BNR performance can be further verified by performing on-site experiments at real WWTPs.

Several questions still remain to be answered based on the results of this thesis. The effect of slowly biodegradable COD to enhance EBPR is slightly better than denitrification. Moreover, the amount of COD required from FSF-derived carbon sources to remove the same amount of nitrogen or release the same amount of phosphorus is greater than the COD of pure substances. In addition, fFSF also has a high phosphate concentration. Phosphate recovery like struvite precipitation could also be considered before BNR.

In general, using FSF-derived carbon sources in BNR is feasible. Future research about the above-mentioned limitations and unresolved issues could further promote and exploit the potential of FSF in BNR.

Bibliography

- Ahmed Shawki Ahmed, Ahmed Khalil, Yuichi Ito, Mark CM van Loosdrecht, Domenico Santoro, Diego Rosso, and George Nakhla. Dynamic impact of cellulose and readily biodegradable substrate on oxygen transfer efficiency in sequencing batch reactors. *Water Research*, 190:116724, 2021.
- Sadegh Aghapour Aktij, Alireza Zirehpour, Arash Mollahosseini, Mohammad J. Taherzadeh, Alberto Tiraferri, and Ahmad Rahimpour. Feasibility of membrane processes for the recovery and purification of bio-based volatile fatty acids: A comprehensive review. *Journal of Industrial and Engineering Chemistry*, 81:24–40, 1 2020. ISSN 22345957. doi: 10.1016/j.jiec.2019.09.009.
- Federico N Andrés, Loreley B Beltramini, Anabela G Guillarducci, Melisa S Romano, and Nestor O Ulibarrie. Lightweight concrete: an alternative for recycling cellulose pulp. *Procedia Materials Science*, 8:831–838, 2015.
- I. Angelidaki, M. Alves, D. Bolzonella, L. Borzacconi, J. L. Campos, A. J. Guwy, S. Kalyuzhnyi, P. Jenicek, and J. B. Van Lier. Defining the biomethane potential (bmp) of solid organic wastes and energy crops: A proposed protocol for batch assays. *Water Science and Technology*, 59:927–934, 2009. ISSN 02731223. doi: 10.2166/wst.2009.040.
- Rodger B Baird et al. Standard methods for the examination of water and wastewater, 23rd, 2017.
- Simon Bengtsson, Jakob Hallquist, Alan Werker, and Thomas Welander. Acidogenic fermentation of industrial wastewaters: Effects of chemostat retention time and ph on volatile fatty acids production. *Biochemical Engineering Journal*, 40(3):492–499, 2008.
- LR Betterman, C Ouyang, and Surendra P Shah. Fiber-matrix interaction in microfiber-reinforced mortar. *Advanced Cement Based Materials*, 2(2):53–61, 1995.
- Bioprocess Control. Ampts ii ampts ii light automatic methane potential test system operation and maintenance manual, 6 2016. URL <https://www.environmental-expert.com/files/27562/download/781453/bioprocess-control-manual-ampts-ii-ampts-ii-light.pdf>.
- Luz Stella Cadavid-Rodríguez and Nigel J. Horan. Production of volatile fatty acids from wastewater screenings using a leach-bed reactor. *Water Research*, 60:242–249, 9 2014. ISSN 18792448. doi: 10.1016/j.watres.2014.05.001.
- Shenbin Cao, Li Wang, Wangwang Yan, and Yan Zhou. Primary sludge as solid carbon source for biological denitrification: System optimization at micro-level. *Environmental Research*, 191:110160, 2020.
- MEF César, PDSC Mariani, LH Innocentini-Mei, and EJBN Cardoso. Particle size and concentration of poly (-caprolactone) and adipate modified starch blend on mineralization in soils with differing textures. *Polymer Testing*, 28(7):680–687, 2009.
- Wei Chen, Gary C Lickfield, and Charles Q Yang. Molecular modeling of cellulose in amorphous state. part i: model building and plastic deformation study. *Polymer*, 45(3):1063–1071, 2004.

- Hosea Cheung, Robin S Tanke, and G Paul Torrence. Acetic acid. *Ullmann's Encyclopedia of Industrial Chemistry*, 2000.
- Selene Chinaglia, Maurizio Tosin, and Francesco Degli-Innocenti. Biodegradation rate of biodegradable plastics at molecular level. *Polymer Degradation and Stability*, 147:237–244, 1 2018. ISSN 01413910. doi: 10.1016/j.polymdegradstab.2017.12.011.
- Cinzia Da Ros, Vincenzo Conca, Anna Laura Eusebi, Nicola Frison, and Francesco Fatone. Sieving of municipal wastewater and recovery of bio-based volatile fatty acids at pilot scale. *Water Research*, 174:115633, 2020.
- DC Devlin, SRR Esteves, RM Dinsdale, and AJ Guwy. The effect of acid pretreatment on the anaerobic digestion and dewatering of waste activated sludge. *Bioresource Technology*, 102(5):4076–4082, 2011.
- Jakub Drewnowski and J Makinia. The role of biodegradable particulate and colloidal organic compounds in biological nutrient removal activated sludge systems. *International Journal of Environmental Science and Technology*, 11(7):1973–1988, 2014.
- P. Elefsiniotis and D. Li. The effect of temperature and carbon source on denitrification using volatile fatty acids. *Biochemical Engineering Journal*, 28:148–155, 2 2006. ISSN 1369703X. doi: 10.1016/j.bej.2005.10.004.
- EUR-Lex. Council directive 91/271/eec of 21 may 1991 concerning urban waste-water treatment, 5 1991. URL <https://eur-lex.europa.eu/legal-content/EN/TXT/?uri=CELEX:31991L0271>.
- Herbert HP Fang and HQ Yu. Effect of hrt on mesophilic acidogenesis of dairy wastewater. *Journal of environmental engineering*, 126(12):1145–1148, 2000.
- Wei Fang, Xuedong Zhang, Panyue Zhang, Jijun Wan, Hongxiao Guo, Dara S.M. Ghasimi, Xavier Carol Morera, and Tao Zhang. Overview of key operation factors and strategies for improving fermentative volatile fatty acid production and product regulation from sewage sludge. *Journal of Environmental Sciences (China)*, 87:93–111, 1 2020. ISSN 18787320. doi: 10.1016/j.jes.2019.05.027.
- Tengfei Fu, Robert J Moon, Pablo Zavattieri, Jeffrey Youngblood, and William Jason Weiss. Cellulose nanomaterials as additives for cementitious materials. In *Cellulose-Reinforced Nanofibre Composites*, pages 455–482. Elsevier, 2017.
- Octavio García-Depraect, Raquel Lebrero, Sara Rodriguez-Vega, Sergio Bordel, Fernando Santos-Beneit, Leonardo J Martínez-Mendoza, Rosa Arago Bórner, Tim Börner, and Raúl Munoz. Biodegradation of bioplastics under aerobic and anaerobic aqueous conditions: Kinetics, carbon fate and particle size effect. *Bioresource Technology*, 344:126265, 2022.
- Shijian Ge, Yongzhen Peng, Congcong Lu, and Shuying Wang. Practical consideration for design and optimization of the step feed process. *Frontiers of Environmental Science & Engineering*, 7(1):135–142, 2013.
- Dara S M Ghasimi. Bio-methanation of fine sieved fraction sequestered from raw municipal sewage, 2016.
- Dara S.M. Ghasimi, Yu Tao, Merle de Kreuk, Ben Abbas, Marcel H. Zandvoort, and Jules B. van Lier. Digester performance and microbial community changes in thermophilic and mesophilic sequencing batch reactors fed with the fine sieved fraction of municipal sewage. *Water Research*, 87:483–493, 2015. ISSN 18792448. doi: 10.1016/j.watres.2015.04.027.

- Dara SM Ghasimi, Marcel H Zandvoort, Michiel Adriaanse, Jules B van Lier, and Merle de Kreuk. Comparative analysis of the digestibility of sewage fine sieved fraction and hygiene paper produced from virgin fibers and recycled fibers. *Waste management*, 53:156–164, 2016.
- Hongxiao Guo. Bio-methane potential test (internal material), 1 2016.
- Hongxiao Guo, Jules B van Lier, and Merle de Kreuk. Digestibility of waste aerobic granular sludge from a full-scale municipal wastewater treatment system. *Water research*, 173:115617, 2020.
- Lange Hach. Tnt 836 nitrate - tnt plus method 10206, 2019.
- Lange Hach. Lck348 - total phosphorus and ortho-phosphorus, 2020.
- Mogens Henze, Mark C.M. van Loosdrecht, George A. Ekama, and Damir Brdjanovic. *Biological Wastewater Treatment Principles, Modelling and Design*. 2008.
- Tim Huber, Jörg Müssig, Owen Curnow, Shusheng Pang, Simon Bickerton, and Mark P Staiger. A critical review of all-cellulose composites. *Journal of Materials Science*, 47(3):1171–1186, 2012.
- S H Isaacs and M Henze. Controlled carbon source addition to an alternating nitrification-denitrification wastewater treatment process including biological p removal, 1995.
- S H Isaacs, M Henze, H Soeberg, and M Kummel. External carbon source addition as a means to control an activated sludge nutrient removal process, 1994.
- Jianguo Jiang, Yujing Zhang, Kaimin Li, Quan Wang, Changxiu Gong, and Menglu Li. Volatile fatty acids production from food waste: effects of ph, temperature, and organic loading rate. *Biore-source technology*, 143:525–530, 2013.
- Robbert Kleerebezem, Bart Joosse, Rene Rozendal, and Mark C.M. Van Loosdrecht. Anaerobic digestion without biogas? *Reviews in Environmental Science and Biotechnology*, 14:787–801, 12 2015. ISSN 15729826. doi: 10.1007/s11157-015-9374-6.
- Jia Hong Kuo, Chiou Liang Lin, Jyh Cherng Chen, Hui Hsin Tseng, and Ming Yen Wey. Emission of carbon dioxide in municipal solid waste incineration in taiwan: A comparison with thermal power plants. *International Journal of Greenhouse Gas Control*, 5:889–898, 7 2011. ISSN 1750-5836. doi: 10.1016/J.IJGGC.2011.03.001.
- Pierre Le-Clech, Vicki Chen, and Tony AG Fane. Fouling in membrane bioreactors used in wastewater treatment. *Journal of membrane science*, 284(1-2):17–53, 2006.
- Wee Shen Lee, Adeline Seak May Chua, Hak Koon Yeoh, and Gek Cheng Ngoh. A review of the production and applications of waste-derived volatile fatty acids. *Chemical Engineering Journal*, 235:83–99, 1 2014. ISSN 13858947. doi: 10.1016/j.cej.2013.09.002.
- Gaopeng Li, Panyue Zhang, Yili Wang, Yiqi Sheng, Xiaoxue Lv, and Jiang Yin. Enhancing biological denitrification with adding sludge liquor of hydrolytic acidification pretreated by high-pressure homogenization. *International Biodeterioration & Biodegradation*, 113:222–227, 2016.
- He Liu, Peng Han, Hongbo Liu, Guangjie Zhou, Bo Fu, and Zhiyong Zheng. Full-scale production of vfas from sewage sludge by anaerobic alkaline fermentation to improve biological nutrients removal in domestic wastewater. *Bioresource Technology*, 260:105–114, 7 2018. ISSN 18732976. doi: 10.1016/j.biortech.2018.03.105.

- Huijun Ma, Xingchun Chen, He Liu, Hongbo Liu, and Bo Fu. Improved volatile fatty acids anaerobic production from waste activated sludge by pH regulation: alkaline or neutral pH? *Waste management*, 48:397–403, 2016.
- AK Misund, S Fjorden, and J Jacobsen. Experiences from primary treatment plants using sedimentation. *Report from Asplan Viak Sør, December*, 10, 2004.
- Alberto Modelli, Barbara Calcagno, and Mariastella Scandola. Kinetics of aerobic polymer degradation in soil by means of the ASTM D 5988-96 standard method. *Journal of environmental polymer degradation*, 7(2):109–116, 1999.
- Phillimon T Odirile, Potlako M Marumoloa, Anthonla Manali, and Petros Gikas. Anaerobic digestion for biogas production from municipal sewage sludge: A comparative study between fine mesh sieved primary sludge and sedimented primary sludge. *Water*, 13(24):3532, 2021.
- Adrian Oehmen, Zhiguo Yuan, Linda L Blackall, and Jürg Keller. Comparison of acetate and propionate uptake by polyphosphate accumulating organisms and glycogen accumulating organisms. *Biotechnology and bioengineering*, 91(2):162–168, 2005.
- Mathijs Oosterhuis, Alexander Hendriks, Gert-Jaap van Dijk, and Laura Castanares. *Verkenndend onderzoek naar de verzuring van zeeffgoed*, 2019.
- Derin Orhon, Esra Ate, Seval Srzen, and Emine Ubay. Characterization and COD fractionation of domestic wastewaters, 1997.
- Jonathan Charles Palm. *Relationship between organic loading, dissolved oxygen concentration, and sludge settleability in the completely-mixed activated sludge process*. University of California, Berkeley, 1982.
- Silvia Palmieri, Giulia Cipolletta, Carlo Pastore, Chiara Giosuè, Çağrı Akyol, Anna Laura Eusebi, Nicola Frison, Francesca Tittarelli, and Francesco Fatone. Pilot scale cellulose recovery from sewage sludge and reuse in building and construction material. *Waste Management*, 100:208–218, 2019.
- Yunmeng Pang and Jianlong Wang. Various electron donors for biological nitrate removal: A review. *Science of the Total Environment*, 794:148699, 2021.
- Bjarne Paulsrud, Bjørn Rusten, and Bjørn Aas. Increasing the sludge energy potential of wastewater treatment plants by introducing fine mesh sieves for primary treatment. *Water Science and Technology*, 69:560–565, 2014. ISSN 02731223. doi: 10.2166/wst.2013.737.
- Supaporn Phanwilai, Pongsak Noophan, Chi Wang Li, and Kwang Ho Choo. Effect of COD:N ratio on biological nitrogen removal using full-scale step-feed in municipal wastewater treatment plants. *Sustainable Environment Research*, 30, 10 2020. ISSN 24682039. doi: 10.1186/s42834-020-00064-6.
- Phenova. Volatile fatty acids - material safety data sheet. 2017. URL <https://phenomenex.blob.core.windows.net/documents/bec1e150-3d2b-4cd3-bbef-c6c16c3f9f6a.pdf>.
- S Puig, Marta Coma, H Monclús, MCM Van Loosdrecht, J Colprim, and MD Balaguer. Selection between alcohols and volatile fatty acids as external carbon sources for EBPR. *Water research*, 42(3):557–566, 2008.
- P Roeleveld, J Roorda, and M Schaafsma. News, the Dutch roadmap for the WWTP of 2030; op weg naar de RWZI van 2030. 2010.

- Angsana Romsaiyud, Warinthorn Songkasiri, Annop Nopharatana, and Pawinee Chairasert. Combination effect of pH and acetate on enzymatic cellulose hydrolysis. *Journal of Environmental Sciences*, 21(7):965–970, 2009.
- Cinzia Da Ros, Vincenzo Conca, Anna Laura Eusebi, Nicola Frison, and Francesco Fatone. Sieving of municipal wastewater and recovery of bio-based volatile fatty acids at pilot scale. *Water Research*, 174, 5 2020. ISSN 18792448. doi: 10.1016/j.watres.2020.115633.
- C. J. Ruiken, G. Breuer, E. Klaversma, T. Santiago, and M. C.M. van Loosdrecht. Sieving wastewater – cellulose recovery, economic and energy evaluation. *Water Research*, 47:43–48, 1 2013. ISSN 0043-1354. doi: 10.1016/J.WATRES.2012.08.023.
- Chris Ruiken, Enna Klaversma, G Breuer, and R Neef. Influent fijnzeven in rwzi's. *Amersfoort, STOWA*, 2010.
- B Rusten and Hallvard Ødegaard. Evaluation and testing of fine mesh sieve technologies for primary treatment of municipal wastewater. *Water Science and Technology*, 54(10):31–38, 2006.
- B. Rusten and Hallvard Ødegaard. Evaluation and testing of fine mesh sieve technologies for primary treatment of municipal wastewater. *Water Science and Technology*, 54:31–38, 2006. ISSN 02731223. doi: 10.2166/wst.2006.710.
- T. Sabbas, A. Poletini, R. Pomi, T. Astrup, O. Hjelm, P. Mostbauer, G. Cappai, G. Magel, S. Salhofer, C. Speiser, S. Heuss-Assbichler, R. Klein, and P. Lechner. Management of municipal solid waste incineration residues. *Waste Management*, 23:61–88, 2003. ISSN 0956053X. doi: 10.1016/S0956-053X(02)00161-7.
- Salsnes. Eco-efficient solids separation systems, 2022. URL <https://www.salsnes-filter.com/products/>.
- C Sans, J Mata-Alvarez, F Cecchi, P Pavan, and A Bassetti. Volatile fatty acids production by mesophilic fermentation of mechanically-sorted urban organic wastes in a plug-flow reactor. *Bioresource Technology*, 51(1):89–96, 1995.
- Robert J Seviour, Takashi Mino, and Motoharu Onuki. The microbiology of biological phosphorus removal in activated sludge systems. *FEMS microbiology reviews*, 27(1):99–127, 2003.
- Irene Siegert and Charles Banks. The effect of volatile fatty acid additions on the anaerobic digestion of cellulose and glucose in batch reactors. *Process Biochemistry*, 40(11):3412–3418, 2005.
- GJF Smolders, J Van der Meij, MCM Van Loosdrecht, and JJ Heijnen. Model of the anaerobic metabolism of the biological phosphorus removal process: stoichiometry and pH influence. *Biotechnology and bioengineering*, 43(6):461–470, 1994.
- Ana Soares, Pantelis Kampas, Sarah Maillard, Elizabeth Wood, Jon Brigg, Martin Tillotson, Simon A Parsons, and Elise Cartmell. Comparison between disintegrated and fermented sewage sludge for production of a carbon source suitable for biological nutrient removal. *Journal of Hazardous Materials*, 175(1-3):733–739, 2010.
- George Tchobanoglous, Franklin Burton, and H David Stensel. *Wastewater Engineering - Treatment and Reuse (4th edition)*. 2004.
- Juan Tong and Yinguang Chen. Enhanced biological phosphorus removal driven by short-chain fatty acids produced from waste activated sludge alkaline fermentation. *Environmental science & technology*, 41(20):7126–7130, 2007.

- USEPA. United states environmental protection agency wastewater treatment fact sheet: External carbon sources for nitrogen removal, 2013.
- Mark C.M. van Loosdrecht, Per Halkjaer Nielsen, Carlos M. Lopez-Vazquez, and Damir Brdjanovic. Experimental methods in wastewater treatment. 2016.
- Stefan Weijers. *Modelling, identification and control of activated sludge plants for nitrogen removal*. Wageningen University and Research, 2000.
- WTW. Bod primer: Determination of biochemical oxygen demand, 2021.
- HATİCE Yesil, AE Tugtas, A Bayrakdar, and BARIŞ Calli. Anaerobic fermentation of organic solid wastes: volatile fatty acid production and separation. *Water science and technology*, 69(10):2132–2138, 2014.
- Haowei Zhang, Jianguo Jiang, Menglu Li, Feng Yan, Changxiu Gong, and Quan Wang. Biological nitrate removal using a food waste-derived carbon source in synthetic wastewater and real sewage. *Journal of Environmental Management*, 166:407–413, 2016.
- Peng Zhang, Yinguang Chen, and Qi Zhou. Waste activated sludge hydrolysis and short-chain fatty acids accumulation under mesophilic and thermophilic conditions: effect of ph. *Water research*, 43(15):3735–3742, 2009.
- Xiong Zheng, Chen Yinguang, and Liu Chenchen. Waste activated sludge alkaline fermentation liquid as carbon source for biological nutrients removal in anaerobic followed by alternating aerobic-anoxic sequencing batch reactors. *Chinese Journal of Chemical Engineering*, 18(3):478–485, 2010.
- Huichuan Zhuang, Jianyu Guan, Shao Yuan Leu, Ying Wang, and Huaimin Wang. Carbon footprint analysis of chemical enhanced primary treatment and sludge incineration for sewage treatment in hong kong. *Journal of Cleaner Production*, 272:122630, 11 2020. ISSN 0959-6526. doi: 10.1016/J.JCLEPRO.2020.122630.

A

Raw data

Table A.1: TS and VS measurement of BOD test. The 1:59 diluted samples were measured, so the original VS and TS concentration of samples were calculated based on measure values and VS of activated sludge.

Sample	No.	Volume	Weight of dish g	After 105 °C g	After 550°C g	TS g/L	VS g/L	VS/TS -
fFSF	1	30	2.3931	2.4072	2.3977	0.470	0.317	0.674
	2	30	2.3710	2.3861	2.3757	0.503	0.347	0.689
	3	30	2.3848	2.3991	2.3897	0.477	0.313	0.657
						0.483 ± 0.014	0.326 ± 0.015	0.673 ± 0.013
Secondary filtrate	4	30	2.3818	2.3905	2.3861	0.290	0.147	0.506
	5	30	2.3986	2.4069	2.4026	0.277	0.143	0.518
	6	30	2.3418	2.3507	2.3464	0.297	0.143	0.483
						0.288 ± 0.008	0.144 ± 0.002	0.502 ± 0.014
raw FSF	7	20	2.3784	2.3944	2.3809	0.800	0.675	0.844
	8	20	2.3821	2.3970	2.3850	0.745	0.600	0.805
	9	20	2.3694	2.3887	-	0.965	-	-
						0.837 ± 0.093	0.638 ± 0.038	0.825 ± 0.019
Activated sludge	10	10	2.6136	2.6497	2.6168	3.610	3.290	0.911
	11	10	2.6280	2.6638	2.6312	3.580	3.260	0.911
	12	10	2.6281	2.6659	2.6316	3.780	3.430	0.907
						3.657 ± 0.088	3.327 ± 0.074	0.910 ± 0.002

Table A.2: tCOD and sCOD measurement for BOD test

Sample	No.	tCOD g O ₂ /L	sCOD g O ₂ /L
fFSF	1	31.1	6.64
	2	32.9	6.89
	3	36.5	6.93
		33.5 ± 2.2	6.82 ± 0.13
Secondary Filtrate	4	15.5	6.12
	5	14.2	5.98
	6	14.1	6.11
		14.6 ± 0.6	6.07 ± 0.06
raw FSF	7	64.1	1.897
	8	62.8	1.914
	9	60.8	1.907
		62.5 ± 1.4	1.906 ± 0.007

Table A.3: BMP raw data, VS,TS measurement

Sample	No.	Volume or mass L or g	Weight of dish g	After 105 °C g	After 550°C g	TS g/L or g/g sample	VS g/L or g/g sample	VS/TS -
Raw FSF	1	3.7115 g	2.3882	2.6307	2.4069	0.065	0.060	0.923
	2	4.7473 g	2.3869	2.6909	2.4120	0.064	0.059	0.917
	3	4.4439 g	2.3103	2.5793	2.3480	0.061	0.052	0.860
						0.063 ± 0.002	0.057 ± 0.004	0.90 ± 0.03
fFSF	4	0.005 L	2.3677	2.4571	2.3998	17.880	11.460	0.641
	5	0.005 L	2.3851	2.4863	2.4188	20.240	13.500	0.667
	6	0.005 L	2.3165	2.4011	2.3488	8.460	10.460	0.618
						18.347 ± 1.395	11.807 ± 1.265	0.642 ± 0.020
Sec FSF	7	3.3321 g	2.3985	2.7188	2.4315	0.096	0.086	0.897
	8	2.7425 g	2.3750	2.6294	2.4003	0.093	0.084	0.901
	9	2.7545 g	2.2660	2.5100	2.2927	0.089	0.079	0.891
						0.092 ± 0.003	0.083 ± 0.003	0.896 ± 0.004
Primary Sludge	10	3.2158 g	2.3753	2.5730	2.4188	0.061	0.048	0.780
	11	2.7755 g	2.4008	2.5714	2.4379	0.061	0.048	0.783
	12	2.5017 g	2.3430	2.4965	2.3755	0.061	0.048	0.788
						0.061 ± 0.001	0.048 ± 0.001	0.784 ± 0.003
Anaerobic Sludge	13	0.01 L	2.3796	2.6811	2.4611	(TSS) 30.150	(VSS) 22.000	(VSS/TSS) 0.730
	14	0.01 L	2.3512	2.7041	2.4459	35.290	25.820	0.732
	15	0.01L	2.3775	2.6954	2.4619	31.790	23.350	0.735
						32.41 ± 2.14	23.72 ± 1.58	0.73 ± 0.01

Table A.4: Biochemical oxygen demand of blank and experiment samples measured by Oxitop system. UFL indicates that the calculated BOD is below the admissible range for the input parameters. fFSF is abbreviation of fermented fine sieved fraction and SF is for secondary filtrate.

No	Time [min]	BOD Values														
		Blank-1 mg/l	Blank-2 mg/l	RawFSF-1 mg/l	RawFSF-2 mg/l	RawFSF-3 mg/l	fFSF-1 mg/l	fFSF-2 mg/l	fFSF-3 mg/l	SF-1 mg/l	SF-2 mg/l	SF-3 mg/l				
0	0	0,0	0,0	0,0	0,0	0,0	0,0	0,0	0,0	0,0	0,0	0,0	0,0	0,0	0,0	0,0
1	240	UFL	UFL	UFL	UFL	UFL	UFL	320	UFL	UFL	UFL	UFL	UFL	UFL	UFL	UFL
2	480	UFL	UFL	160	480	1441	UFL	1441	480	UFL	UFL	UFL	UFL	UFL	UFL	UFL
3	720	UFL	UFL	961	1121	2402	UFL	2402	1121	UFL	UFL	UFL	0,0	UFL	UFL	0,0
4	960	UFL	UFL	2082	2082	3363	UFL	3363	2082	UFL	UFL	UFL	801	UFL	UFL	801
5	1200	UFL	UFL	2563	2563	4004	160	4004	2563	160	320	1441	1441	320	160	1441
6	1440	UFL	UFL	2563	2402	4004	UFL	4004	2402	UFL	UFL	1441	1441	UFL	UFL	1281
7	1680	UFL	UFL	2883	2723	4485	UFL	4485	2723	UFL	320	1762	1762	160	160	1602
8	1920	UFL	UFL	3363	3043	4965	UFL	4965	3043	UFL	961	2402	2402	801	801	2242
9	2160	UFL	UFL	4164	3844	5606	UFL	5606	3844	UFL	1762	3203	3203	1281	1281	2723
10	2400	UFL	0,7	5285	4965	6567	UFL	6567	4965	UFL	2723	4004	4004	1922	2082	3524
11	2640	UFL	1,4	6086	5606	7207	UFL	7207	5606	UFL	3043	4324	4324	2402	2563	3844
12	2880	UFL	0,7	7047	5926	7688	UFL	7688	5926	UFL	3363	4645	4645	2723	2563	4004
13	3120	UFL	0,0	8008	6567	8329	UFL	8329	6567	UFL	3844	4965	4965	3043	3043	4324
14	3360	UFL	1,4	9129	7207	9290	UFL	9290	7207	UFL	4485	5606	5606	3524	3524	4805
15	3600	UFL	2,1	9930	7848	10251	UFL	10251	7848	UFL	5125	6086	6086	4004	4164	5285
16	3840	UFL	3,5	10891	8489	11051	UFL	11051	8489	UFL	5926	6727	6727	4485	4645	5766
17	4080	0,0	4,9	11692	9129	11692	UFL	11692	9129	UFL	6407	7207	7207	4965	4965	6086
18	4320	UFL	2,8	11852	9129	11692	UFL	11692	9129	UFL	6407	7207	7207	4805	4965	5926
19	4560	UFL	3,5	12333	9610	12173	UFL	12173	9610	UFL	6887	7528	7528	4805	5125	6086
20	4800	UFL	4,9	13134	10411	12973	UFL	12973	10411	UFL	7688	8168	8168	5125	5446	6567
21	5040	0,0	4,9	13774	10731	13294	UFL	13294	10731	UFL	8008	8649	8649	5446	5926	6887
22	5280	0,7	6,3	14575	11372	13934	UFL	13934	11372	UFL	8649	9129	9129	5766	6246	7207
23	5520	1,4	7,0	15376	11852	14575	UFL	14575	11852	UFL	9129	9610	9610	6086	6407	7528
24	5760	2,1	7,0	16017	12173	14895	UFL	14895	12173	UFL	9450	9770	9770	6407	6567	7688
25	6000	1,4	7,0	16497	12493	15216	UFL	15216	12493	UFL	9770	10090	10090	6407	6567	7688
26	6240	2,1	7,7	17298	12973	15856	UFL	15856	12973	UFL	10251	10411	10411	6567	6727	7848
27	6480	3,5	9,1	18099	13614	16657	UFL	16657	13614	UFL	10731	10891	10891	6727	7047	8168
28	6720	2,1	7,7	18579	13774	17138	UFL	17138	13774	UFL	11051	11212	11212	6887	7047	8329
29	6960	2,1	7,7	19220	14255	17778	UFL	17778	14255	UFL	11212	11372	11372	6887	7047	8329

Continued on next page

Table A.4 – Continued from previous page

No	Time [min]	Blank-1 mg/l	Blank-2 mg/l	RawFSF-1 mg/l	RawFSF-2 mg/l	RawFSF-3 mg/l	BOD Values						SF-1 mg/l	SF-2 mg/l	SF-3 mg/l
							UFL	fFSF-1 mg/l	fFSF-2 mg/l	fFSF-3 mg/l	UFL	UFL			
30	7200	2,1	7,7	19700	14735	18259	UFL	11692	11692	11692	7047	7207	8489		
31	7440	2,8	8,4	20021	15056	18900	UFL	12012	12012	12012	7047	7368	8649		
32	7680	2,8	8,4	20341	15376	19380	UFL	12333	12333	12333	7207	7368	8809		
33	7920	3,5	9,1	20661	15856	20181	UFL	12653	12653	12653	7368	7528	8809		
34	8160	4,2	9,1	20982	16337	20661	UFL	13134	13134	13134	7528	7528	8969		
35	8400	3,5	9,1	20982	16657	21142	UFL	13134	13134	13294	7528	7688	8969		
36	8640	2,8	7,7	20982	16817	21462	UFL	13134	13454	13454	7207	7368	8809		
37	8880	2,8	8,4	21142	17298	21943	UFL	13454	13614	13614	7207	7368	8809		
38	9120	3,5	9,1	21462	17778	22744	UFL	13774	14095	14095	7528	7688	9129		
39	9360	4,2	9,1	21622	18259	23224	UFL	14095	14575	14575	7688	8008	9290		
40	9600	4,9	10,5	21943	18739	24025	UFL	14255	14895	14895	7848	8008	9450		
41	9840	4,9	10,5	22103	19220	24505	320	14575	15056	15056	7848	8168	9450		
42	10080	3,5	8,4	22103	19220	24666	801	14255	14895	14895	7688	7848	9290		
43	10320	3,5	8,4	22263	19540	25146	1602	14415	15056	15056	7848	8008	9450		
44	10560	4,9	9,8	22423	20181	25787	2402	14735	15216	15216	7848	8008	9450		
45	10800	5,6	10,5	22583	20661	26587	3203	15056	15536	15536	8008	8168	9610		
46	11040	6,3	11,2	22904	21142	27068	4164	15216	15856	15856	8168	8329	9930		
47	11280	7,7	11,9	23224	21622	27548	4965	15536	16017	16017	8168	8489	9770		
48	11520	4,2	9,1	22904	21302	27548	5125	15056	15696	15696	8008	8168	9610		
49	11760	4,2	8,4	22904	21783	28029	5766	15056	15856	15856	8008	8008	9450		
50	12000	5,6	9,8	23384	22423	28670	6727	15376	16177	16177	8008	8168	9770		
51	12240	6,3	10,5	23705	22904	29310	7688	15696	16497	16497	8329	8329	9930		
52	12480	7,0	11,9	24025	23384	29951	8489	16017	16657	16657	8489	8649	10090		
53	12720	7,7	11,9	24185	23865	30431	9129	16177	16817	16817	8649	8649	10090		
54	12960	6,3	10,5	24345	24025	30592	9450	15696	16497	16497	8329	8489	9930		
55	13200	3,5	7,7	24185	24025	30752	9770	15536	16337	16337	8168	8329	9770		
56	13440	5,6	9,8	25146	24666	31553	10731	16017	16657	16657	8489	8489	9930		
57	13680	6,3	10,5	25627	25146	32033	11372	16017	16978	16978	8489	8489	10090		
58	13920	7,0	11,2	26267	25627	32514	12173	16337	17138	17138	8649	8649	10251		
59	14160	7,7	11,9	26908	25947	32674	12813	16337	17298	17298	8649	8649	10251		
60	14400	6,3	9,8	27068	25947	32514	12973	16177	16978	16978	8489	8489	10090		
61	14640	5,6	9,1	27388	26267	32674	13454	16017	16978	16978	8329	8329	9930		

Continued on next page

Table A.4 – Continued from previous page

No	Time [min]	Blank-1 mg/l	Blank-2 mg/l	RawFSF-1 mg/l	RawFSF-2 mg/l	RawFSF-3 mg/l	BOD Values					
							fFSF-1 mg/l	fFSF-2 mg/l	fFSF-3 mg/l	SF-1 mg/l	SF-2 mg/l	SF-3 mg/l
62	14880	7,0	11,2	28029	26908	32994	14095	16497	17298	8489	8489	10090
63	15120	7,7	11,2	28349	27068	33154	14575	16657	17458	8649	8649	10251
64	15360	8,4	12,6	28830	27548	33314	15216	16817	17778	8969	8809	10411
65	15600	10,5	14,0	29310	28029	33475	15856	17298	17939	8969	9129	10731
66	15840	9,1	11,9	29470	27869	33154	16017	16978	17778	8969	8969	10571
67	16080	9,1	11,9	29631	28189	33154	16337	17138	17939	8969	8969	10571
68	16320	9,8	13,3	29951	28509	33475	16817	17298	18099	9129	9129	10731
69	16560	11,2	14,0	30431	28830	33475	17138	17458	18259	9290	9290	10891
70	16800	10,5	14,0	30592	28830	33475	17458	17618	18419	9450	9290	10891
71	17040	11,2	14,7	30912	29150	33475	17778	17618	18579	9450	9290	11051
72	17280	10,5	13,3	30912	28990	33314	17618	17618	18419	9290	9290	10891
73	17520	9,8	13,3	31072	29150	33314	17778	17618	18419	9450	9290	10891
74	17760	10,5	14,0	31232	29470	33475	17939	17778	18739	9450	9290	11051
75	18000	11,9	15,4	31553	29791	33635	18099	18099	18900	9450	9450	11212
76	18240	11,9	14,7	31713	29951	33635	18419	18099	18900	9770	9610	11372
77	18480	11,2	14,7	31713	29791	33475	18259	17939	18900	9450	9450	11212
78	18720	9,1	11,9	31553	29470	33154	17939	17618	18419	9290	9129	10731
79	18960	8,4	11,9	31713	29470	33154	17939	17458	18419	9129	8969	10731
80	19200	9,8	13,3	31873	29791	33314	18099	17618	18579	9290	8969	10891
81	19440	9,8	13,3	32033	29951	33314	18259	17939	18739	9450	9129	11051
82	19680	11,2	14,7	32193	30111	33475	18579	18099	19060	9610	9290	11212
83	19920	11,2	14,7	32193	30271	33475	18739	18099	18900	9610	9290	11212
84	20160	9,8	13,3	32033	30111	33154	18419	17939	18739	9450	9129	10891
85	20400	9,8	13,3	32033	30271	33154	18419	18259	18900	9290	9129	10891
86	20640	9,8	13,3	32033	30271	33154	18579	18099	18900	9450	9129	11051
87	20880	10,5	14,0	32193	30431	33314	18739	18259	19060	9610	9290	11212
88	21120	11,2	14,7	32193	30592	33475	19060	18419	19380	9930	9450	11372
89	21360	11,2	14,7	32193	30592	33314	19060	18419	19220	9610	9450	11372
90	21600	10,5	13,3	32033	30431	33154	18900	18259	19060	9450	9129	11051
91	21840	9,8	13,3	31873	30431	33154	18900	18259	19220	9290	9129	11051
92	22080	10,5	14,0	32033	30752	33314	19220	18579	19380	9610	9290	11212
93	22320	11,2	14,7	32193	30912	33314	19380	18739	19540	9770	9450	11372

Continued on next page

Table A.4 – Continued from previous page

No	Time [min]	Blank-1 mg/l	Blank-2 mg/l	RawFSF-1 mg/l	RawFSF-2 mg/l	RawFSF-3 mg/l	BOD Values					
							RawFSF-1 mg/l	RawFSF-2 mg/l	RawFSF-3 mg/l	fFSF-1 mg/l	fFSF-2 mg/l	fFSF-3 mg/l
94	22560	11,9	15,4	32353	31232	33635	19700	19060	19861	10090	9610	11692
95	22800	13,3	16,8	32353	31232	33635	19700	19060	20021	9930	9610	11692
96	23040	9,1	12,6	31873	30752	33154	19540	18579	19540	9770	9290	11372
97	23280	9,1	11,9	31873	30752	32994	19540	18419	19380	9610	9129	11212
98	23520	9,8	13,3	31873	30912	32994	19700	18739	19540	9610	9290	11372
99	23760	11,2	14,0	32193	31232	33314	20021	18900	19861	9930	9450	11532
100	24000	12,6	16,1	32353	31713	33475	20661	19220	20181	10251	9770	11852
101	24240	14,0	16,1	32353	31713	33475	20822	19380	20181	10090	9770	11852
102	24480	11,9	14,7	32193	31392	33154	20661	19220	19861	10090	9450	11532
103	24720	11,9	14,7	32193	31392	33154	20661	19220	19861	10090	9450	11532
104	24960	12,6	15,4	32193	31713	33314	20822	19380	20181	10090	9610	11692
105	25200	12,6	15,4	32193	31713	33314	21142	19540	20181	10251	9610	11852
106	25440	13,3	15,4	32353	31873	33475	21142	19700	20341	10411	9770	11852
107	25680	14,0	17,5	32353	32193	33475	21462	20021	20501	10731	9930	12012
108	25920	14,0	16,8	32353	32193	33475	21302	20021	20661	10731	9930	12012
109	26160	14,0	16,8	32514	32193	33475	21622	20021	20661	10891	9930	12012
110	26400	14,0	16,8	32353	32193	33475	21462	20021	20661	11051	9930	12173
111	26640	14,0	16,8	32353	32193	33475	21622	20181	20822	11212	9930	12173
112	26880	14,0	16,8	32353	32353	33475	21622	20341	20982	11372	10090	12173
113	27120	14,0	16,8	32353	32193	33314	21622	20341	20982	11372	9930	12173
114	27360	14,7	17,5	32353	32353	33314	21783	20501	21142	11372	10090	12173
115	27600	14,0	16,8	32193	32193	33314	21622	20501	21142	11372	9930	12173
116	27840	14,0	16,8	32353	32353	33314	21622	20661	21302	11532	10090	12173
117	28080	14,0	16,8	32353	32353	33154	21783	20661	21462	11532	10090	12173
118	28320	14,0	16,8	32353	32514	33314	21783	20661	21462	11532	10090	12333
119	28560	14,0	16,8	32353	32353	33154	21943	20822	21622	11692	10251	12333
120	28800	13,3	16,1	32193	32193	32994	21783	20501	21462	11532	10090	12173
121	29040	13,3	16,1	32193	32193	32994	21783	20661	21622	11532	10090	12173
122	29280	13,3	15,4	32033	32193	32994	21783	20661	21622	11532	10090	12173
123	29520	13,3	15,4	32033	32193	32994	21783	20661	21622	11692	10251	12173
124	29760	14,7	16,8	32193	32514	33154	21943	20982	21943	11852	10571	12333
125	30000	14,0	16,1	32193	32353	33154	21943	20822	21783	11692	10571	12333

Continued on next page

Table A.4 – Continued from previous page

No	Time [min]	BOD Values										
		Blank-1 mg/l	Blank-2 mg/l	RawFSF-1 mg/l	RawFSF-2 mg/l	RawFSF-3 mg/l	fFSF-1 mg/l	fFSF-2 mg/l	fFSF-3 mg/l	SF-1 mg/l	SF-2 mg/l	SF-3 mg/l
126	30240	12,6	15,4	32033	32193	32994	21783	20661	21783	11692	10411	12333
127	30480	12,6	14,7	31873	32193	32834	21783	20661	21783	11372	10411	12333
128	30720	13,3	15,4	32033	32193	32994	21943	20822	21783	11532	10411	12333
129	30960	13,3	15,4	32033	32353	32994	21943	20822	21783	11532	10571	12493
130	31200	14,0	16,1	32193	32353	33154	22103	20982	21943	11692	10731	12493
131	31440	14,0	16,8	32193	32514	33154	22103	20982	21943	11692	10731	12653
132	31680	13,3	15,4	32033	32193	32994	22103	20822	21783	11692	10731	12493
133	31920	12,6	14,7	31873	32033	32834	21943	20822	21943	11532	10571	12493
134	32160	13,3	16,1	32033	32353	32994	22103	20982	21943	11532	10731	12653
135	32400	13,3	15,4	32033	32353	32994	22263	20982	21943	11692	10891	12813
136	32640	14,0	16,1	32193	32353	32994	22423	21142	22103	12012	11051	12973
137	32880	14,0	16,1	32193	32353	32994	22423	20982	22103	12012	11051	12973
138	33120	12,6	15,4	32033	32193	32834	22263	20822	21943	11852	10731	12813
139	33360	12,6	14,7	31873	32033	32834	22263	20822	21943	11692	10731	12973
140	33600	12,6	14,7	31873	32193	32834	22263	20982	21943	11692	10891	12973
141	33840	14,0	16,1	32033	32353	32994	22423	21142	22263	11852	11051	13134
142	34080	14,0	16,8	32193	32353	32994	22744	21302	22263	12012	11051	13294
143	34320	14,0	16,1	32033	32353	32994	22583	21142	22263	12012	11051	13294
144	34560	11,9	14,0	31873	32033	32674	22423	20982	22103	11852	10891	13134
145	34800	11,9	14,0	31873	32033	32674	22423	20982	22103	11852	10891	13134
146	35040	14,0	16,1	32033	32353	32834	22583	21142	22263	11852	11051	13134
147	35280	14,0	16,1	32193	32353	32994	22744	21302	22263	12173	11212	13294
148	35520	15,4	17,5	32353	32514	33154	23064	21622	22583	12333	11372	13614
149	35760	16,1	18,2	32353	32514	33154	23224	21783	22744	12493	11532	13614
150	36000	16,1	18,2	32353	32514	33154	23224	21622	22583	12653	11532	13614
151	36240	16,1	18,2	32353	32514	33154	23224	21622	22744	12653	11532	13614
152	36480	16,8	18,9	32514	32674	33314	23384	21783	22904	12653	11692	13774
153	36720	17,5	19,6	32674	32834	33314	23544	22103	23064	12813	11852	13934
154	36960	18,2	20,3	32834	32834	33475	23705	22263	23224	13134	12012	14095
155	37200	18,2	20,3	32834	32994	33475	23865	22263	23224	13294	12012	14095
156	37440	18,9	20,3	32834	32994	33475	23865	22263	23224	13294	12173	14095
157	37680	18,9	20,3	32834	32834	33475	23865	22263	23224	13294	12173	14095

Continued on next page

Table A.4 – Continued from previous page

No	Time [min]	BOD Values										
		Blank-1 mg/l	Blank-2 mg/l	RawFSF-1 mg/l	RawFSF-2 mg/l	RawFSF-3 mg/l	fFSF-1 mg/l	fFSF-2 mg/l	fFSF-3 mg/l	SF-1 mg/l	SF-2 mg/l	SF-3 mg/l
158	37920	18,9	21,0	32834	32994	33635	24025	22263	23224	13454	12173	14255
159	38160	20,3	21,7	32994	33154	33635	24185	22583	23384	13454	12333	14415
160	38400	21,0	22,4	33154	33314	33795	24345	22583	23544	13614	12333	14575
161	38640	20,3	21,0	32994	32994	33475	24185	22423	23224	13294	12173	14095
162	38880	18,2	19,6	32514	32674	33154	23705	21943	22904	12973	11852	13934
163	39120	16,8	18,2	32353	32514	32994	23544	21943	22744	12813	11692	13774
164	39360	17,5	18,9	32353	32514	33154	23384	21943	22904	12813	11692	13934
165	39600	16,8	18,9	32353	32514	33154	23384	21943	22904	12653	11692	13774
166	39840	16,8	18,9	32193	32514	33154	23384	21943	22904	12813	11852	13934
167	40080	16,8	18,2	32193	32514	33154	23384	21943	22904	12653	11692	13774
168	40320	14,7	16,1	31873	32033	32674	23064	21462	22583	12333	11372	13614
169	40560	14,0	16,1	31873	32033	32674	22904	21462	22583	12493	11532	13614
170	40800	15,4	17,5	32033	32353	32994	23064	21943	22744	12493	11692	13774
171	41040	15,4	17,5	32033	32353	32994	23224	21943	22904	12653	11692	13774
172	41280	16,1	18,2	32033	32514	32994	23384	21943	23064	12653	11692	13934
173	41520	15,4	17,5	32033	32353	32994	23224	21943	22904	12493	11532	13774
174	41760	13,3	14,7	31713	31873	32514	23064	21462	22583	12333	11372	13454
175	42000	11,9	14,7	31553	31873	32514	22904	21302	22423	12173	11212	13294
176	42240	14,0	16,1	31713	32033	32834	22904	21622	22744	12173	11372	13454
177	42480	14,0	16,1	31713	32033	32674	22904	21622	22744	12333	11372	13614
178	42720	14,7	16,8	31873	32353	32834	23064	21783	22904	12333	11532	13614
179	42960	14,0	16,1	31713	32033	32674	23064	21622	22744	12333	11372	13614
180	43200	10,5	12,6	31232	31553	32353	22744	21142	22423	12012	11212	13294

Table A.5: BMP raw data

Day	Raw FSF		fFSF		Secondary FSF		Primary sludge		Cellulose		Blank	
	NmL CH ₄ / g VS		NmL CH ₄ / g VS		NmL CH ₄ / g VS		NmL CH ₄ / g VS		NmL CH ₄ / g VS		NmL CH ₄ / g VS	
	Average	STD										
0	0.0	0.0	0.0	0.0	0.0	0.0	0.0	0.0	0.0	0.0	0.0	0.0
1	43.5	1.9	44.3	0.5	57.7	3.0	111.2	5.6	23.9	10.9	11.4	1.8
2	112.6	7.6	100.2	5.9	116.9	7.3	187.8	5.7	78.4	9.9	19.8	2.9
3	198.3	4.8	156.5	4.3	211.2	4.3	230.8	4.5	165.5	18.4	29.1	4.9
4	240.4	6.4	176.5	3.6	275.3	6.0	259.2	5.3	219.9	24.3	37.2	7.0
5	276.7	7.1	196.8	4.0	335.6	7.3	284.0	4.9	273.6	26.2	46.2	9.9
6	309.8	5.4	219.7	5.7	378.5	10.0	305.1	2.6	328.6	34.2	55.5	12.3
7	334.4	8.0	240.8	8.0	401.3	9.6	319.0	1.6	361.0	33.4	62.8	13.3
8	355.2	11.6	263.4	9.9	420.0	9.1	332.2	0.1	379.7	18.8	69.0	13.9
9	373.3	16.3	289.4	11.2	433.9	8.9	342.2	1.6	393.9	6.0	73.2	13.3
10	393.2	20.7	323.7	13.1	446.9	8.1	353.3	2.5	404.6	7.2	77.4	12.9
11	412.9	30.0	367.8	17.0	458.4	7.5	363.2	3.8	407.8	8.2	80.6	12.0
12	418.8	35.2	425.6	21.8	466.9	6.9	372.3	4.9	409.2	7.4	83.5	11.2
13	420.7	37.1	468.8	2.9	476.3	6.2	383.8	5.2	410.8	7.0	86.9	10.1
15	423.4	40.1	495.8	7.8	488.7	3.4	400.3	5.2	413.5	7.9	92.5	7.5
17	423.6	40.3	526.1	3.8	493.5	1.3	410.2	4.8	413.5	7.9	95.1	5.9
19	423.6	40.3	556.5	0.7	497.4	5.3	419.9	6.6	413.5	7.9	97.7	4.5
21	423.6	40.3	583.9	3.4	501.5	9.3	427.6	13.3	413.5	7.9	99.1	4.8
23	423.6	40.3	607.1	6.4	503.9	11.8	433.0	18.8	419.1	7.9	100.1	5.5
25	423.6	40.3	622.5	6.5	506.4	14.2	433.0	18.8	413.5	7.9	101.1	6.5
27	423.6	40.3	630.8	5.2	506.4	14.3	433.0	18.8	413.5	7.9	101.8	7.2
29	423.6	40.3	632.5	6.1	506.4	14.3	433.0	18.8	413.5	7.9	101.8	7.2
31	423.6	40.3	633.6	7.2	506.4	14.3	433.0	18.8	413.5	7.9	101.8	7.2
33	423.6	40.3	635.0	8.6	506.4	14.3	433.0	18.8	413.5	7.9	101.8	7.2
35	423.6	40.3	635.0	8.6	506.4	14.3	433.0	18.8	413.5	7.9	101.8	7.2

Table A.6: Raw data - fFSF - Denitrification

Time	NO3-N Concentration mg NO3/L					VFAs_Conc mg/L				
	1	2	Average	STD	NaAc	1	2	Average	STD	NaAc
0	107.4	103.3	105.3	2.0	105.1	10.0	10.6	10.3	0.3	33.0
5	104.1	96.4	100.2	3.8	100.6	6.9	5.0	5.9	0.9	21.4
10	102.1	92.6	97.4	4.7	97.0	0.0	0.0	0.0	0.0	9.9
15	98.8	88.4	93.6	5.2	93.3	0.0	0.0	0.0	0.0	0.0
20	95.6	86.4	91.0	4.6	90.8	0.0	0.0	0.0	0.0	0.0
30	92.5	83.5	88.0	4.5	85.3	0.0	0.0	0.0	0.0	3.1
45	90.2	77.0	83.6	6.6	79.0	0.0	0.0	0.0	0.0	0.0
60	85.5	71.6	78.5	7.0	72.2	0.0	0.0	0.0	0.0	0.0
75						0.0	0.0	0.0	0.0	0.0
90	77.4	62.3	69.8	7.6	61.8	0.0	0.0	0.0	0.0	
120	69.9	53.4	61.7	8.3	51.7	0.0	0.0	0.0	0.0	0.0
150	65.1	45.9	55.5	9.6	42.9	0.0	0.0	0.0	0.0	3.4
180	59.9	39.0	49.5	10.5	35.4	0.0	0.0	0.0	0.0	0.0
210	55.6	33.2	44.4	11.2	22.3	0.0	0.0	0.0	0.0	0.0
240	52.4	27.8	40.1	12.3	18.6	0.0	0.0	0.0	0.0	0.0

Table A.7: Raw data - fFSF - P release

Time	PO4-P Concentration mg PO4/L					VFAs_Conc mg/L				
	1	2	Average	STD	NaAc	1	2	Average	STD	NaAc
0	52.8	58.0	55.4	2.6	56.2	59.1	42.6	50.9	8.3	92.8
5	60.8	66.8	63.8	3.0	70.2	42.4	22.8	32.6	9.8	81.4
10	66.1	71.4	68.8	2.7	78.7	38.2	19.6	28.9	9.3	69.0
15	71.9	80.2	76.0	4.1	93.8	20.5	8.7	14.6	5.9	57.5
20		86.2	86.2	0.0	110.5	8.0	0.0	4.0	4.0	49.0
30	95.8	98.9	97.4	1.5	137.1	0.0	0.0	0.0	0.0	31.8
45	104.2	107.0	105.6	1.4	173.0	0.0	0.0	0.0	0.0	9.7
60	110.6	113.2	111.9	1.3	193.1	0.0	0.0	0.0	0.0	0.0
75						0.0	0.0			0.0
90	119.9	122.0	121.0	1.1	200.6	0.0	0.0	0.0	0.0	0.0
120	128.8	130.7	129.7	1.0	206.2	0.0	0.0	0.0	0.0	0.0
150	135.9	139.1	137.5	1.6	212.6	0.0	0.0	0.0	0.0	0.0
180	141.9	145.8	143.8	1.9	219.2	0.0	0.0	0.0	0.0	0.0
210	148.5	151.6	150.0	1.5		0.0	0.0	0.0	0.0	0.0
240	153.2	156.6	154.9	1.7	228.4	0.0	0.0	0.0	0.0	0.0

Table A.8: Raw data - Secondary Filtrate - Denitrification

Time	NO3-N Concentration					VFAs_Conc				
	mg NO3/L					mg/L				
	1	2	Average	STD	NaAc	1	2	Average	STD	NaAc
0	128.4	114.2	121.3	7.1	136.0	26.6	25.5	26.1	0.6	34.7
5	121.7	114.7	118.2	3.5	130.0	20.1	18.6	19.3	0.7	21.4
10	117.3	109.9	113.6	3.7	125.6	15.5	10.6	13.1	2.5	8.7
15	114.5	105.3	109.9	4.6	121.3	11.3	5.4	8.3	2.9	0.0
20	111.5	104.9	108.2	3.3	120.4	5.1	0.0	2.6	2.6	0.0
30	104.2	98.8	101.5	2.7	116.0	0.0	0.0		0.0	0.0
45	98.5	92.4	95.5	3.1	109.6	4.1	0.0	2.0	2.0	0.0
60	93.7	85.5	89.6	4.1	104.3	3.2	0.0	1.6	1.6	0.0
75										0.0
90	86.7	76.4	81.5	5.2	94.4	0.0	0.0	0.0	0.0	0.0
120	80.5	68.0	74.3	6.3	87.9	0.0	0.0	0.0	0.0	0.0
150	73.9	60.9	67.4	6.5	81.3	0.0	0.0	0.0	0.0	0.0
180	68.2	53.9	61.1	7.1	74.9	0.0	0.0	0.0	0.0	0.0
210	62.7	46.7	54.7	8.0	68.5	0.0	0.0	0.0	0.0	0.0
240	55.7	38.7	47.2	8.5	62.6	3.1	0.0	1.6	1.6	

Table A.9: Raw data - Secondary Filtrate - P release

Time	PO4-P Concentration					VFAs_Conc				
	mg PO4/L					mg/L				
	1	2	Average	STD	NaAc	1	2	Average	STD	NaAc
0	8.4	8.4	8.4	0.0	8.4	88.0	87.2	87.6	0.4	88.1
5	18.9	15.0	16.9	2.0	22.9	84.7	82.1	83.4	1.3	75.9
10					42.2					
15	26.7	28.6	27.6	0.9	63.7	58.7	56.7	57.7	1.0	62.3
20	35.1	34.2	34.6	0.4	78.6	47.9	48.6	48.2	0.3	50.9
30	45.1	44.1	44.6	0.5	115.7	38.2	37.1	37.6	0.6	31.4
45	53.6	51.1	52.4	1.3	155.9	21.2	18.8	20.0	1.2	12.5
60	63.1	59.0	61.1	2.1	186.4	3.6	8.7	6.1	2.5	0.0
75					190.2					0.0
90	67.6	62.6	65.1	2.5	195.9	3.6	3.2	3.4	0.2	0.0
120	68.2	65.6	66.9	1.3	203.0	4.8	3.4	4.1	0.7	0.0
150	72.4	69.3	70.9	1.5	207.5	4.7	3.7	4.2	0.5	0.0
180	80.0	74.7	77.4	2.6	212.2	0.0	0.0	0.0	0.0	0.0
210	84.8	80.0	82.4	2.4	218.0	0.0	4.0	2.0	2.0	0.0
240	91.8	80.9	86.4	5.5	221.0	0.0	4.3	2.2	2.2	0.0

B

Solution preparation and program settings

Table B.1: Program settings for the determination of VFAs by gas chromatography

Setting		Value
ALS		
Injection Volume		1 μ L
Ultrapure water	Pre-injection	3 times
	Post-injection	3 times
Sample washes		3 times
Column		
Type		Agilent 19091F-112
Size		25m * 320 μ m * 0.5 μ m
Maximum Temperature		240
Carrier gas		Helium
Flow		24.82 mL/min
Pressure		11 psi
Oven		
Oven temperature	Initial	80 °C for 1 min
	Ramp 1	120 °C for 3 min
	Ramp 2	180 °C for 10.5 min
	Maximum	240 °C
	Post Run	50 °C
FID		
Heater Temperature		240 °C
H ₂ Flow		40 mL/min
Air Flow		400 mL/min
Makeup Flow (He)		10 mL/min
Flame signal value		5 pA

Table B.2: Stock solutions for Biochemical oxygen demand test. All chemicals were purchased from Sigma-Aldrich (United states).

Solution	Chemicals	Concentration
Phosphate buffer solution	KH ₂ PO ₄	8.5 g/L
	K ₂ HPO ₄	21.75 g/L
	Na ₂ HPO ₄ · 7H ₂ O	33.4 g/L
	NH ₄ Cl	1.7 g/L
Magnesium sulfate solution	MgSO ₄ · 7H ₂ O	22.5 g/L
Calcium chloride solution	CaCl ₂	27.5 g/L
Ferric chloride solution	FeCl ₃	0.25 g/L
Dilution water	Phosphate buffer solution	1 mL/L
	Magnesium sulfate solution	1 mL/L
	Calcium chloride solution	1 mL/L
	Ferric chloride solution	1 mL/L
HCl solution	HCl	1 mol/L
Alkali solution	NaOH	1 mol/L
Nitrification inhibitor solution	Allylthiourea	2.0 g/L
Glucose-Glutamic acid solution	Glucose	150 mg/L
	Glutamic acid	150 mg/L

Table B.3: Experimental settings of the BOD test

			Blank	Standard	Control	Test
Type of sample			Dilution water	GGA solution	fFSF	Secondary filtrate
Oxitop® Setting	Bottle Vol.	mL	300	300	300	300 [t]
	Fill. Vol.	mL	200	100	25	25
	Meas. Range	mg/L	107	408	22123	22123
	Dilution 1+	-	0	0	9	9
Concentration	FSF	mL/L	0	0	100	100
	Dilution	Sample: di- dution water	N.A.	1:49	1:9	1:9
	Seed	mL/L	10	10	10	10
	Phosphate buffer	mL/L	0.9875	0.9676	0.8876	0.8876
	MgSO ₄ solution	mL/L	0.9875	0.9676	0.8876	0.8876
	CaCl ₂ solution	mL/L	0.9875	0.9676	0.8876	0.8876
	FeCl ₃ solution	mL/L	0.9875	0.9676	0.8876	0.8876
	ATU Conc.	mg/L	5	5	5	5
	GGA	mL/L	0	20	0	0

Table B.4: Experimental settings of the BMP test

Group	V _{demi} mL	V _{BufferA} mL	V _{BufferB} mL	V _{Micro} mL	V _{Macro} mL	V _{Sludge} mL	Sample dosage mL or g	V _{tot} mL	V _{Sini} g/L	C _{VFAs,ini} mg/L
Blank	304.86	7.6	4.9	0.24	2.4	80	0	400	2.375	0
Raw FSF	288.2	7.6	4.9	0.24	2.4	80	16.65 g	400	2.375	79.1
fFSF	144.1	7.6	4.9	0.24	2.4	80	80.4 mL	400	2.375	830.1
Secondary FSF	293.4	7.6	4.9	0.24	2.4	80	11.43 g	400	2.375	108.6
Primary sludge	285.1	7.6	4.9	0.24	2.4	80	19.77 g	400	2.375	177.9
Cellulose	209.98	7.6	4.9	0.24	2.4	80	94.9mL	400	2.375	0

Table B.5: Chemicals and dosage of standard solutions required for BMP experiments

Solution	Chemicals	Concentration	Dosage
Phosphate Buffer A	K ₂ HPO ₄ *3H ₂ O	45.65 g/L	30.5 mL/L
Phosphate Buffer B	NaH ₂ PO ₄ *2H ₂ O	31.20 g/L	19.5 mL/L
Macronutrients	CaCl ₂ * 2H ₂ O	8 g/L	6 mL/L
	MgSO ₄ *7H ₂ O	9 g/L	
	NH ₄ Cl	170 g/L	
Micronutrients	FeCl ₃ * 4H ₂ O	2 g/L	0.6 mL/L
	Na ₂ SeO ₃ *5H ₂ O	100 mg/L	
	CoCl ₂ *6H ₂ O	2 g/L	
	NiCl ₂ * 6H ₂ O	50 mg/L	
	MnCl ₂ * 4H ₂ O	0.5 g/L	
	EDTA	1 g/L	
	CuCl ₂ * 2H ₂ O	30 mg/L	
	36% HCl	1 mL/L	
	ZnCl ₂	50 mg/L	
	Resazurine	0.5 g/L	
	HBO ₃	50 mg/L	
	Yeast extract	2 g/L	
(NH ₄) ₆ Mo ₇ O ₂ ·4H ₂ O	90 mg/L		

Table B.6: Experiment parameters of denitrification test. Mass is used in stead of volume if solid samples are tested. Initial concentrations are expected concentration in each bottle at the beginning of the test. Micro: micronutrients stock solution, Macro: macronutrients stock solution. The composition of micro & macronutrients solutions are listed in table B.5. The concentration of nitrate stock solution is 14 g NO₃-N/L. The activated sludge concentration is 3.3 g VSS/L.

Sample	V_{sludge} L	V_{macro} mL	V_{micro} mL	V_{sample} mL or g	V_{nitrate} mL	V_{tot} L	C_{nitrate,ini} mg NO ₃ -N/ L	VS_{ini} mg/L
Raw FSF	0.8	5	0.5	2.10	1.3	0.808	22.5	50
fFSF	0.8	5	0.5	3.62	1.3	0.809	22.5	50
Secondary filtrate	0.8	5	0.5	7.38	1.3	0.813	22.4	50
Sodium acetate	0.8	5	0.5	4.94	1.3	0.810	22.5	50

Table B.7: Experiment parameters of denitrification test. F/M indicates food to biomass ratio at the beginning of the P-release test.

Sample	V_{sludge} L	V_{macro} mL	V_{micro} mL	V_{sample} mL or g	V_{tot} L	VS_{ini} mg/L	F/M g VS / g VSS
Raw FSF	0.8	5	0.5	5.50	0.811	130.2	0.05
fFSF	0.8	5	0.5	9.44	0.815	129.6	0.05
Secondary filtrate	0.8	5	0.5	19.17	0.825	128.1	0.05
Sodium acetate	0.8	5	0.5	12.88	0.818	129.0	0.05